INVESTIGATION OF PROPERTIES AFFECTING CONTROLLED RELEASE OF MACROMOLECULES FROM PLGA MICROSPHERES

BY

KALENA DIONNE STOVALL

DISSERTATION

Submitted in partial fulfillment of the requirements
for the degree of Doctor of Philosophy in Chemical Engineering
in the Graduate College of the
University of Illinois at Urbana-Champaign, 2009

Urbana, Illinois

Doctoral Committee:

Professor Daniel Pack, Chair
Professor Richard Braatz
Professor Jianjun Chen
Professor Jonathan Higdon

Abstract

Poly(lactide-co-glycolide), or PLGA, microspheres offer a widely-studied biodegradable option for controlled release of therapeutics. An array of fabrication methodologies have been developed to produce these microspheres with the capacity to encapsulate therapeutics of various types; and produce microspheres of a wide range of sizes for different methods of delivery. The encapsulation, stability, and release profiles of therapeutic release based on physical and thermodynamic properties has also been studied and modeled to an extent. Much research has been devoted to tailoring formulations for improved therapeutic encapsulation and stability as well as selective release profiles.

Despite the breadth of available research on PLGA microspheres, further analysis of fundamental principles regarding the microsphere degradation, formation, and therapeutic encapsulation is necessary. This work aims to examine additional fundamental principles related to PLGA microsphere formation and degradation from solvent-evaporation of preformed polymer. In particular, mapping the development of the acidic microenvironment inside the microsphere during degradation and erosion is discussed. Also, the effect of macromolecule size and conformation is examined with respect to microsphere diameter and PLGA molecular weight. Lastly, the effects of mechanical shearing and protein exposure to aqueous media during microsphere formation are examined.

In an effort to better understand the acidic microenvironment development across the microsphere diameter, pH sensitive dye conjugated to protein that undergoes conformational change at different acidic pH values was encapsulated in PLGA microspheres of diameters ranging from 40 μm to 80 μm, and used in conjunction with fluorescence resonance energy transfer to measure the radial pH change in the microspheres. Qualitative analysis of confocal micrographs was used to correlate fluorescence intensity with pH value, and obtain the radial pH across the center of the microsphere.

Therapeutic encapsulation and release from polymeric microspheres is governed by an interconnected variety of factors, including the therapeutic itself. The globular protein bovine serum albumin, and the elongated and significantly smaller enzyme, lysozyme, were

encapsulated in PLGA microspheres ranging from 40 μm to 80 μm in diameter. The initial surface morphology upon microsphere formation, release profiles, and microsphere erosion characteristics were explored in an effort to better understand the effect of protein size, conformation, and known PLGA interaction on the formation and degradation of PLGA microspheres and macromolecule release, with respect to PLGA molecular weight and microsphere diameter.

In addition to PLGA behavior and macromolecule behavior, the effect of mechanical stresses during fabrication was examined. Two similar solvent extraction techniques were compared for the fabrication of albumin loaded microspheres. In particular, the homogeneity of the microspheres as well as capacity to retain encapsulated albumin were compared. This preliminary study paves the way for a more rigorous treatment of the effect of mechanical forces present in popular microsphere fabrication.

Several factors affecting protein release from PLGA microspheres are examined herein. The technique explored for spatial resolution of the pH inside the microsphere proved mildly effective in producing a reliable method of mapping microsphere pH changes. However, notable trends with respect to microsphere size, PLGA molecular weight, and microsphere porosity were observed. Proposed methods of improving spatial resolution of the acidic microenvironment are also provided. With respect to microsphere formation, studies showed that albumin and lysozyme had little effect on the internal homogeneity of the microsphere. Rather, ionic interactions with PLGA played a more significant role in the encapsulation and release of each macromolecule. Studies also showed that higher instances of mechanical stress led to less homogeneous microspheres with lower protein encapsulation. This suggests that perhaps instead of or in addition to modifying the microsphere formation formulation, the fabrication technique itself should be more closely considered in achieving homogeneous microspheres with desired loading.

To Our Sovereign Lord God Almighty

My Eternal Father

All Glory, Honor, and Everlasting Praise to You

To Snookums

I Love You

Truly. Deeply. Always.

Kook

Acknowledgements

To my mother…
How do I put into words the deep love, admiration, and respect I have for you in my heart? Truly, truly, there would be no me without you. I cherish you deeply, and pray only the best of everything for you. I can never repay the many things you have done for me. I can never thank you enough for your unconditional love and support. As a token of my appreciation, I dedicate this work to you. All my love…

To my family…
Words can not express my gratitude to you all. You all are the ones who gave me friendship, and taught me love, sacrifice, and how to survive. I will always count it a great blessing to call myself family to all of you. Thank you so much.

Colleagues and friends: Thank y'all for letting this southern girl be a part of your lives.

Cynthia, you are an amazing friend. I'll never forget the horseback riding lessons and trips along corn fields to get there with the amazing conversations along the way; the introduction to contra dancing; walking down the sidewalk and [well you fill in the blank here – ha!]. Thanks for everything.

Kara, girl, what can I say! We've done so much together in that wonderful basement lab in RAL. From sandwich hugs, to fighting the PPF, to undergrad fun, to G.A.M.E.S. camp. So much – and it's been an amazing time. Thanks for introducing me to spaghetti squash (definitely one of my favorite foods now), and for showing me so often just how much you care.

Lisa, you are awesome. Thanks so much for rugby training a few summers ago, and for teaching me how to run! Seriously, I still consider that one of my great personal triumphs in grad school. Thanks for letting me be a part of your life as you and Gregg started your family. You two are amazing people and amazing parents.

Rahul, I'll never forget the huggin' luvin' fun – squeezing you silly; plucking your hair; you falling down in the hall at my house screaming in premature fear when I showed up during that gumbo party.

Neel, how could I ever forget the crazy back rubs I used to give you in exchange for chocolate peanut butter oatmeal cookies with chocolate chips.

Tony, what a great friend you have been to me. Who would have thought that my roommate during my first year of grad school would turn into one of my best friends – my workout buddy, dinner buddy, Chicago trip buddy, you name it. I am going to miss your crazy jokes.

Dr. Waldyke, it is hard to imagine that anyone who meets you isn't immediately hooked on you! You are such a wonderful person, and it comes from the heart. Thanks for putting up with me in your office on average at least once a month, and for the Thanksgiving dinners – an absolute blast!

Eldress Moore, you have been my family away from home here. I can't thank you enough for that.

Dr. Pack and Dr. Higdon, thank you for your mentorship and guidance. If there was one lesson that truly stood out, it was the lesson of motivated responsibility. I only wish I could have made better strides in this work, but thank you for your patience with me.

Dr. Demetrius McCormick (aka Meko), you gave me my first experience in the lab, and taught me so much and so well. Thanks for being such an amazing mentor and friend.

To my professors both in undergrad and grad school, my McNair Scholar colleagues, AGEM scholars, and MAMP / IMAGE scholars, thank you so much for everything.

Last but not least, this work would not have been possible without the financial resources provided by the NSF Graduate Research Fellowship Program, the SURGE Fellowship Program,

and NIH Grant 1R01EB005181. Also, special thanks go to the Materials Research Laboratory at UIUC, the Imaging Technology Group at the Beckman Institute, and the Center for Microscopic Imaging at UIUC for microscopy resources and analysis expertise.

May this work mark the beginning of new and better things to come.

Table of Contents

Chapter 1. Introduction

1.1 Motivation for Controlled Release

Controlled therapeutic release has been a topic of interest for decades. Controlled release of therapeutics is often preferred over traditional therapeutic administration, in which the drug is delivered as a bolus, potentially resulting in drug concentrations exceeding the maximum tolerated dose upon initial administration, and having a limited time frame for efficacy as the concentration in the body is depleted. A delivery method that provides nearly constant drug concentration within the therapeutic window would allow more effective treatment of diseases and would minimize the toxicity risks to the body. Additionally, controlled release may reduce the dosage frequency, and offer site-specific delivery of the therapeutic.

1.2 Methods of Controlled Release

A wide variety of controlled release devices are currently available. These include implantable devices, which are implanted into muscle tissue or under the skin. Such implantable devices include Biophan™'s nanomagnetic drug eluting devices; InterStim® Therapy for urinary control from Medtronic™; and active and inactive drug delivery systems offered by MicroCHIPS™. These systems provide high localized therapeutic concentrations, preferred for targeted delivery. However, they are sometimes doubly invasive since non-biodegradable components must be removed once the therapeutic is depleted. Other delivery methods include implantable pumps, which provide excellent control of drug concentration and release rate and allow for extended release (up to 1 year), but must be removed upon drug depletion.

Preferred controlled release options involve the use of minimally invasive biodegradable materials to administer therapeutics. Several types of biodegradable systems are currently employed, including gels and hydrogels, liposomes, polymeric microspheres and other geometries. In addition to biodegradability, these options are advantageous in that they can be locally injected. Gels are further advantageous because of their potential for tailored response to the local environment, including temperature and pH. One of the main disadvantages of gels is their poor mechanical strength. Liposomes have been explored for controlled release, but provide poor control of drug release rates and are relatively unstable.

1.3 Polymeric Microspheres for Drug Delivery

Biodegradable polymeric microspheres are of major interest due to their ease of fabrication and administration. Microspheres can be administered by several routes. The route of administration selected depends heavily upon the stability of the therapeutic and the type of delivery desired. Oral administration is limited to systemic delivery of highly stable therapeutics. Injection allows both systemic and localized delivery of sturdy and some delicate therapeutics. Small micron and nanosphere preparations allow administration by inhalation.

A variety of polymers have been studied for drug delivery applications, including polyorthoesters and polyanhydrides [1], which degrade by surface erosion; naturally occurring polymers such as chitosan and cellulose [2-4]; and bulk eroding polyesters such as poly(lactide-co-glycolide). Several factors can be adjusted to help tailor the encapsulation efficiency, stability and release of therapeutic [5-12]. The mechanism of polymer degradation is one of the controlling factors in therapeutic release behavior. Constant therapeutic release rates can be achieved by using surface eroding polymers, such as polyanhydrides [13]. Such hydrophobic polymers minimize the absorption of water in the polymer matrix, allowing surface erosion to dominate. The rate of release is then proportional to the surface area of the microsphere. Bulk-eroding polymers, such as poly(lactide-co-glycolide), allow water to penetrate the polymer matrix, causing degradation to occur both topically and throughout the polymer matrix. This leads to an early period of release exemplified by surface erosion, but a later burst caused by erosion in the bulk, typically giving a sigmoidal release trend.

Additional characteristics of the polymer and drug affect therapeutic release and polymer degradation. For example, research has shown that by increasing the lactide:glycolide ratio, the polymer degradation rate, and thus the therapeutic release rate can be slowed significantly [9]. Polymer molecular weight can also be adjusted to tailor release profiles. Typically, increasing polymer molecular weight gives slower release and polymer degradation [6-9]. Studies have also shown that smaller microspheres exhibit faster release in both surface and bulk eroding microspheres. However, in the case of bulk erosion, the mechanism of release can be more complex. In the case of PLGA microspheres, the rate of release in larger microspheres exhibits a

marked increased after some period of incubation by the presence of an “erosive burst” from the bulk [14]. This erosive burst is caused by the buildup of acidic byproducts inside the microsphere, which accelerates the rate of polymer degradation, leading to a more significant increase in release rate when the pore sizes and pore network throughout the microsphere have developed such that greater diffusion can occur. Research has also shown that drug distribution in larger microspheres can be increased toward the surface of the microsphere, due to slower solvent evaporation during microsphere hardening caused by longer diffusion distances [6]. This aggregation of drug toward the surface can in some cases negate the previously described release behavior in larger microspheres.

Therapeutic release behavior can also be affected by the thermodynamics of the encapsulated material. Since release is dominated by diffusion, in theory, smaller molecules release faster than larger molecules. However, studies have suggested that the positively charged enzyme lysozyme interacts with PLGA inside the matrix, slowing its release rate [15]. Depending on the polymer used, the composition of the polymer can mitigate these interactions, as is the case with poly[1,6-bis(p-carboxyphenoxy)hexane] and poly(sebacic anhydride) copolymer (CPH:SA). Research has shown that with CPH:SA copolymer, the interactions of the encapsulated compounds with a selected monomer in the copolymer composition led to release mimicking the degradation behavior of the monomer toward which each compound preferentially migrated [16].

1.4 PLGA Microspheres

The biocompatible polymers poly(lactide-co-glycolide), or PLGA, and poly(lactic acid), or PLA, have been studied for decades for drug delivery applications. As previously mentioned, varying the ratio of lactide to glycolide in PLGA can significantly influence the rate of degradation, with longer release profiles observed for compositions containing more lactide [17-18]. Studies have also shown that increasing the molecular weight of PLGA, as with other bulk-eroding polymers, slows the release rate of model protein [19-20]. Unique release profiles have been achieved from PLGA microspheres by varying the microsphere diameter [6,21]. Additionally, comparative studies have shown a slight effect on the release rate with varying protein size at low loading concentrations [22]. Lysozyme has been shown to release more slowly than albumin from PLGA microspheres due to interaction of the lysozyme with PLGA [18].

1.4.1 PLGA Microsphere Modification and Protein Stability

The fabrication process, which typically involves the use of an organic solvent, can be damaging to therapeutics. In addition, hydrophilic PLGA microspheres will allow water diffusion into the polymer matrix, causing bulk-erosion and the development of an acidic microenvironment [23-25]. This microenvironment can destabilize an encapsulated therapeutic. A variety of methods have been employed to better control the porosity and encapsulation of proteins, as well as to stabilize therapeutic while inside PLGA microspheres [26-27]. Emulsion stabilizers such as Pluronic and poly(vinyl alcohol) are often employed to control solvent evaporation rate. Studies have shown that by increasing the concentration of poly(vinyl alcohol) in the secondary emulsion, the solvent evaporation rate can be reduced, leading to more homogeneous microspheres [28]. Researchers have successfully stabilized drugs inside PLGA microspheres by adding pH buffering agents, and other excipients [29-30].

1.4.2. pH Dependence of PLGA Degradation and Protein Release

Ester-based polymeric microspheres degrade by autocatalytic degradation. During degradation, acidic byproducts are generated and the polymer hydrolysis is acid catalyzed. The rate of diffusion of these byproducts out of the microsphere is limited in proportion to the radius and porosity of the microsphere. Entrapment of these acidic moieties causes a drop in the internal pH of the microspheres and leads to more rapid degradation in the core compared to near the surface. This pH drop expectedly becomes more pronounced as the size of microspheres increases, and as the polymer molecular weight increases due to diffusion limitations. This decreased pH threatens to denature and/or inactivate encapsulated therapeutics. The presence of a low pH microenvironment inside degrading microspheres incubated at neutral pH has been observed, and determined to be as low as pH 1.5 [26-28]. Little work has been done to provide a more rigorous treatment that maps the pH across the microsphere to its lowest value, and examines the internal pH based on microsphere size.

1.5 Microsphere Fabrication Methods

Polymeric microspheres are formed either during the polymerization process or using preformed polymer. Commonly used methods for polymerization-based polymeric microsphere fabrication

include interfacial polymerization, emulsion/solvent extraction, and polymer extrusion. The applicability of each technique is limited by the polymer and therapeutic. Interfacial polymerization [30-32] commonly employs suspension [33-34], emulsion [36-38], or dispersion polymerization [39] to achieve particle fabrication during the polymerization process.

Particles formed by suspension polymerization are limited to the solvent droplet sizes in solution once the polymer-drug mixture is added to an immiscible bath. This method also requires mechanical agitation for the formation of microspheres. Emulsion polymerization requires the formation of micelles in an aqueous solution, and poses problems with encapsulation of the drug if it is not trapped with the polymer inside the micelle. It is subsequently limited to water-insoluble proteins and therapeutics. Particles formed using dispersion polymerization are made in a single-phase solution. This technique affords the use of a variety of monomers, but requires that the therapeutic and monomers are both miscible in the chosen solvent.

Microsphere formation using preformed polymer typically requires some form of solvent removal. Solvent extraction involves dissolving preformed polymers and the therapeutic either separately or in the same solvent, then breaking the solution into droplets using external physical force, such as through homogenization or sonication [40-42]. The solvent is then removed by dissolution into aqueous media, or by gas based drying. The presence of residual solvents in the final particles must be monitored, as they pose toxicity threats. Also, the amount of microspheres that can be made is limited by the batch size.

Microspheres from preformed polymer can also be produced by extrusion of the polymer-drug solution from a narrow orifice [43-44]. Unlike the aforementioned techniques, this process is continuous, and allows more precise control of particle size. Control of particle size is necessary for improved control of therapeutic release profiles, i.e. concentration of drug released and the length of time for release. Thus, techniques that provide a narrower size distribution are favored.

A variety of techniques that produce microspheres of narrow size-distribution have been developed [45-49]. Narrow size distributions can be achieved using an extrusion-style technique developed at the University of Illinois, Urbana-Champaign, in which acoustic excitation is used

to break a polymer stream into particles of a single size [5, 50-54]. This method employs a dual-nozzle setup for microsphere formation in which emulsified or co dissolved drug and polymer are fed through an inner nozzle, and surrounded by a carrier phase. A schematic of the precision fabricator is shown in Figure 1.1. By varying parameters such as the flow rates of the organic phase and the carrier phase, and the frequency and amplitude of vibration, microsphere size can be controlled. In addition, a variety of microsphere and microcapsule compositions can be used with this technique. [5,6,21,55-58]

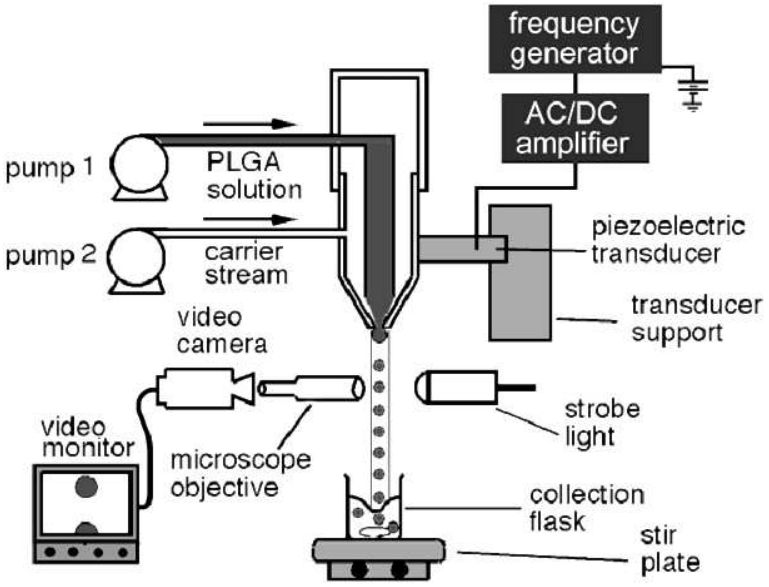

Figure 1.1. Schematic of Precision Fabrication Device. [5]

1.6 Research Aims

A wide variety of studies on PLGA microspheres have been done to date. Researchers have not only attempted to understand the fundamental governing principles of PLGA microsphere degradation and protein release and stability, but have also developed formulations and methods of fabrication that overcome many obstacles associated with employing PLGA microspheres in pharmaceutical applications. Nevertheless, additional understanding of the governing principles that influence PLGA microsphere behavior is needed. Using precision fabrication technology previously described, this study focuses on three aims. Particularly with respect to microsphere size and PLGA molecular weight, this study aims to better understand the development of the

acidic microenvironment inside degrading PLGA microspheres; to understand differences in release of macromolecules of different size and conformation; and to gain insight into the effect of shearing by the fabrication process on the formation of PLGA microspheres. Chapter 2 focuses on the development of a technique to map intraparticle pH. Chapter 3 focuses on the release behavior of albumin and lysozyme from PLGA microspheres of varying diameter produced from PLGA of varying molecular weight. Chapter 4 examines the effect of precision fabrication and homogenization on the production of PLGA microspheres.

1.7 References

[1] Rosen, H., J. Chang, G. Wnek, R. Linhardt, and R. Langer. Bioerodible Polyanhydrides for Controlled Drug Delivery. Biomaterials, 4(2):131–133, 1983.

[2] Tansey, R.. Sustained Release Therapeutic Tablet Compositions Comprising Organic Solvent-Gelled Gums. U. S. Patent, US 3133863, May 1964.

[3] Miyazaki, S., K. Ishii, and T. Nadai. Pharmaceutical Application of Biomedical Polymers. Part IV. The Use of Chitin and Chitosan as Drug Carriers. Chemical and Pharmaceutical Bulletin, 29(10):3067–3069, 1981.

[4] Arshady, R. Preparation of Microspheres and Microcapsules by Interfacial Polycondensation Techniques, Journal of Microencapsulation 6:13-28, 1989.

[5] C. Berkland, K. Kim, and D. Pack. Fabrication of PLG Microspheres with Precisely Controlled and Monodisperse Size Distributions. Journal of Controlled Release, 73:59–74, 2001.

[6] C. Berkland, K. Kim, and D. Pack. PLGA Microsphere Size Controls Drug Release Rate Through Several Competing Factors. Pharmaceutical Research, 20(7):1055–1062, 2003.

[7] Bezemer, J., R. Radersma, D. Grijpma, P. Dijkstra, C. van Blitterswijk, and F. Feijen. Microspheres for Protein Delivery Preprared from Amphiphilic Multiblock Copolymers 2. Journal of Controlled Release, 67(2-3):249–260, 2000.

[8] Crotts, G., H. Sah, and T. Park. Adsorption Determines In-Vitro Protein Release Rate from Biodegradable Microspheres: Quantitative Analysis of Surface Area During Degradation. Journal of Controlled Release, 47(1):101–111, 1997.

[9] Ouellette, A., and N A. Peppas. Controlled Release of Triamterene from Poly(dl-lactide-co-glycolide) Microspheres. Materials Research Society Symposium Proceedings, 331 (Biomaterials for drug and cell delivery):91–96, 1994.

[10] Najib, N., M. Suleiman, and A. Malakh. Characteristics of the In-Vitro Release of Ibuprofen from Polyvinylpyrrolidone Solid Dispersions. International Journal of Pharmaceutics, 32(2-3):229–236, 1986.

[11] H. Robson, D. Q. Craig, and D. Deutsch. An Investigation into the Release of Cefuroxime Axetil from Taste-Masked Stearic Acid Microspheres. III. The use of DSC and HSDSC as Means of Characterising the Interaction of the Microspheres with Buffered Media. International Journal of Pharmaceutics, 201(2):211–219, 2000.

[12] Shukla, A., and J. Price. Effect of Drug Loading and Molecular Weight of Cellulose Acetate Propionate on the Release Characteristics of Theophylline Microspheres.

[13] Saltzman, W. Drug Delivery-Engineering Principles for Drug Therapy. Oxford University Press, New York 2001.
[14] Saltzman, W., and R. Langer. Transport Rates of Proteins in Porous Polymers with Known Microgeometry. Biophysical Journal, 55:163–171, 1989.
[15] Blanco, D., M. Alonso. Protein Encapsulation and Release from Poly(lactide-co-glycolide) Microspheres: Effect of the Protein and Polymer Properties and of the Co-Encapsulation of Surfactants. European Journal of Pharmaceutics and Biopharmaceutics, 45:285–294, 1998.
[16] Kpper, M. E. Shen, A. Determan, B. Narasimhan. Design of an Injectable System Based on Bioerodible Polyanlydride Microspheres for Sustained Drug Delivery. Biomaterials 23:4405-4412, 2002.
[17] Park. T. Degradation of Poly(lactic-co-glycolic acid) Microspheres: Effect of Copolymer Composition. Biomaterials, 16(15):1123–1130, 1995.
[18] Crotts, G., H. Sah, and T. Park. Adsorption Determines In-Vitro Protein Release Rate from Biodegradable Microspheres: Quantitative Analysis of Surface Area During Degradation. Journal of Controlled Release, 47(1):101–111, 1997.
[19] Blanco, D., and M. Alonso. Protein Encapsulation and Release from Poly(lactide-co-glycolide) Microspheres: Effect of the Protein and Polymer Properties and of the Co-Encapsulation of Surfactants. European Journal of Pharmaceutics and Biopharmaceutics, 45:285–294, 1998.
[20] Soriano, I., M. Llabres, and C. Evora. Release Control of Albumin from Polylactic Acid Microspheres. International Journal of Pharmaceutics, 125(2):223–230, 1995.
[21] Berkland, C., E. Pollauf, C. Raman, R. Silverman, K. Kim, and D. Pack. Macromolecule Release from Monodisperse PLGA Microspheres: Control of Release Rates and Investigation of Release Mechanism. Journal of Pharmaceutical Science, 96(5):1176-91, 2007.
[22] Sandor, M., D. Enscore, P. Weston, and E. Mathiowitz. Effect of Protein Molecular Weight on Release from Micron Sized PLGA Microspheres. Journal of Controlled Release, 76:291–311, 2001.
[23] Shenderova, A., T. Burke, and S. Schwendeman. The Acidic Microclimate in Poly(lactide-co-glycolide) Microspheres Stabilizes Camptothecins. Pharmaceutical Research. 16(2):241–248, 1999.
[24] Fu, K., D. Pack, A. Klibanov, and R. Langer. Visual Evidence of Acidic Environment Within Degrading Poly(lactic-co-glycolic acid) (PLGA) Microspheres. Pharmaceutical Research, 17(1):100–106, 2000.
[25] Brunner, A., K. M¨ader, and A. G¨opferich. pH and Osmotic Pressure Inside Biodegradable Microspheres During Erosion. Pharmaceutical Research, 16(6):847– 853, 1999.
[26] Pavanetto, F., B. Conti, I. Genta, P. Giunchedi. Solvent Evaporation, Solvent Extraction and Spray Drying for Polylactide Microsphere Preparation. International Journal of Pharmaceutics 84(2):151-159, 1992.
[27] O'Donnell, P., J. McGinity. Preparation of Microspheres by the Solvent Evaporation Technique. Advanced Drug Delivery Reviews, 28:25–42, 1997.
[28] Li, W., K. Anderson, R. Mehta, P. DeLuca. Prediction of Solvent Removal Profile and Effect on Properties for Peptide-Loaded PLGA Microspheres Prepared by Solvent Extraction / Evaporation Method. Journal of Controlled Release, 37:199–214, 1995.

[29] Jong-Ho, K., Ajay, T., Kristine, K., Bae, Y. Stability of Bovine Serum Albumin Complexed with PEG-poly(L-histidine) Diblock Copolymer in PLGA Microspheres. Journal of Controlled Release, 109:86-100, 2005.
[30] Jain, R., C. Rhodes, A. Railkar, A. Malick, N. Shah. Controlled Release of Drugs fom Injectable In-Situ formed Biodegradable PLGA Microspheres: Effect of Various Formulation Variables. European Journal of Pharmaceutics and Biopharmceutics, 50:257-262, 2000.
[31] Arshady, R. Suspension, Emulsion, and Dispersion Polymerization: A Methodological Survey. Colloid and Polymer Science, 270:717-732, 1992.
[32] Kamiyama, M., K. Kikuhiko, H. Matsuda, Y. Sano, Micron-Sized Polymeric Microsphere by Suspension Polymerization. Journal of Applied Polymer Science, 50:107-113, 1993.
[33] Sahin, S., S. Handan, G. Ponchel, M. Ercan, M. Sargon, A. Hincal, and H. Kas. Preparation, Characterization and In-Vivo Distribution of Terbutaline Sulfate Loaded Albumin Microspheres. Journal of Controlled Release, 82:345-358, 2002.
[34] Singh, J., and K. Tripathi. Preparation, Characterization, and In-Vitro Release Kinetics of Aminophylline-Loaded Albumin Microspheres. Pharmazeutische Industrie, 56:1076-1080, 1994.
[35] Kriwet, B., E. Walter, and T. Kissel. Synthesis of Bioadhesive Poly(acrylic acid) Nano- and Microparticles Using an Inverse Emulsion Polymerization Method for the Entrapment of Hydrophilic Drug Candidates. Journal of Controlled Release, 56:149-158, 1998.
[36] Zimmer, A., Antisense Oligonucleotide Delivery with Polyhexylcyanoacrylate Nanoparticles as Carriers. Methods, 18:286-295, 1999.
[37] Radwan, M., I. Zaghloul, and Z. Aly. In-vivo Performance of Parenteral Theophylline-Loaded Polyisobutylcyanoacrylate Nanoparticles in Rats, European Journal of Pharmaceutical Sciences 8:95-98, 1999.
[38] Jayachandran, K., and P. Rangorath. Preparation of Linear and Crosslinked Polymer Microspheres by Dispersion Polymerization, Journal of Macromolecular Science, Polymer Reviews, 41:79-9, 2001.
[39] Cohen, S., T. Yoshioka, M. Lucarelli, L. Hwang, and R. Langer. Controlled Delivery Systems for Proteins Based on Poly(Lactic/Glycolic Acid) Microspheres. Pharmaceutical Research, 8:713-720, 1991.
[40] Mylonas, C., R. Langer, and Y. Zohar. Preparation and Evaluation of Polyanhydride Microspheres Containing Gonadotropin-Releasing Hormone (GnRH), for Inducing Ovulation and Spermiation in Fish, Journal of Controlled Release 35:23-34, 1995.
[41] Sah, H. Protein Instability Toward Organic Solvent/Water Emulsification: Implications for Protein Microencapsulation into Microspheres. Journal of Pharmaceutical Science and Technology, 53:3-10, 1999.
[42] Ma, G., M. Nagai, and S. Oni. Preparation of Uniform Poly(lactide) Microspheres by Employing the Shirasu Porous Glass (SPG) Emulsification Technique. Colloids and Surfaces A: Physicochemical and Engineering Aspects. 153:383-394, 1999.
[43] Hatate, Y., H. Ohta, Y. Uemura, K. Ijichi, and H. Yoshizawa. Preparation of Monodispersed Polymeric Microspheres for Toner Particles by the Shirasu Porous Glass Membrane Emulsification Technique. Journal of Applied Polymer Science, 64:1107-1113, 1996.

[44] Amsden, B. The Production of Uniformly Sized Polymer Microspheres, Pharmaceutical Research 16:1140-1143, 1999.

[45] Shiga, K., N. Muramatsu, and T. Kondo. Preparation of Poly(D,L-lactide) and Poly(lactide-glycolide) Microspheres of Uniform Size. Journal of Pharmaceutics and Pharmacology, 48:891-895, 1996.

[46] Sansdrap, P., and A. Moes. Influence of Manufacturing Parameters on the Size Characteristics and the Release Profiles of Nifedipine from Poly(DL-lactide-co-glycolide) Microspheres. International Journal of Pharmceutics, 98:157-164, 1993.

[47] Leelarasamee, N., S. Howard, C. Malanga, and J. Ma. A Method for the Preparation of Polylactic Acid Microcapsules of Controlled Particle Size and Drug Loading. Journal of Microencapsulation, 5:147-157, 1998.

[48] Amsden, B., and M. Goosen. An Examination of the Factors Affecting the Size, Distribution, and Release Characteristics of Polymer Microbeads Made Using Electrostatics. Journal of Controlled Release, 43:183-196, 1997.

[49] Amsden, B. The Production of Uniformly Sized Polymer Microspheres. Pharmaceutical Research, 16:1140-1143, 1999.

[50] Guttman, J., C. Hendricks, K. Kim, and R. Turnbull. An Investigation of the Effects of System Parameters on the Production of Hollow Hydrogen Droplets. Journal of Applied Physics, 50:4139–4142, 1979.

[51] Kim, N., K. Kim, D. Payne, and R. Upadhye. Fabrication of Hollow Silica Aerogel Spheres by a Droplet Generation Method and Sol-Gel Processing. Journal of Vacuum Science and Technology A, 7:1181–1184, 1989.

[52] Jang, K., K. Kim, and R. Upadhye. Study of Sol-Gel Processing for Fabrication of Hollow Silica-Aerogel Spheres. Journal of Vacuum Science and Technology A, 8:1732–1735, 1990.

[53] Kim, K., K. Jang, and R. Upadhye. Hollow Ssilica Spheres of Controlled Size and Porosity by Sol-Gel Processing. Journal of the American Ceramic Society, 74:1987–1992, 1991.

[54] Jang, K., and K. Kim. Evaluation of Sol-Gel Processing as a Method for Fabricating Spherical-Shell Silica Aerogel ICF Targets. Journal of Vacuum Science and Technology A, 10:1152–1157, 1992.

[55] Berkland, C., E. Pollauf, N. Varde, D. Pack and K. Kim. Monodisperse Liquid-Filled Biodegradable Microcapsules. Pharmaceutical Research, 24(5):1007-1013, 2007.

[56] Berkland, C., M. Kipper, B. Narasimhan, K. Kim, and D Pack. Microsphere Size, Precipitation Kinetics and Drug Distribution Control Drug Release from Biodegradable Polyanhydride Microspheres. Journal of Controlled Release, 94(1):129-141, 2004.

[57] Pollauf, E. K. Kim, D. Pack. Small-Molecule Release from Poly(D,L-lactide)/Poly(D,L-lactide-co-glycolide) Composite Microparticles. Journal of Pharmaceutical Sciences, 94(9):2013-2022, 2005.

[58] Berkland, C., E. Pollauf, D. Pack, K. Kim. Uniform Double-Walled Polymer Microspheres of Controllable Shell Thickness. Journal of Controlled Release, 96(1):101-111, 2004.

Chapter 2. Measurement of Intraparticle pH in Degrading PLGA Microspheres

2.1 Motivation

Though PLGA is a heavily studied material for drug delivery, some characteristics of its behavior warrant further investigation. In particular, the rate of diffusion of acidic degradation byproducts out of the microsphere is limited in proportion to the square of the radius and porosity of the microsphere. Accumulation of these acidic moieties causes a drop in the internal pH of the microspheres and leads to more rapid degradation in the core compared to near the surface. This pH drop expectedly becomes more pronounced as the size of microspheres increases, and as the polymer molecular weight increases due to diffusion limitations. This decreased pH threatens to denature and/or inactivate encapsulated therapeutics.

The presence of a low pH microenvironment inside degrading microspheres has been established, and determined to be as low as pH 1.5 [1-3]. Little work has been done to provide a more rigorous treatment that maps the pH across the microsphere and examines the internal pH based on microsphere size. Herein, the radial development of the acidic microenvironment inside PLGA microspheres is determined with respect to PLGA molecular weight and microsphere diameter.

2.2 Previous Work

In an earlier study, an initial attempt at using pH sensitive fluorescent dye to map the internal pH across microspheres was made [5]. The pH sensitive dye fluorescein-5-isothiocyanate (FITC) and pH insensitive dye AlexaFluor 633 (AF 633) were used to map the pH inside degrading PLGA microspheres from pH 6.5 to pH 4. Figure 2.1 shows the variation in radial pH of 12 microspheres of 32 μm diameter at day 3. Data showed a swift drop in pH toward the center of the microspheres, with pH reaching the lowest measurable value as early as 3 days. The most significant effect was the tapering of the pH across the microsphere. The pH drops quickly with decreasing radial position near the surface.

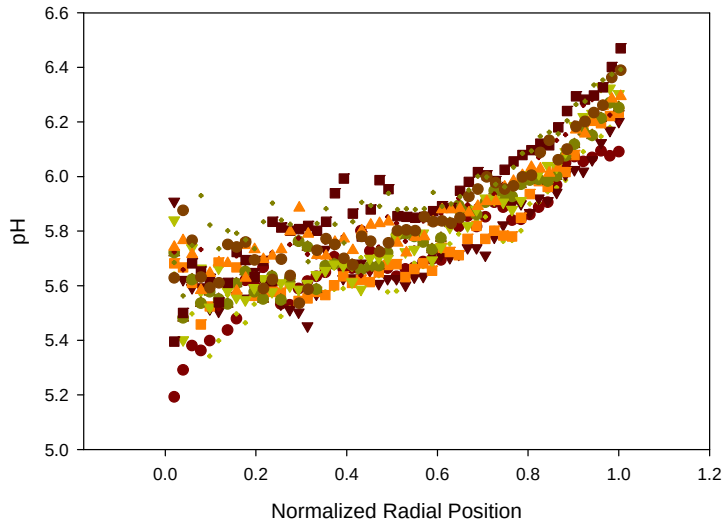

Figure 2.1. pH of twelve individual microspheres used to find the average pH of the 32 µm microspheres at day 3.

The extent of the pH drop at the center of the microsphere and across the radial distance, along with the rate of this change in pH are of great interest. Thus this study aimed to determine the extent of the pH drop by employing the principles of fluorescence resonance energy transfer (FRET) in conjunction with the pH-induced conformational change of BSA at low pH. Efforts to accomplish this goal are discussed herein.

2.3 Methods

2.3.1 Materials

Poly(D,L-lactide-*co*-glycolide) (PLGA) polymers of 50:50 lactide:glycolide ratio and inherent viscosities (i.v.) of 0.20, 0.41, and 0.61 dL/g, were obtained from Durect Corporation. These PLGA polymers are hereafter referred to by their relative molecular weights of 11 kDa, 25 kDa, and 48 kDa, respectively. Lyophilized bovine serum albumin was obtained from Sigma-Aldrich. Carboxyfluorescein or FAM, obtained from Molecular Probes, was selected as a pH sensitive dye in the range of pH 4-7. 5-(and-6)-Carboxytetramethylrhodamine succinimidyl ester (TAMRA), obtained from Molecular Probes, was selected as a pH insensitive dye in the range of pH 4-7. Additionally, its excitation wavelength falls inside the range of FAM's emission spectra, which is a necessary component for FRET. Dimethyl sulfoxide (DMSO) was purchased from

Fisher Scientific. PD-10 desalting columns were purchased from Amersham Biosciences. Tween 80 was obtained from Fisher Scientific, and used as a surfactant during release studies. Phosphate buffered saline tablets were obtained from MP Biomedicals, and dissolved in milli-Q water. Poly(vinyl alcohol) (PVA), 88% hydrolyzed, was obtained from Polysciences, dissolved in Milli-Q water, and diluted to the specified concentrations. Reagent grade dichloromethane (DCM) and HPLC grade chloroform were obtained from Fisher Scientific.

2.3.2 Protein Labeling

Dual labeled bovine serum albumin was made by covalently conjugating FAM and TAMRA to albumin. Briefly, for each formulation, 40 milligrams of albumin were dissolved in 4 mL of sodium bicarbonate at pH 8.3±0.05. Several formulations containing varied amounts of FAM and TAMRA dissolved in 40 µL of DMSO each were pipetted into the foil-wrapped vial containing dissolved albumin. The solution was stirred on a stir plate for 60 minutes at room temperature. The labeled albumin and unattached dye were then separated using a PD-10 desalting column pre-equilibrated with sodium bicarbonate buffer. The collected protein was then frozen and lyophilized.

The degree of labeling for each conjugate was determined by dissolving 1.0 mg of labeled protein in 1.0 mL of milli-Q H_2O. The absorbance was taken at the wavelengths shown in Table 2.1. Readings were zeroed against 1.0 mL of milli-Q H_2O. The values were then used to calculate the degree of labeling according to the method established by Molecular Probes (www.probes.com). Labeling results are discussed in further details in the section 2.4.1. For microspheres discussed herein, the labeling ratio FAM : TAMRA was 7.1 : 1.

Table 2.1. Excitation wavelengths of selected dyes and Albumin

Dye or Protein	Excitation Wavelength (nm)	Extinction Coefficient
FAM	494	68000
TAMRA	555	65000
Albumin	280	--

2.3.3 Microsphere Fabrication and Sizing

Uniform microspheres of roughly 40 µm, 60 µm, and 80 µm diameter were fabricated using the precision fabrication technique described in chapter 1. In short, PLGA was dissolved in DCM at 10 % (w/v). Albumin was dissolved in milli-Q water. The amount of water used was maintained at a 1:10 (H_2O : DCM) ratio. Albumin concentration was selected to provide 10 % (w/w) loading of the PLGA, with dual-labeled albumin comprising 2.5% of the total albumin concentration. The PLGA and macromolecule solutions were emulsified by sonication on ice at 60% amplitude for 1 minute, and fed into the precision fabricator. Carrier phase and emulsion phase flow rates, and frequency and amplitude of vibration were selected to produce the desired microsphere size.

Microspheres were collected in 1% PVA solution, and allowed to harden under stirring for three hours. Microspheres were subsequently washed with three aliquots of milli-Q water, then frozen and lyophilized for 48 hours prior to use. Lyophilized microspheres were stored at -20ºC under desiccant. Microspheres were sized using a Beckman-Coulter Multi-Sizer III, with a minimum count of 10,000 microspheres. Microsphere diameters are reported as the mean diameter, and include the standard deviation and R_{90}, which is the ratio of the largest to smallest microsphere within the 10% outer limits of measurement.

2.3.4 Albumin Loading

For each set of microspheres, approximately 5 mg of microspheres were dissolved in 100 µL of DMSO. Twenty microliters of the dissolved PLGA and macromolecule solution were pipetted into 1 mL of PBS while vortexing. Samples were incubated at 37ºC for 1 hour with agitation, and then centrifuged at 10000 rpm for 10 minutes to pellet the polymer. The supernatant was removed and replaced with 1 mL of fresh PBS while vortexing. The samples were then incubated for an additional 30 minutes at 37ºC. The concentration of protein in the supernatant was determined for both supernatants using BCA assay, then summed for each set of microspheres. The encapsulation efficiency or loading is reported as the measured concentration of albumin as a percent of theoretical loading during encapsulation.

2.3.5 In-Vitro Release and PLGA Degradation Studies

To obtain protein release behavior, 10 mg of microspheres were suspended in 1.25 mL of PBS with 0.05% Tween 80 (pH 7.2 ± 0.05), and incubated at 37ºC with agitation. One mL of supernatant was extracted at various time points, and replaced with fresh buffer. Protein concentration in supernatants was determined using BCA assay.

Microsphere surface morphology and porosity changes were observed by scanning electron microscopy. Microspheres were washed with milli-Q water three times, then freeze-fractured and mounted on carbon tape, and allowed to dry. Prepped samples were sputter coated for 30 seconds at 20 mA with gold-palladium using an Emitech K-575 Sputter Coater. Scanning electron micrographs were then acquired using a JEOL 6060 LV scanning electron microscope at 5 kV accelerating voltage.

2.3.6 Radial pH Mapping

The radial pH of the microspheres was determined by quantitative analysis of confocal fluorescence micrographs obtained from dual-labeled protein loaded microspheres. Stock solutions of 500 mM pH buffers ranging from pH 1.5 to 7 were prepared using acid-salt combinations given in Table 2.2. Buffers were titrated to the desired pH using 0.1 M HCl and 0.1 M NaOH. To determine a calibration curve, microspheres were soaked for 12 hours at 37ºC in buffers of pH 1.5 to 7 ± 0.05. Microspheres were then imaged using a Leica SP2 Laser Scanning Confocal Microscope with Leica Confocal Software. The microscope was focused at the center of the microspheres by adjusting the focus to achieve an image of the largest diameter. Optimal PMT and Offset settings were determined by saturating images of microspheres at each pH, then decreasing the PMT and gain until saturation was eliminated. Images were analyzed using IMAGE J (http://rsb.info.nih.gov/ij/) software. The images were first converted to 8-bit format and smoothed once. The FAM or FRET image was then divided by the TAMRA image, and a 32-bit result obtained, using the Image Calculator feature. The radial intensities of a minimum of ten microspheres per batch were determined using the Radial Profile Plugin feature, and then averaged to determine a single average intensity inside the microsphere. Fluorescence intensity ratio versus pH calibration curves were created for each set of microspheres.

Microspheres from each set of size and polymer molecular weight were subjected to a 40-day degradation study. For each set approximately 10.0 mg of microspheres were suspended in 1.25 mL of PBS (pH 7.2±0.5) with 0.05% Tween 80. Microspheres were incubated on a roto-rack at 37ºC. At various time points during the study, a sample of microspheres was removed. Also, 1.0 mL of supernatant was removed from each sample and replaced with 1.0 mL of fresh PBS (pH 7.2±0.5) with 0.05% Tween 80 every seven days to maintain buffer pH. Microspheres were imaged using confocal microscopy at the optimal PMT and gain settings determined during calibration. The average radial intensity for a minimum of ten microspheres was determined using IMAGE J. The values obtained were compared with pH versus intensity ratio calibration plots to determine the pH across the microspheres.

Table 2.2. pH Buffer Compositions for pH versus Fluorescence Intensity Calibration Curves.

Acid / Salt Pair	pH	Acid Concentration (g/L)	Salt Concentration (g/L)
HOCOCH:CHCOOH / $HO_2CCH=CHCO_2H$	1.5	16.8	2.5
	2	10.5	6.4
	2.5	4.8	12.7
	3	1.8	18.4
	3.5	0.6	21.4
CH_3COOH / $CH_3COONa\ 3H_2O$	4	14.0	1.8
	4.5	10.6	4.2
	5	6.0	7.6
	5.5	2.5	10.2
KH_2PO_4 / K_2HPO_4	6	23.9	4.2
	6.5	18.9	10.6
	7	11.4	20.2

2.4 Results and Discussion

2.4.1 Dual-Labeled Albumin Selection

To optimize the incremental fluorescence intensity with respect to pH, FAM and TAMRA concentrations were selected to vary the labeling ratio from (FAM : TAMRA) 1:1, 1:2, 2:1, and so on. After the degree of labeling was determined, dissolved protein was pipetted into pH buffer standards and the fluorescence intensity at each pH determined for FAM (488 nm / 518 nm), TAMRA (555 nm / 580 nm), and FRET (488 nm / 580 nm). Although it is recommended to use 494 nm for FAM, the confocal microscope has only 488 nm laser available, thus solution testing was performed at 488 nm. Figure 2.2 shows fluorescence intensity versus pH for 2:1 dual-labeled albumin and 7:1 dual-labeled albumin using FRET. The increments are larger for 7:1 than 2:1. However, over the pH range of interest with FRET (pH 1 to 4), the total change in intensity is only 0.2. Previous studies have demonstrated that a smaller incremental change in intensity is observed with confocal than with fluorescence in solution. A change of 0.2 over such a large pH range would equate to between 0.1 to 0.15 incremental change over the same pH range with confocal. Given the propensity for larger variations in intensity across the microsphere when using confocal microscopy than in solution, the values would overlap, and not provide useful determination between pH values. Ultimately, it was determined that a ratio of 7:1 was the most promising, with an incremental change of 0.4 in fluorescence intensity in solution from pH 1.5 to 4, as shown in Figure 2.2.

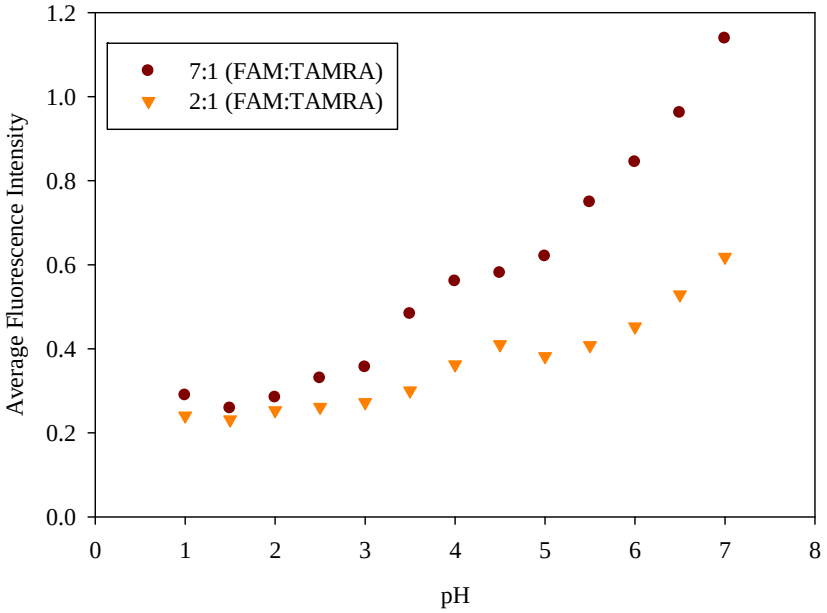

Figure 2.2. Fluorescence intensity versus pH of dual-labeled albumin in pH buffer solution.

2.4.2 pH Standard Curves

Analysis of microspheres containing 2.5% dual-labeled albumin showed that the concentration of dual-labeled albumin was too high. Standard curves could not be obtained due to inconsistencies in the measured intensities between pH values, which were likely caused by self-quenching of the dye fluorescence. Thereafter, the dual-labeled albumin was again tested in pH buffer solution to determine the concentration that exhibited no quenching. It was determined that dual-labeled albumin incorporated at 1% of the total albumin concentration would be of utility. Microspheres were fabricated at 40 µm, 60 µm, and 80 µm for each PLGA molecular weight.

Standard curves were established using 500 mM pH buffers. Confocal micrographs of microspheres soaked in pH buffer for 12 hours are shown in Figure 2.3. Standard curves for each set of microspheres are shown by PLGA molecular weight in Figures 2.4 – 2.6. Notice that there are two curves present for each set. To map pH from neutral to acidic, the natural pH sensitivity of fluorescein was used over the pH 4 to 7 range, and FRET was used from pH 1.5 to 4. The excitation and emission wavelengths for each are given in section 2.4.1. The two curves do overlap in intensity readings, but the values are exclusive to the technique employed. In theory, when the pH reaches 4, further analysis would be performed using FRET. The standard curves

for 11 kDa PLGA are skewed, making them difficult to use over the full pH range. However, the curves are much cleaner for the 25 kDa and 48 kDa PLGA. Note also that the 80 μm microspheres allow the best incremental change in FRET intensity versus pH in the 25 kDa and 48 kDa microspheres. Because these images are taken at the center of the microsphere, the higher PLGA molecular weight and larger focus distance help minimize quenching of the energy transfer, allowing greater resolution of the FRET behavior.

In all curves, there is a distinctive drop in the FRET intensity at pH 4. This is expected due to the conformational change of albumin near pH 4. At lower pH, albumin exists in a partially unfolded form. The properly folded conformation above pH 4 puts the dyes in even closer proximity, likely leading to quenching at pH 4. Thus, pH 4 is omitted from the FRET analysis. Also, there is clear quenching in the 11 kDa microspheres, which increasingly skews the FRET curves with decreasing microsphere size. Thus, analysis would only be useful for pH 1.5 to 3. However, the extent of the gap between pH 4 and pH 3 make it difficult to determine the point at which FRET analysis should be employed. Therefore, 11 kDa PLGA microspheres can only be analyzed using the natural fluorescence of FAM, which is useful from pH 4 only to pH 6 for all microsphere diameters.

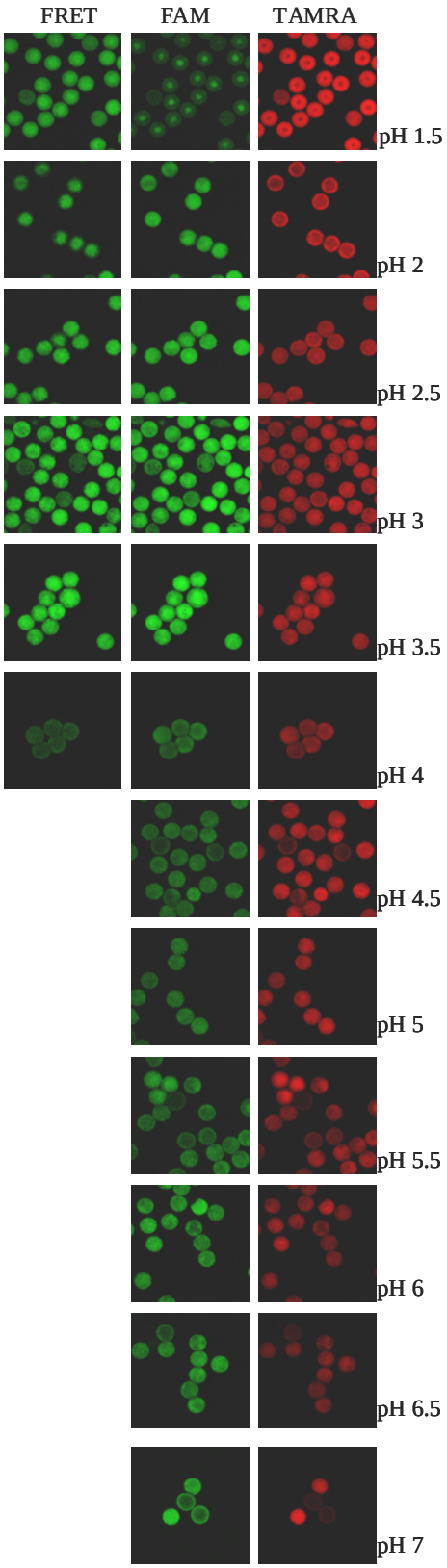

Figure 2.3. Confocal micrographs of microspheres soaked in pH buffer for 12 hours.

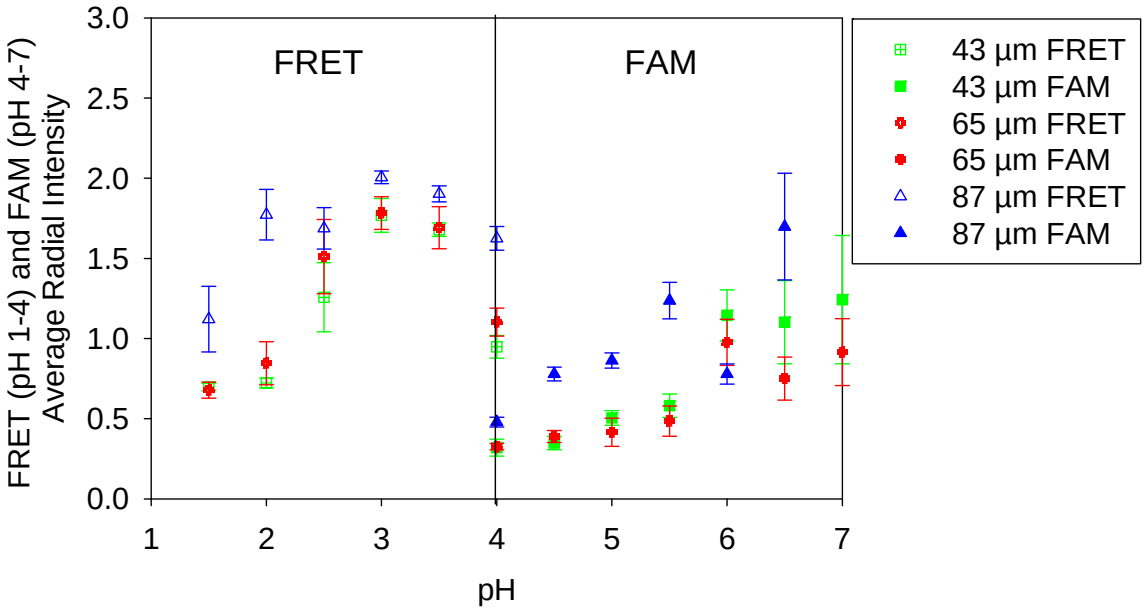

Figure 2.4. FRET (left) and FAM (right) Based Standard Curves for 11 kDa PLGA Microspheres.

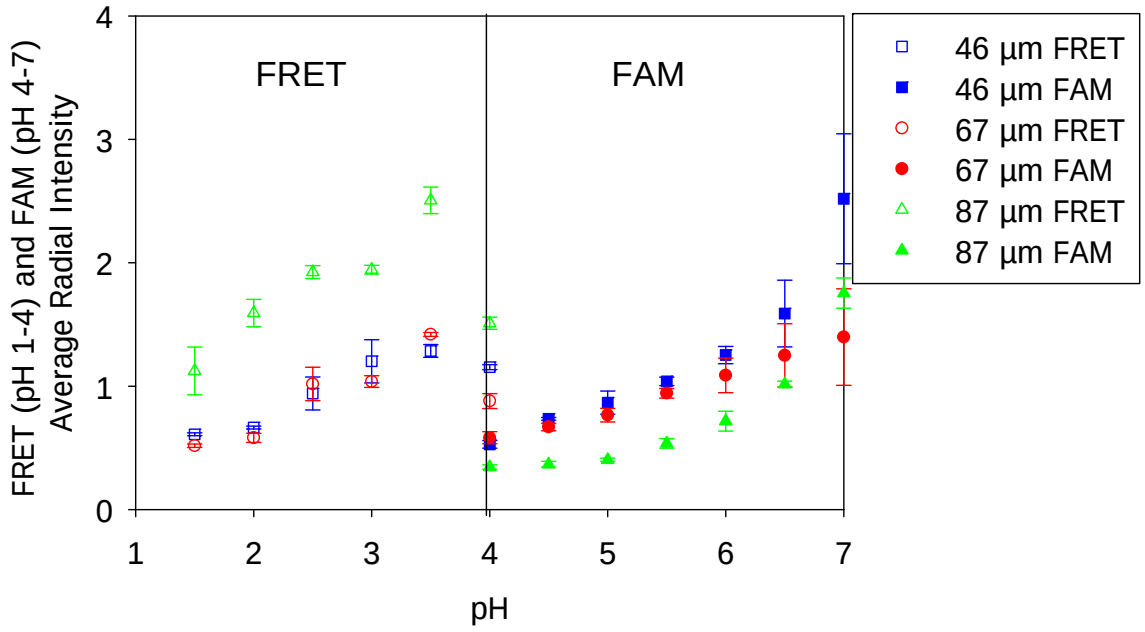

Figure 2.5. FRET (left) and FAM (right) Based Standard Curves for 25 kDa PLGA Microspheres.

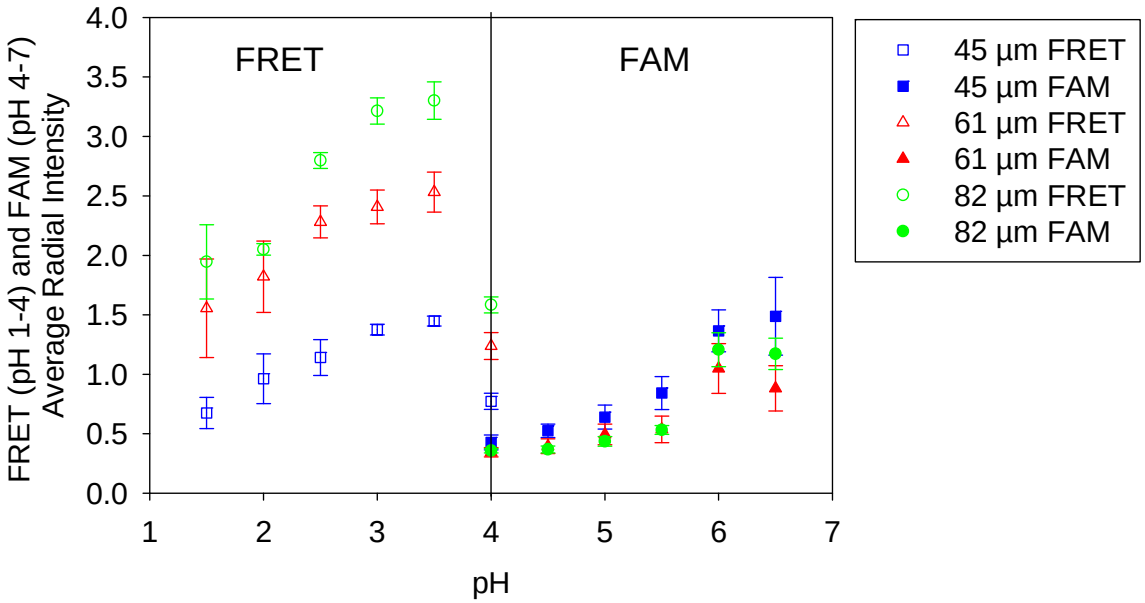

Figure 2.6. FRET (left) and FAM (right) Based Standard Curves for 48 kDa PLGA Microspheres.

2.4.3 pH Mapping

Figure 2.8 shows confocal micrographs of microspheres over 21 days. Some change in intensity throughout the microsphere is visible, but cannot be clearly distinguished in these images. It is interesting to see the swell of the microspheres over time. The 45 µm microspheres from 48 kDa PLGA shown in Figure 2.7 exhibit a 14% increase in diameter. This swelling effect is even more pronounced in larger microspheres at lower molecular weight, with up to 62% swelling visible by day 21 in 87 µm, 11 kDa PLGA microspheres (not shown). Loss of spherical form occurs by day 21 in larger microspheres as well.

The normalized radial pH of 48 kDa PLGA microspheres incubated at various time points are shown in Figures 2.8 to 2.10. All values shown were obtained using the natural fluorescence of FAM. Values were not adjusted within the limitations of the standard curve to maintain the integrity of the curvature of the radial profiles. It should be noted that for reasons described in the next section, the data presented are not necessarily valid pH measurements. However, the data are discussed in relation to the shift of the radial distribution as opposed to actual pH values.

These data show a significant decrease in pH across the microsphere within the first 3 days of incubation. For all three sizes, the pH does not appear to fall below pH 4 during the first 21 days of incubation, making incorporation of the FRET analysis unnecessary.

The normalized radial pH of 25 kDa PLGA microspheres incubated at various time points are shown in Figures 2.11 to 2.13. As with 48 kDa PLGA microspheres, all values shown were obtained using the natural fluorescence of FAM. Values were not adjusted above the values within the limits of the standard curve to maintain the integrity of the curve. The pH behavior is similar to that observed in the 48 kDa PLGA microspheres, showing a significant decrease in the pH in the first 3 days of incubation. Again, the pH does not appear to fall below pH 4 during the first 21 days of incubation, making incorporation of the FRET analysis negligible.

Previous efforts to map the radial pH change showed the pH falling to and below pH 4 within the first 7 days for most microspheres, along with a radial decrease in the pH with decreasing radial position. [5] This low pH is expected due to the autocatalytic degradation taking place inside the microspheres. However, the pH in this data tends to reach a point of consistency between pH 4 and 5, dropping to pH 4, then rising to pH 5 and holding in neutral pH ranges thereafter. It is possible that the pH genuinely does not reach the levels of acidity previously observed, given the level of surface porosity in these microspheres, as shown in Figure 2.14. Ding et al. showed in a similar study that the pH was maintained around 5 during the first month of incubation in porous microspheres [4]. Transport limitations are minimized by the increased porosity, and acidic byproducts are able to diffuse quickly out of the microsphere, allowing opportunity for a less acidic microenvironment. Thus, a similar effect may be experienced in the microspheres used for this study.

Though the pH is not clearly defined at the highest pH, the shape of the pH curves are of importance. For both PLGA molecular weights, variations in the shape of the pH curve from the center to the edge of the microsphere become less distinguishable with increasing microsphere diameter. The pH becomes more consistent across the diameter of the microsphere in microspheres above 40 μm in size. This phenomenon is inconsistent with the previous study involving less porous microspheres, which showed the radial pH drop is faster with larger

microspheres, with the radial pH clearly falling below pH 4 as early as day 3 in the 87 μm microspheres [5].

It is also interesting to see the pH change that occurs at day 21. For all microspheres, the pH increases from the lowest pH at day 14. In 40 μm microspheres, the increase in pH is significant compared with the increase in 60 μm and 80 μm microspheres. GPC studies have shown a roughly 20% decrease in PLGA molecular weight at day 14, 21, or both [6-7]. This increase in pH at day 21 is further confirmation of a burst release from the microspheres around this time due to bulk erosion.

Figures 2.15 to 2.17 show the radial pH in 11 kDa microspheres. The trends observed at higher PLGA molecular weight are not visible with the 11 kDa microspheres. In particular, the data suggest that the 11 kDa microspheres undergo an erosive burst around day 14, but the pH drops again around day 21. This scenario could occur, given that the PLGA will continue to degrade by autocatalytic degradation. However, the extent of the drop would likely be greater in less porous microspheres for all sizes and PLGA molecular weights.

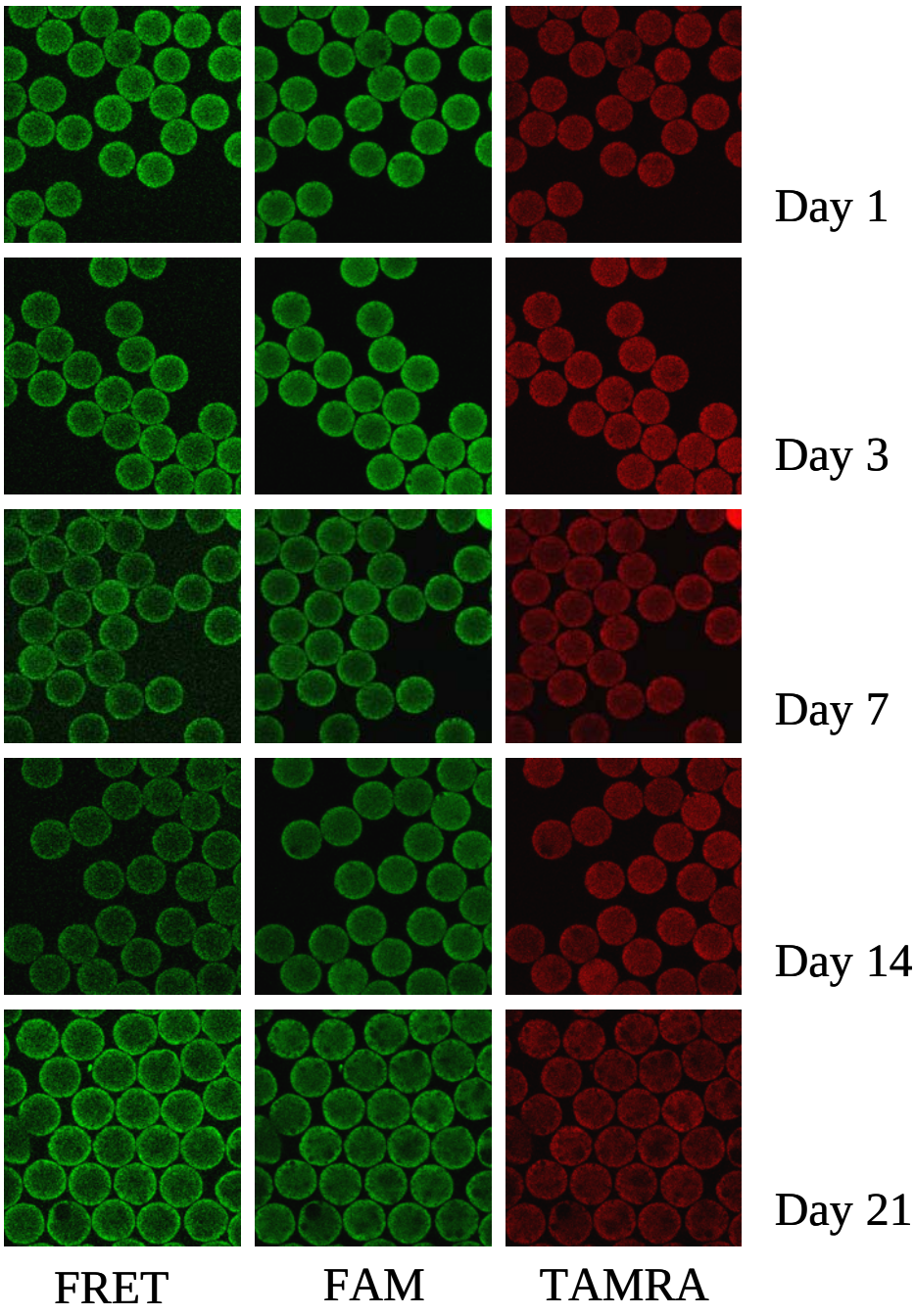

Figure 2.7. Confocal micrographs of 45 µm microspheres from 48 kDa PLGA at various times during incubation.

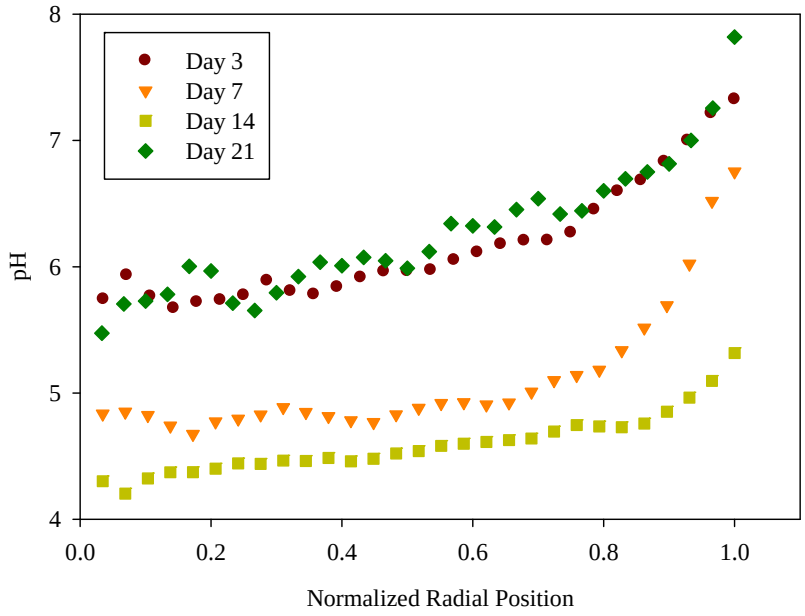

Figure 2.8. Normalized radial pH of 45 µm from 48 kDa PLGA at various times during incubation showing decrease in radial pH over time, with increasing pH at day 21.

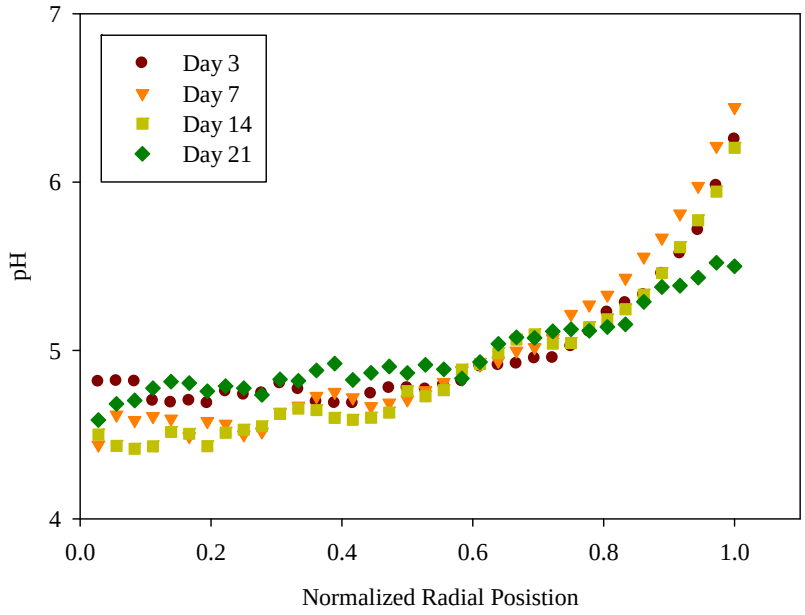

Figure 2.9. Normalized radial pH of 61 µm from 48 kDa PLGA at various times during incubation showing similar radial pH over time, with slight increase in pH at day 21.

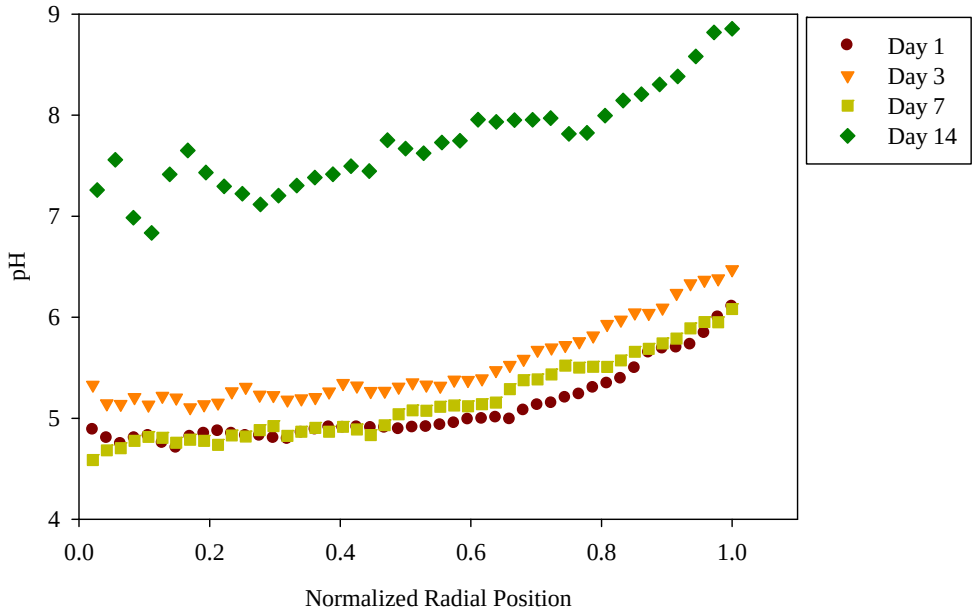

Figure 2.10. Normalized radial pH of 82 µm from 48 kDa PLGA at various times during incubation showing similar radial pH over time, with increase in pH at day 14.

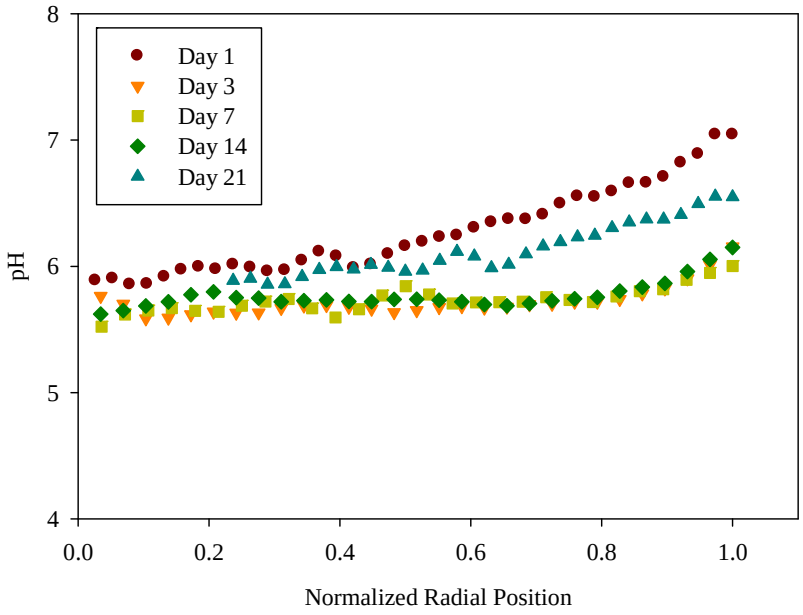

Figure 2.11. Normalized radial pH of 46 µm from 25 kDa PLGA at various times during incubation showing similar radial pH over time, with slight increase in pH at day 21.

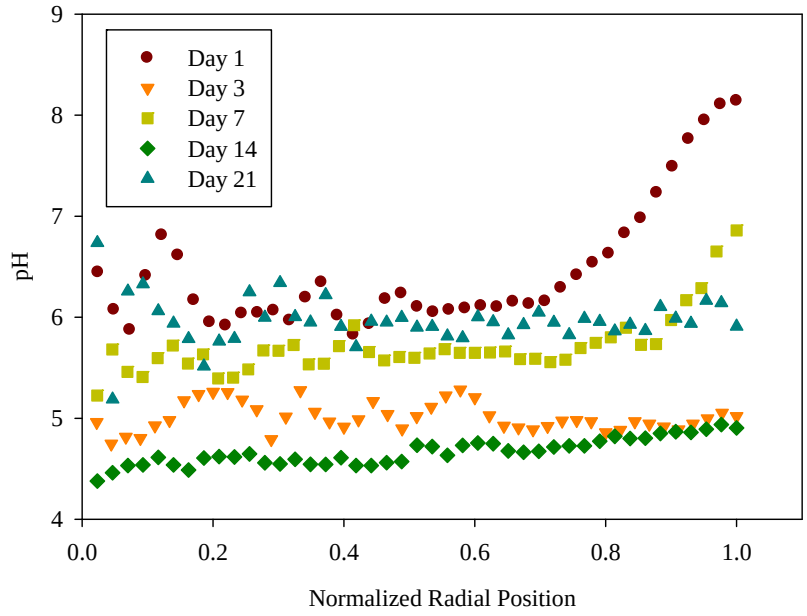

Figure 2.12. Normalized radial pH of 67 µm from 25 kDa PLGA at various times during incubation showing varied radial pH over time, with increase in pH at day 21.

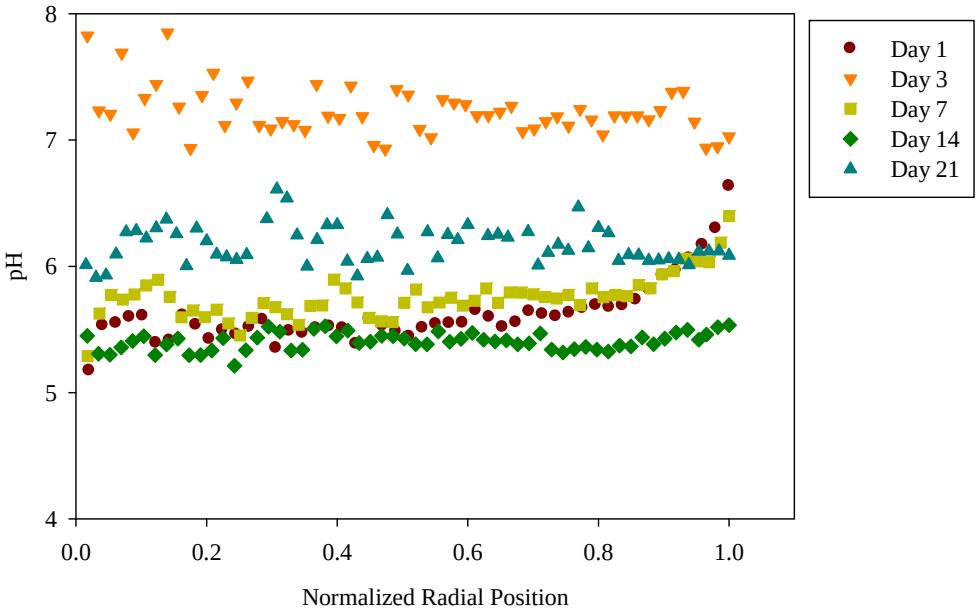

Figure 2.13. Normalized radial pH of 87 µm from 25 kDa PLGA at various times during incubation showing varied radial pH over time, with increase in pH at day 21.

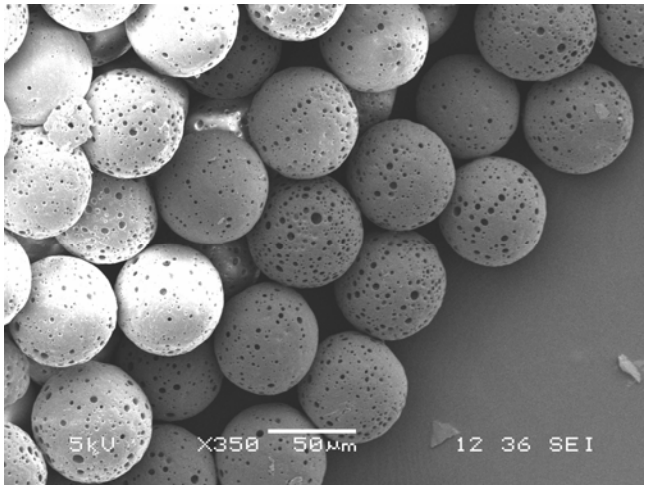

Figure 2.14. Scanning electron micrographs of 87 µm Microspheres from 48 kDa PLGA showing initial surface porosity at day 0.

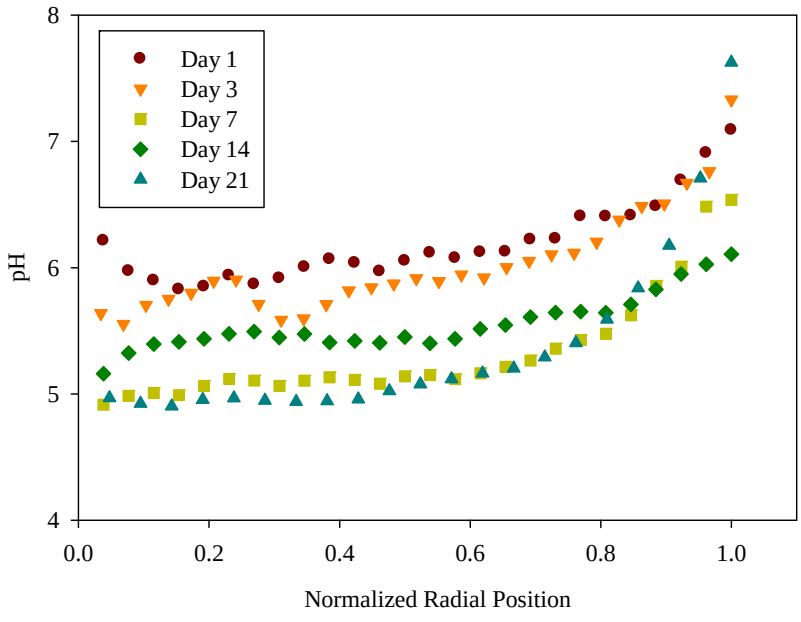

/

Figure 2.15. Normalized radial pH of 43 µm from 11 kDa PLGA at various times during incubation showing varied radial pH over time.

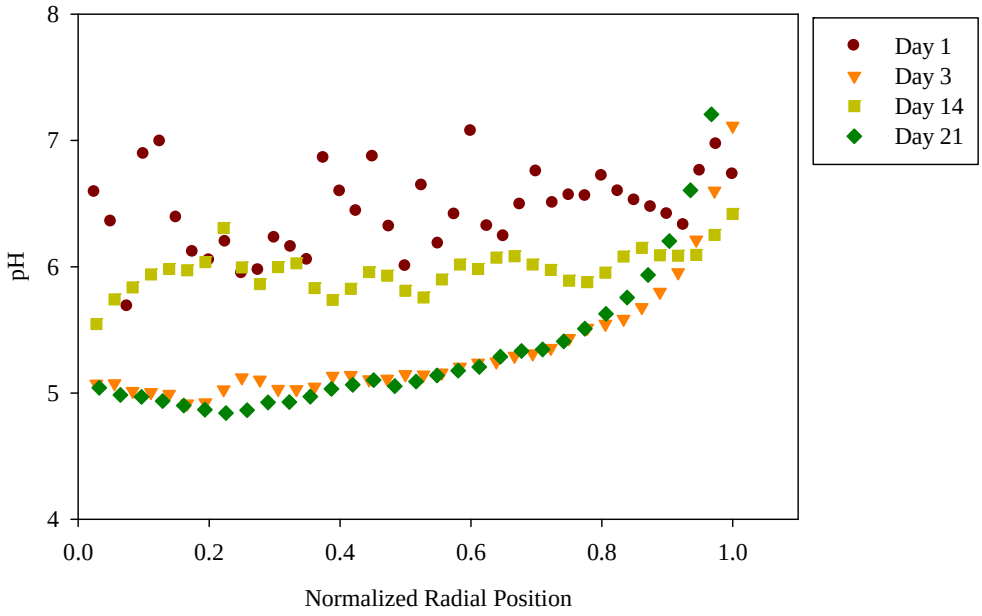

Figure 2.16. Normalized radial pH of 65 µm from 11 kDa PLGA at various times during incubation showing varied radial pH over time.

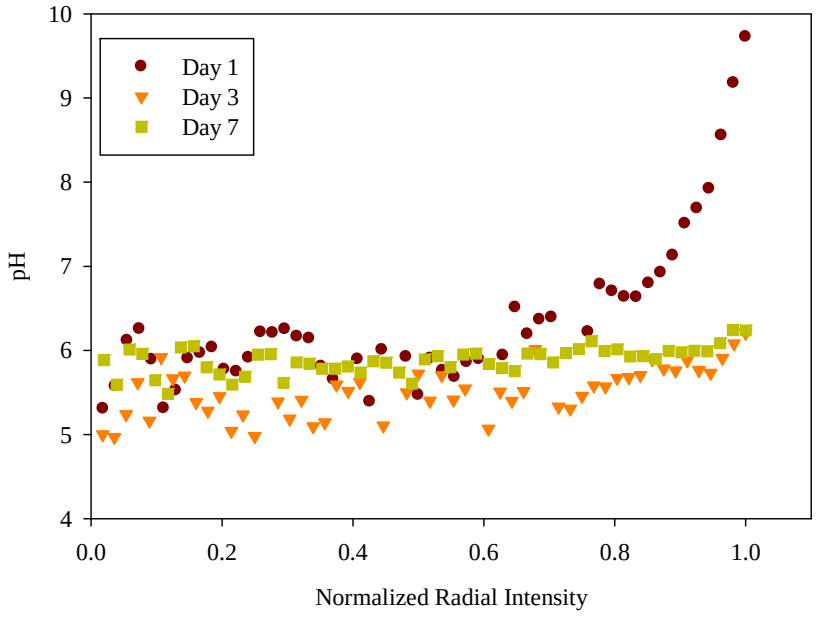

Figure 2.17. Normalized radial pH of 87 µm from 11 kDa PLGA at various times during incubation showing similar radial pH over time.

2.4.4 Study Validity

The validity of results observed using the selected dye pair is questionable. The extent of the decrease in intensity with decreasing radial position is rather shallow in most microspheres regardless of diameter or PLGA molecular weight. Additionally, given the degradation behavior of PLGA, it is highly unlikely that the pH would remain basic inside the microsphere, especially during the first two weeks of incubation.

Several factors can affect the accuracy of pH measurement in this study. Accurately measuring the intensity at the center of the microsphere and relating that intensity to the intensity observed at a particular pH inside pH buffered microspheres depends heavily on the ability of the fluorescence of the fluorophore to be fully emitted in confocal microscopy. It was mentioned that the microspheres exhibit some degree of swelling over time, up to 62%. This swelling increases the distance over which the microscope must measure the intensity of fluorescence. Thus, the data points may be skewed. It could be that where the radial pH seems to become equal across the microsphere diameter, the intensity readings are being affected by the swelling of the microspheres.

The intensity values also make determining the pH difficult. If the data were considered to be real data, particularly when the pH reaches a value of 4.5, there is no definitive way to determine if it would be best to employ FRET analysis at this point, because there is little justification for switching to FRET if there are no values across the microsphere that fall below pH 4 when using the calibration obtained from natural fluorescence.

Though the pH behavior can be explained in part by diffusion effects, another phenomenon must be taken into consideration. Given the clear instances of quenching observed in the standard curves, it is difficult to say whether the pH values obtained are real values after the first occurrence of pH 4.5. According to the data, most microspheres reach a center pH of around 4.5 by day 7. It could be that the pH is truly much lower, as shown in previous studies. However, low pH does induce a conformational change in albumin that may reduce the instance of energy transfer to the acceptor dye at more acidic pH. Thus, the intensities seen may be the full intensity

of FAM at low pH. Given that the pH sensitivity of FAM is limited to the range of pH 4 to 7, this may also explain why, in some instances, the profiles are flat.

2.5 Conclusions and Future Work

Overall, this study has shown that pH mapping inside degrading microspheres is of great importance. Between previously obtained results and the results of this study, it is clear that the pH is heavily influenced by the morphological characteristics of the degrading microsphere, including microsphere diameter and initial porosity.

The complexity and sensitivity of fluorescence resonance energy transfer make it a difficult technique for application in mapping the radial pH change in degrading PLGA microspheres. The combined effect of albumin conformation change and dye pH sensitivity leads to dye quenching with changes in pH, making pH mapping difficult to accomplish without questioning the validity of the results.

An additional factor is the standard curves themselves. Although a dual dye-conjugated protein was found that accomplished FRET for establishing standard curves, two separate curves were necessary to fully determine pH: one in the FRET region of interest, one where the natural pH sensitivity of the dye was able to provide a standard curve. Only in the higher molecular weight PLGA and larger microsphere sizes is quenching minimized to obtain a more consistent standard curve over a wider pH range. Also the unpredictable nature of the pH change inside the microsphere coupled with the unknown effects of dye quenching made determining the region where the FRET curve should be used after the pH first reached a value of 4 an inconclusive task.

FRET could still be an option for future work on mapping microsphere pH changes. However, it is extremely critical to find a system that would allow observation of pH change without the likelihood of quenching interference. This could potentially be accomplished by using a different protein that also undergoes pH-induced conformational change. Alginate may be a reasonable option, as it has the capacity for greater incremental conformation changes at varying acidic pH [8]. Alginate requires a more complex chemistry than albumin for conjugation with the

dyes, and crosslinking must be avoided. It may also be of utility to incorporate LysoSensor yellow blue from Molecular Probes, which is attached to high molecular weight dextran, to consistently measure pH down to pH 3. Since LysoSensor can only measure to pH 3, it would be a useful aid in determining the effectiveness of a modified FRET model. If the size or conformation of the encapsulated macromolecule is of interest with respect to pH changes, LysoSensor yellow blue could comprise only the pH sensitive portion of the composition.

Upon development of a sound system of measuring the pH, it would be of great interest to examine the change in pH not only with respect to PLGA molecular weight and microsphere diameter, but with varying degrees of porosity. Porosity can be tailored by varying the PLGA concentration and the PVA content in the hardening phase. This would allow coupling of porosity parameters with pH change, which is a known critical feature of PLGA degradation, erosion, and macromolecule encapsulation behavior. It would also be of interest to develop the mapping protocol such that the system of measuring pH can be used consistently between encapsulated materials, regardless of protein interactions with PLGA and ionic behaviors inside the microsphere. This could be accomplished by a more rigorous treatment of the mapping process.

2.6 References

[1] Shenderova, A., T. Burke, and S. Schwendeman. The Acidic Microclimate in Poly(lactide-co-glycolide) Microspheres Stabilizes Camptothecins. Pharmaceutical Research. 16(2):241–248, 1999.

[2] Fu, K., D. Pack, A. Klibanov, and R. Langer. Visual Evidence of Acidic Environment Within Degrading Poly(lactic-co-glycolic acid) (PLGA) Microspheres. Pharmaceutical Research, 17(1):100–106, 2000.

[3] Brunner, A., K. M¨ader, and A. G¨opferich. pH and Osmotic Pressure Inside Biodegradable Microspheres During Erosion. Pharmaceutical Research, 16(6):847– 853, 1999.

[4] Ding, A., S. Schwendeman. Acidic Microclimate pH Distribution in PLGA Microspheres Monitored by Confocal Laser Scanning Microscopy. Pharmaceutical Research, 25(9):2041- 2062, 2008.

[5] Stovall, K., Mapping pH Microenvironment Inside Degrading PLGA Microspheres. Masters Thesis. University of Illinois at Urbana-Champaign 2007.

[6] Blanco, D., M. Alonso. Protein Encapsulation and Release from Poly(lactide-co-glycolide) Microspheres: Effect of the Protein and Polymer Properties and of the Co-Encapsulation of Surfactants. European Journal of Pharmaceutics and Biopharmaceutics, 45:285-294, 1998.

[7] Raman, C. Computational and Experimental Studies of Controlled Release Drug Delivery: Effect of Microsphere Diameter and Drug Size on In-Vitro Release Kinetics. Dissertation University of Illinois at Urbana-Champaign 2005.
[8] Kong, H. C. Kim, N. Huebsch, D. Weitz, and D. Mooney. Noninvasive Probing of the Spatial Organization of Polymer Chains in Hydrogels Using Fluorescence Resonance Energy Transfer (FRET). Journal of the American Chemical Society, 129:4518-4519, 2007.

Chapter 3. Effect of Macromolecule Size on Release from PLGA Microspheres

3.1 Motivation

PLGA microspheres have been heavily investigated for use in therapeutic delivery. Research has shown that, among other factors, the PLGA composition and molecular weight as well as the diameter of the microsphere all contribute to the type of therapeutic release [1-6]. The pattern of release has also been investigated for several macromolecules and small molecules [1-2, 7-8]. Comparative studies have shown a slight effect on the release rate of drug with varying protein size at low loading concentrations [9]. However, a deeper understanding of the effect of the macromolecule itself on the type of release is still needed. Herein, focus is on the release behavior of macromolecules of different size and conformation encapsulated in microspheres of PLGA 50:50 lactide:glycolide ratio with molecular weights from 11 kDa to 48 kDa. In particular, this study compares the release behavior of bovine serum albumin (66,000 Da) and hen egg-white lysozyme (14,400 Da). These two macromolecules were chosen for their size and conformational differences. Albumin is a globular protein, whereas lysozyme is a smaller, elongated compound. This study also examines the potential differences in microsphere surface morphology and porosity after formation, and PLGA degradation with respect to each macromolecule.

3.2 Methods

3.2.1 Materials

Poly(D,L-lactide-*co*-glycolide) (PLGA) polymers of 50:50 lactide:glycolide ratio and inherent viscosities (i.v.) of 0.20, 0.41, and 0.61 dL/g, were obtained from Durect Corporation. These PLGA polymers are hereafter referred to by their relative molecular weights of 11 kDa, 25 kDa, and 48 kDa, respectively. Lyophilized bovine serum albumin was obtained from Sigma-Aldrich, and chosen for its large size (66 kDa) and globular form. Lyophilized hen egg-white lysozyme was obtained from Sigma-Aldrich, and was chosen for its elongated form and small size (14 kDa) compared with albumin. Tween 80 was obtained from Fisher Scientific, and used as a surfactant during release studies. Phosphate buffered saline tablets were obtained from MP Biomedicals, and dissolved in milli-Q water. Poly(vinyl alcohol) (PVA), 88% hydrolyzed, was

obtained from Polysciences, dissolved in Milli-Q water, and diluted to the specified concentrations. Reagent grade dichloromethane (DCM) and HPLC grade chloroform were obtained from Fisher Scientific.

3.2.2 Microsphere Fabrication and Sizing

Uniform microspheres of roughly 40 µm, 60 µm, and 80 µm diameter were fabricated using the precision fabrication technique described in chapter 1. In short, PLGA was dissolved in DCM at 10 % (w/v). Lysozyme or albumin was dissolved in milli-Q water. The amount of water used was maintained at a 1:10 (H_2O : DCM) ratio. Lysozyme and albumin concentrations were selected to provide 10 % (w/w) loading of the PLGA. The PLGA and macromolecule solutions were emulsified by sonication on ice at 60% amplitude for 1 minute, and fed into the precision fabricator. Carrier phase and emulsion phase flow rates, and frequency and amplitude of vibration were selected to produce the desired microsphere size.

Microspheres were collected in 1% PVA solution, and allowed to harden under stirring for three hours at room temperature. Microspheres were subsequently washed with three aliquots of milli-Q water, then frozen and lyophilized for 48 hours prior to use. Lyophilized microspheres were stored at -20ºC under desiccant. Microspheres were sized using a Beckman-Coulter Multi-Sizer III, with a minimum count of 10,000 microspheres. Microsphere diameters are reported as the mean diameter, and include the standard deviation and R_{90}, which is the ratio of the largest to smallest microsphere diameters within the 10% outer limits of measurement.

3.2.3 Macromolecule Loading

For each set of microspheres, approximately 5 mg of microspheres were dissolved in 100 µL of DMSO. Twenty microliters of the dissolved PLGA and macromolecule solution were pipetted into 1 mL of PBS while vortexing. Samples were then incubated at 37ºC for 1 hour with agitation, then centrifuged at 10000 rpm for 10 minutes to pellet the polymer. The supernatant was removed and replaced with 1 mL of fresh PBS while vortexing. The samples were then incubated for an additional 30 minutes at 37ºC. The concentration of protein in the supernatant was determined for both supernatants using BCA assay, then summed per set of microspheres.

The encapsulation efficiency or loading is reported as the measured concentration of macromolecule as a percent of theoretical loading during encapsulation.

3.2.4 In-Vitro Macromolecule Release and PLGA Degradation Studies

Microspheres were subjected to protein release and PLGA degradation using the protocol given in chapter 2. Briefly, 10 mg of microspheres were suspended in 1.25 mL of PBS with 0.05% Tween 80 (pH 7.2 ± 0.05), and incubated at 37ºC with agitation. One mL of supernatant was extracted at various time points, and replaced with fresh buffer. Protein concentration in supernatants was determined using BCA assay.

Microsphere surface morphology and porosity changes were observed by scanning electron microscopy. Microspheres were washed with milli-Q water three times, then freeze-fractured and mounted on carbon tape, and allowed to dry. Prepped samples were sputter coated for 30 seconds at 20 mA with gold-palladium using an Emitech K-575 Sputter Coater. Scanning electron micrographs were then acquired using a JEOL 6060 LV scanning electron microscope at 5 kV accelerating voltage.

PLGA molecular weight changes were monitored using gel permeation chromatography. Briefly, samples were washed with milli-Q water three times to remove PBS salt residue, then frozen and lyophilized. Lyophilized samples were dissolved in HPLC grade chloroform at 0.1 g/mL, and then filtered using a 0.45 µm filter. Samples were then analyzed using a Waters 1515 Isocratic HPLC Pump in conjunction with a Waters 717Plus Autosampler and Waters 2414 Refractive Index Detector. Three Waters Styragel columns HR 3, HR 4, and HR 4E were used to separate the molecular weights. The relative molecular weights were determined against polystyrene standards at 0.1g/mL ranging from 580 Da to 299,400 Da. Samples were injected at 40ºC with a flow of 1.0 mL/min and HPLC grade chloroform as the mobile phase. Two injections were made per sample.

3.3 Results and Discussion

3.3.1 Microsphere Fabrication and Initial Characteristics

PLGA molecular weight was determined prior to and after fabrication of macromolecule loaded microspheres. The initial molecular weight of the PLGA by intrinsic viscosity based on information provided by the manufacturer and from in-lab GPC is shown in Table 3.1. The differences in molecular weight can be attributed to the measurement technique itself. GPC results are heavily dependent on the GPC unit used, as well as the standards and solvent used. Thus all GPC data are relative, and the PLGA molecular weight values presented herein are based on the values obtained from in-lab GPC. PLGA molecular weight was not affected by the fabrication process.

Table 3.1. PLGA Molecular Weight Prior to Macromolecule Encapsulation

PLGA Intrinsic Viscosity	Durect® Molecular Weight	In-lab Molecular Weight
0.20 dL/g	10 kDa	11 kDa
0.41 dL/g	33.9 kDa	25 kDa
0.61 dL/g	56.7 kDa	48 kDa

Lysozyme and albumin microspheres were fabricated according to the previously described precision fabrication protocol. The size distributions of microspheres are shown in Figures 3.1 and 3.2 for lysozyme and albumin, respectively. The size distributions and encapsulation efficiency of lysozyme and albumin are shown in Tables 3.2 and 3.3, respectively. No clear trend in encapsulation efficiency by particle size or PLGA molecular weight is observable. However, the encapsulation efficiency of albumin is 9% higher on average than lysozyme. The lysozyme encapsulation efficiency ranges from 51.5% to 92.3%, and is on average 75.5%. The albumin encapsulation efficiency is at the lowest 72.3% and at the highest 99.4%, with an average of 84.2%. Albumin's higher encapsulation efficiency may also be attributed to its well-known capacity to interact with PLGA to form a stabilizing film at the water-oil interface of the emulsion [10].

The internal porosity of the microspheres is shown in Figure 3. Generally, the surface appears relatively smooth and homogeneous with minor porosity at the surface regardless of PLGA molecular weight, microsphere diameter, or encapsulated macromolecule. Studies have shown that increasing the solvent extraction rate leads to higher porosity microspheres [15]. Thus, it is likely that at the chosen polymer concentration of 10%, the solvent evaporation rate is high enough to cause non-homogeneous formation of the microsphere. Thus greater porosity is observed at both the surface and inside the microspheres.

Overall, the formation of the microspheres was weakly affected by the size of the encapsulated macromolecule. Rather, the dominating effect in microsphere formation and homogeneity appears to be the solvent extraction rate. This study has suggested that the behavior of the macromolecule during the solidification phase can directly affect the encapsulation efficiency of the macromolecule, but not necessarily the formation of the microsphere itself.

Table 3.2. Lysozyme Loading and Microsphere Diameter

PLGA (MW)	Microsphere Diameter (μm) / R_{90}	Encapsulation Efficiency (%)
11 kDa	44 ± 3 / 1.1	51.5
	58 ± 6 / 1.1	86.5
	82 ± 8 / 1.8	67.6
25 kDa	43 ± 3 / 1.0	88.2
	62 ± 6 / 1.0	62.9
	80 ± 9 / 1.1	80.9
48 kDa	40 ± 4 / 1.1	92.3
	60 ± 5 / 1.1	69.9
	80 ± 8 / 1.1	79.4

Table 3.3. Albumin Loading and Microsphere Diameter

PLGA (MW)	Microsphere Diameter (μm) / R_{90}	Encapsulation Efficiency (%)
11 kDa	45 ± 3 / 1.1	99.4
	65 ± 9 / 1.3	85.1
	83 ± 7 / 2.0	74.6
25 kDa	39 ± 6 / 1.1	72.3
	63 ± 5 / 1.0	95.8
	80 ± 4 / 1.0	95.0
48 kDa	38 ± 5 / 1.1	76.7
	57 ± 6 / 1.0	77.7
	79 ± 8 / 1.0	81.0

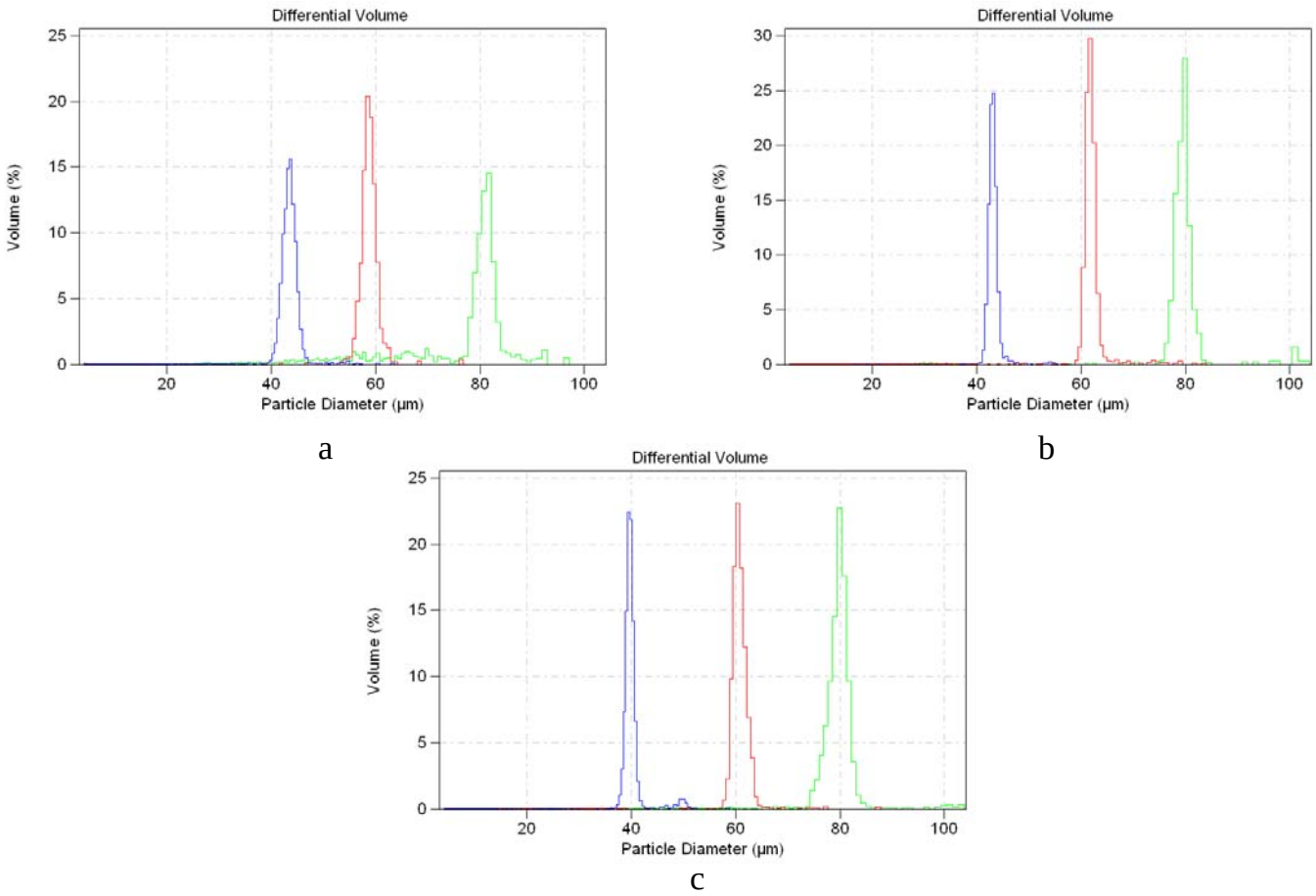

Figure 3.1. Lysozyme Microsphere Size Distributions from a) 11 kDa, b) 25 kDa, and c) 48 kDa PLGA

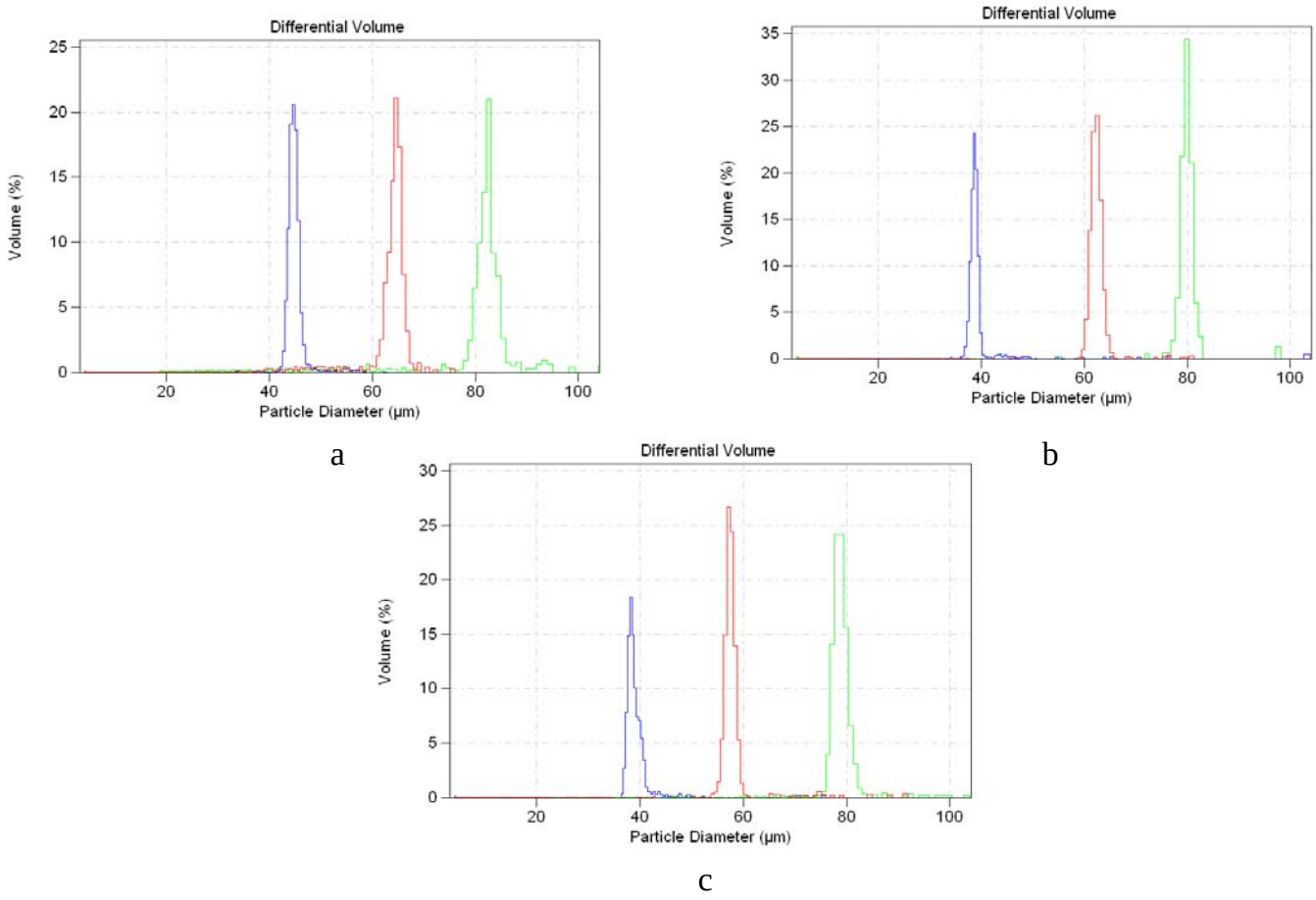

Figure 3.2. Albumin Microsphere Size Distributions from a) 11 kDa, b) 25 kDa, and c) 48 kDa PLGA

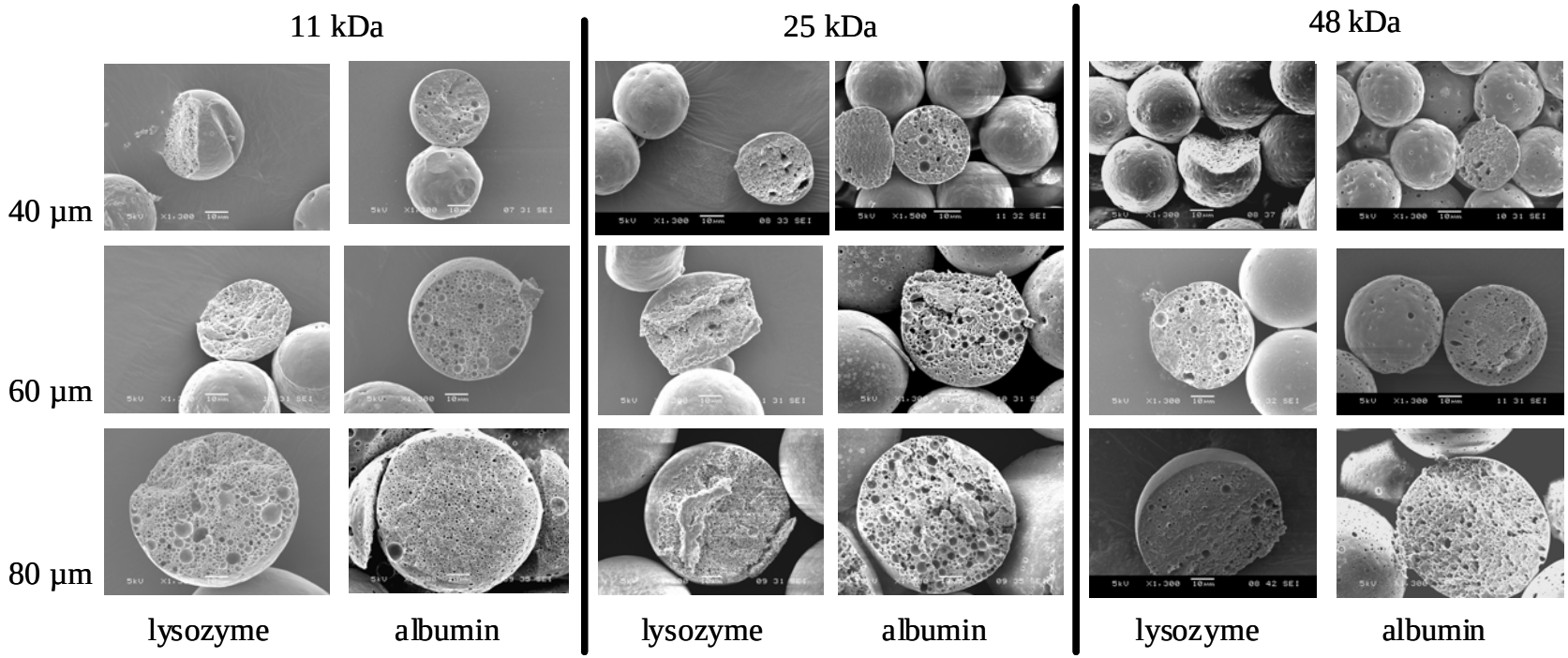

Figure 3.3. Scanning electron micrographs of lysozyme and albumin microsphere cross-sections at day 0, showing no distinctive trend in internal porosity based on encapsulated macromolecule, microsphere diameter, or PLGA molecular weight.

3.3.2 Lysozyme Release and Microsphere Surface Morphology

Figures 3.4 – 3.6 show the percent of lysozyme released over time with respect to microsphere diameter. Figures 3.7 – 3.9 show the percent of lysozyme released over time with respect to PLGA molecular weight. Eight to 23 percent lysozyme release was observed during the first seven days of incubation, with little initial burst. However, around day 14 or day 21 a noticeable increase in the percent of lysozyme released is observed for all microsphere diameters and PLGA molecular weights. As shown in Table 3.4, the percent increase in lysozyme release roughly doubles between 40 μm and 80 μm for all three molecular weights, and is slightly greater between those microspheres made using 48 kDa PLGA. This increase in release rate marks the onset of a noticeable trend in the lysozyme release profiles. Particularly, the largest microspheres exhibit a greater percentage of release than the 40 μm and 60 μm microspheres from day 14 onward. This trend becomes increasingly pronounced with increasing PLGA molecular weight. This overall trend is expected due to the combined effect of PLGA autocatalytic degradation and slowed byproduct diffusion out of larger microspheres. The larger microspheres retain the acidic byproducts produced during the degradation process. By day 14, the microspheres have eroded enough to reach the threshold pore network and pore sizes across the microsphere to allow diffusion of the degradation byproducts and available lysozyme out of the microsphere. Several studies have shown a marked 20% decrease in PLGA molecular weight around day 14 and even day 21 of incubation under similar conditions [11-12]. The SEM micrograph shown in Figure 3.10 is representative of the deformation the microspheres undergo at day 14. This deformation is an indicator of a loss of mass, i.e. erosion, inside the microspheres. In addition, it should be noted that lysozyme, which carries a positive charge, may interact with negatively charged PLGA byproduct species. This could aid its transport out of the microspheres in such large quantities at this critical point.

Table 3.4. Percent Increase in Lysozyme Release at Critical Burst

Microsphere Set	% Burst	Time of Burst
44 µm, 11 kDa	17.2	Day 21
58 µm, 11 kDa	25.0	Day 14
82 µm, 11 kDa	34.9	Day 21
43 µm, 25 kDa	16.9	Day 21
62 µm, 25 kDa	18.9	Day 14
80 µm, 25 kDa	33.2	Day 14
40 µm, 48 kDa	18.9	Day 14
60 µm, 48 kDa	31.6	Day 14
80 µm, 48 kDa	43.8	Day 14

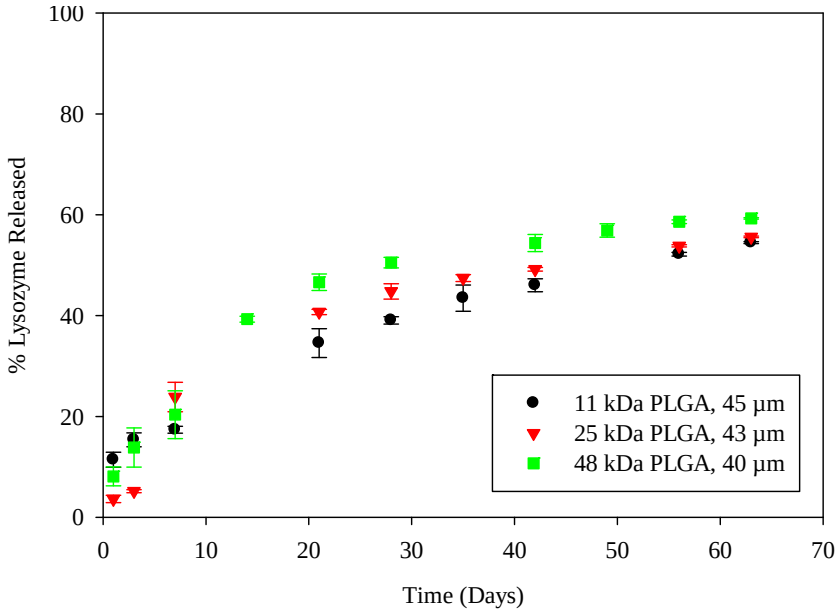

Figure 3.4. Lysozyme release from 40 µm PLGA microspheres showing fastest release from 48 kDa PLGA microspheres and distinctive burst release.

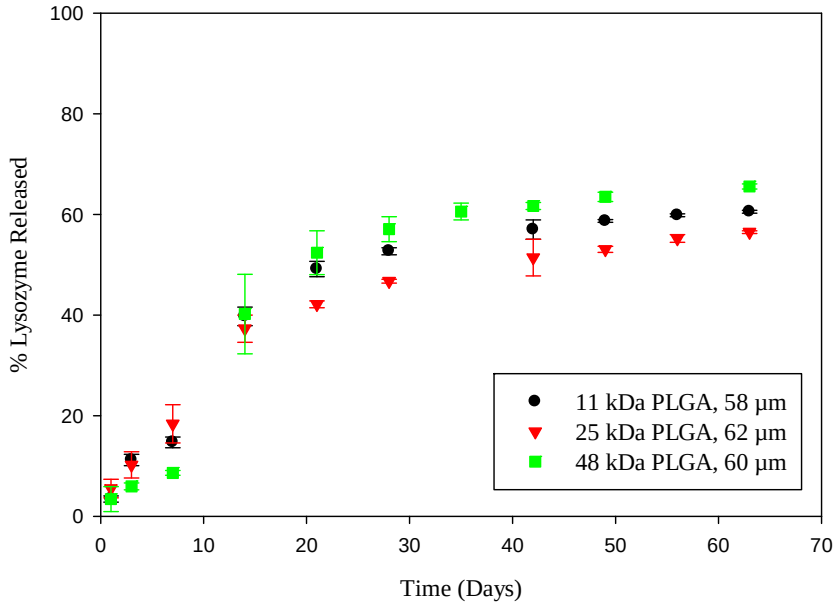

Figure 3.5. Lysozyme release from 60 µm PLGA microspheres showing fastest release from 48 kDa PLGA microspheres and distinctive burst release.

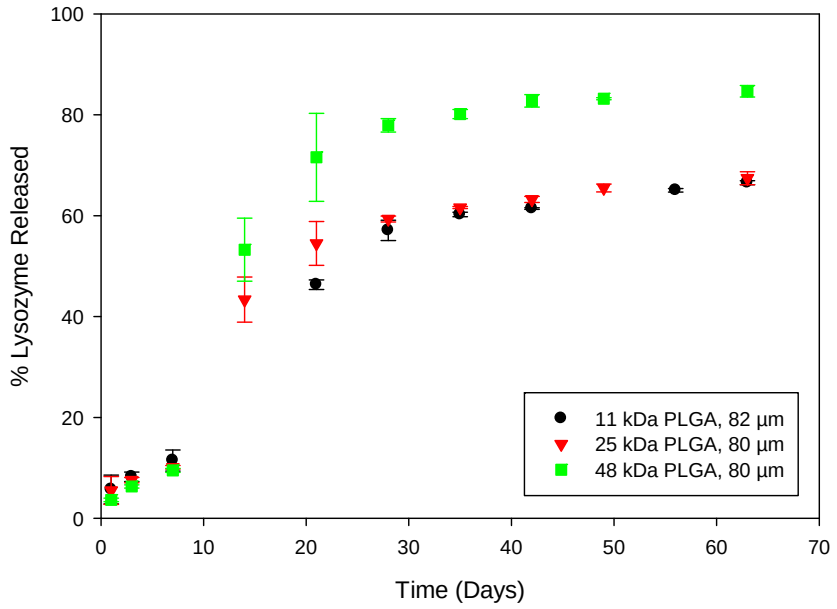

Figure 3.6. Lysozyme release from 80 µm PLGA microspheres showing fastest release from 48 kDa PLGA microspheres and distinctive burst release.

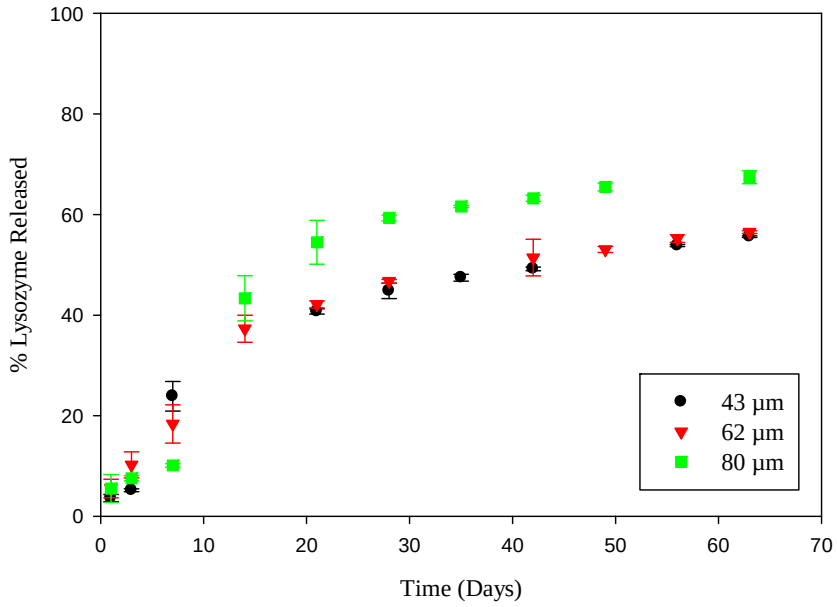

Figure 3.7. Lysozyme release from 11 kDa PLGA microspheres showing fastest release from 80 µm microspheres and distinctive burst release.

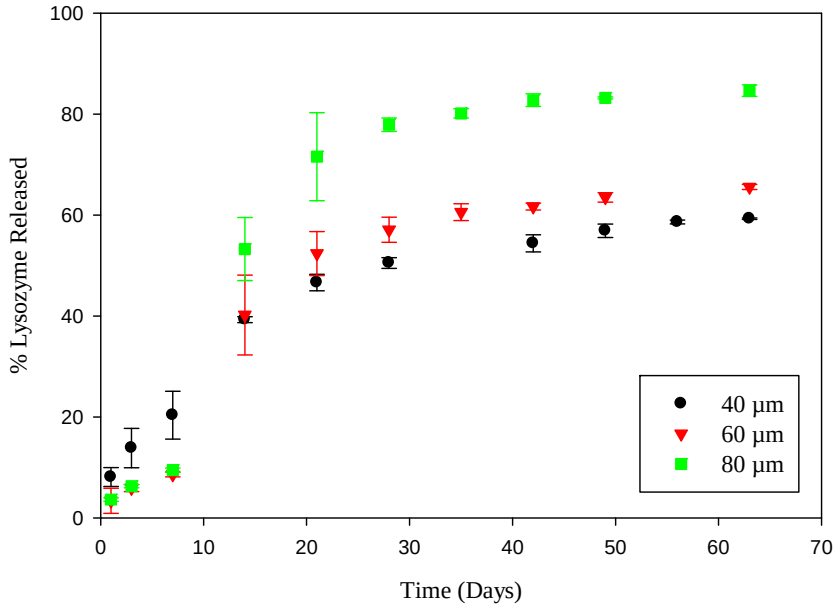

Figure 3.8. Lysozyme release from 25 kDa PLGA microspheres showing fastest release from 80 µm microspheres and distinctive burst release.

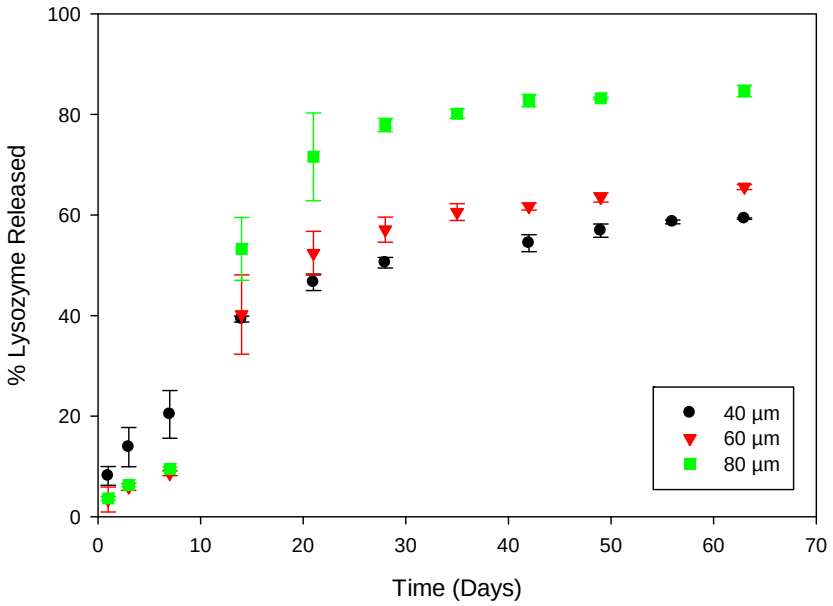

Figure 3.9. Lysozyme release from 48 kDa PLGA microspheres showing fastest release from 80 µm microspheres and distinctive burst release.

3.3.3 Albumin Release, and Microsphere Surface Morphology

Figures 3.11 – 3.13 show the percent of albumin released over time with respect to microsphere diameter. Figures 3.14 – 3.16 show the percent of albumin released over time with respect to PLGA molecular weight. Similar to lysozyme, little initial burst release is observed. However, the percentage of albumin released in the first seven days is double that of lysozyme, averaging between 16 and 40 percent. Also similar to the lysozyme release, a noticeable increase in the percent of albumin released is observed for some microspheres around day 14, and is tabulated in Table 3.5. This increase leads to a slightly higher overall percent release in the 80 µm microspheres compared with the 40 µm and 60 µm microspheres. However, the trend becomes less noticeable with increasing PLGA molecular weight, though the percent burst release shows the inverse trend of releasing more with increasing PLGA molecular weight. The increase in release that ultimately leads to the higher percent albumin released in the largest microspheres is expected, due to the same PLGA erosion and diffusion behavior that affects lysozyme release.

Table 3.5. Percent Increase in Albumin Release at Critical Burst

Microsphere Set	% Burst	Time of Burst
45 µm, 11 kDa	8.3	Day 21
65 µm, 11 kDa	9.3	Day 14
83 µm, 11 kDa	13.4	Day 21
39 µm, 25 kDa	20.0	Day 21
63 µm, 25 kDa	15.9	Day 21
80 µm, 25 kDa	7.1	Day 14
38 µm, 48 kDa	31.9	Day 21
57 µm, 48 kDa	17.7	Day 21
79 µm, 48 kDa	49.1	Day 21

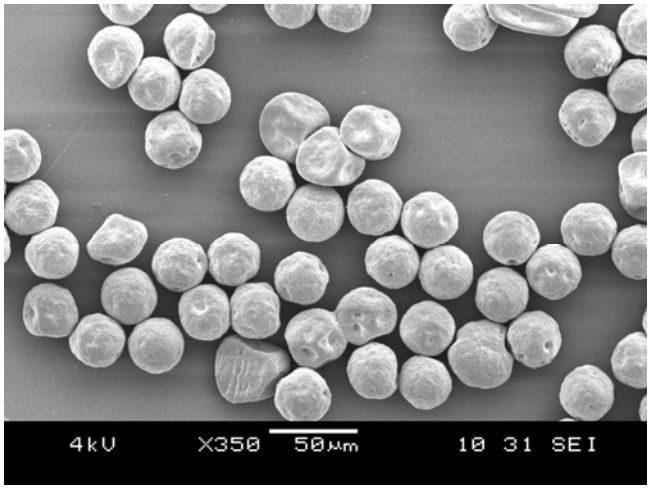

Figure 3.10. Scanning electron micrograph of day 14 39 µm, 25 kDa PLGA microspheres showing loss of spherical form.

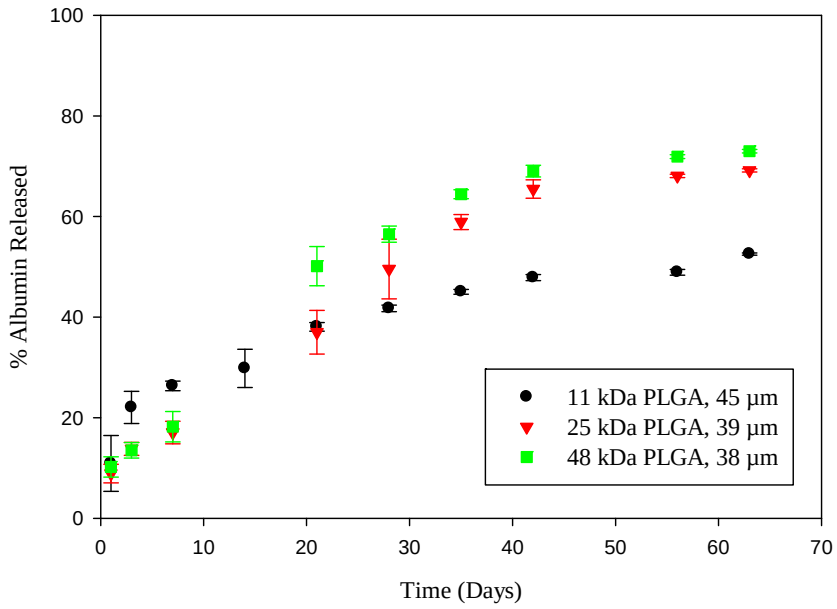

Figure 3.11. Albumin release from 40 µm PLGA microspheres showing increase in release rate of 48 kDa microspheres after distinctive burst release.

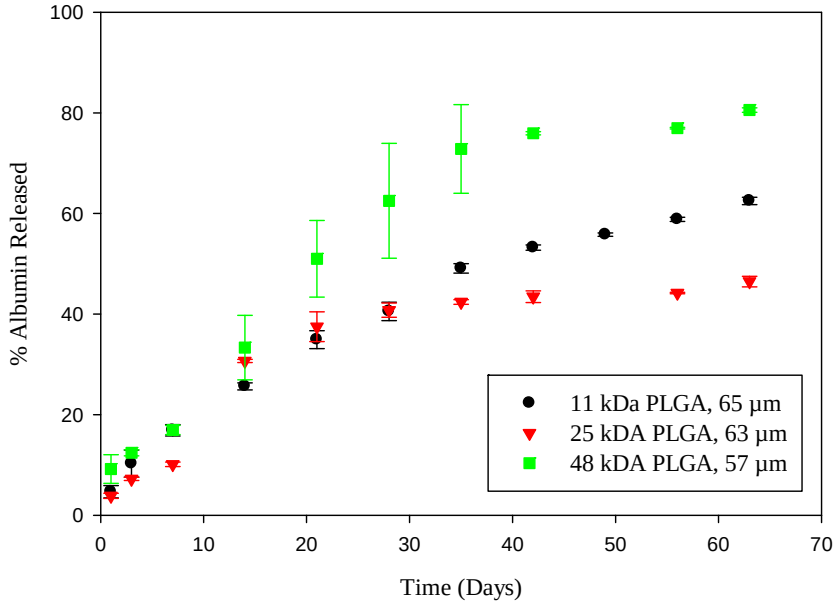

Figure 3.12. Albumin release from 60 µm PLGA microspheres showing fastest release from 48 kDa microspheres and distinctive burst release.

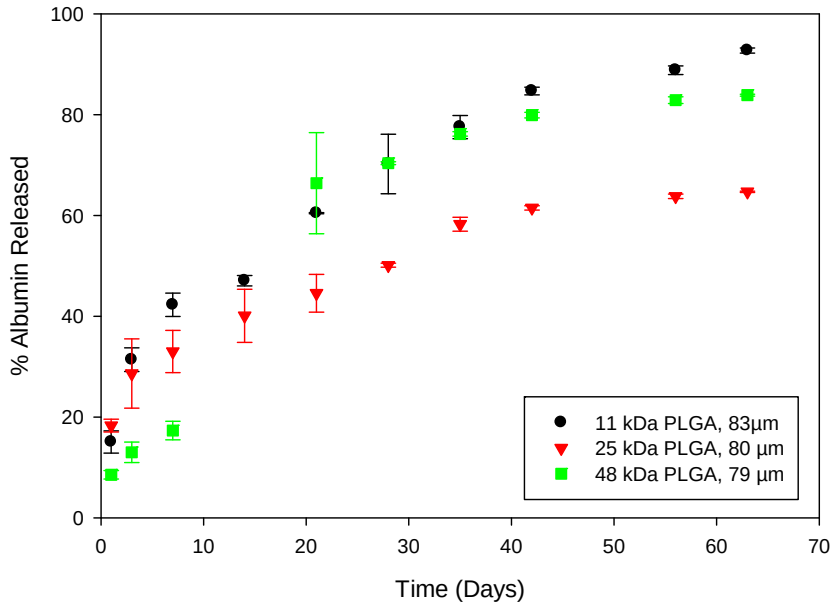

Figure 3.13. Albumin release from 80 µm PLGA microspheres showing increase in release rate of 48 kDa microspheres after distinctive burst release..

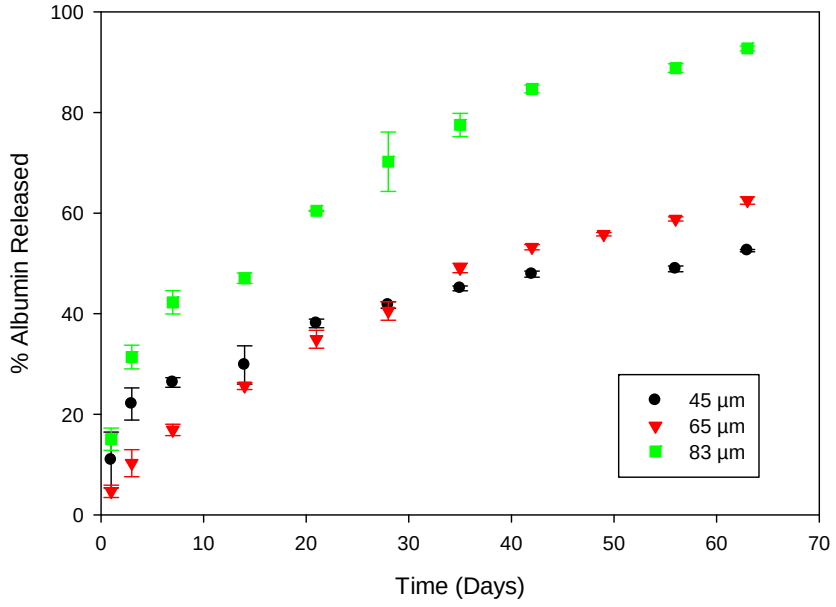

Figure 3.14. Albumin release from 11 kDa PLGA microspheres showing fastest release from 80 µm microspheres.

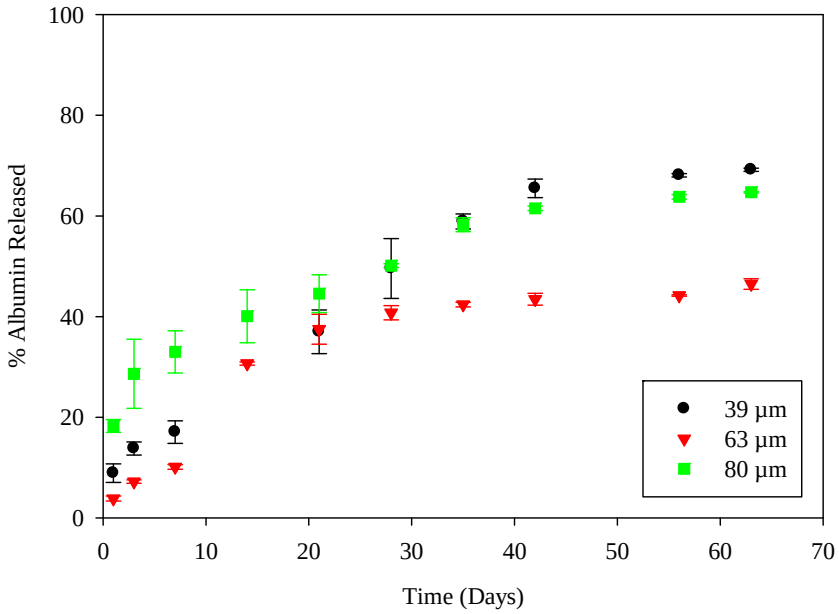

Figure 3.15. Albumin release from 25 kDa PLGA microspheres showing fastest release from 80 µm microspheres during the first 30 days.

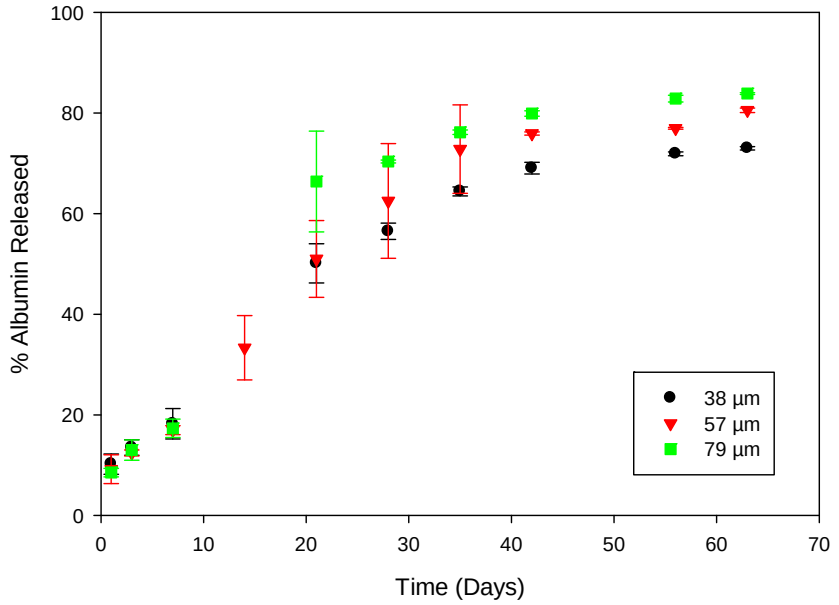

Figure 3.16. Albumin release from 48 kDa PLGA microspheres showing similar release from 60 µm and 80 µm microspheres.

3.3.4 Macromolecule Comparison

Figures 3.17 – 3.22 show lysozyme and albumin release for each microsphere diameter and PLGA molecular weight. Surprisingly in most cases, albumin exhibits a higher percent release overall compared with lysozyme. However, lysozyme shows a propensity for a higher burst release around day 14. In Table 3.6, lysozyme clearly has a higher percent burst release than albumin, with the exception of the 40 μm and 80 μm microspheres from 48 kDa PLGA and 40 μm microspheres from 25 kDa PLGA. Previous studies have shown that lysozyme tends to aggregate toward the surface of the microsphere during fabrication more than albumin [13-14]. As previously mentioned, lysozyme's interaction with PLGA may also contribute to its higher burst release around day 14. Note that the internal porosity and spherical form of the lysozyme and albumin loaded microspheres remain similar over time, as shown in Figure 3.23, alluding to the dominance of the macromolecule behavior in obtaining the release profiles observed.

Curiously, there are a series of inverse release trends observable by both microsphere diameter and PLGA molecular weight. At the lowest PLGA molecular weight, there is an increase in the distinction between the lysozyme and albumin release by microsphere diameter, where at 80 μm the albumin clearly releases at a faster rate than lysozyme. However, the inverse of this trend is observed with both the 25 kDa and 48 kDa PLGA. With respect to microsphere diameter, the behavior of the 40 μm and 60 μm microspheres is similar to that of the 11 kDa PLGA. The albumin release is 14% greater for the 25 kDa PLGA and 13% greater for the 48 kDa PLGA than lysozyme in the 40 μm microspheres, but nearly the same for both macromolecules in the 11 kDa PLGA. An even more definitive trend exists among the 60 μm microspheres, where albumin release is 10% greater for the 25 kDa PLGA and 15% greater for the 48 kDa PLGA than lysozyme. Oddly, the highest PLGA molecular weight microspheres do not continue this trend. Rather, the distinctively larger albumin release is no longer visible beginning with the 60 μm microspheres. Closer observation reveals that during the first 7 days of release, albumin releases faster than or at the same rate as lysozyme. However, the high burst that lysozyme exhibits around day 14 causes the percent release to be similar for both macromolecules. Most interestingly, lysozyme release rate decreases significantly compared with the rate of albumin release after this burst. As a result, the percentage of albumin released either equals or exceeds that of lysozyme at later time points.

The differences between lysozyme and albumin release can be explained by several factors, namely macromolecule size, aggregation, diffusion, and PLGA erosion. As mentioned previously, lysozyme has a propensity to aggregate toward the surface of the microsphere during the fabrication process. Thus, a higher percentage of lysozyme is released quickly compared with albumin. After the burst around day 14, fundamental diffusion characteristics come into play, and lysozyme appears to release more slowly because the remaining portion must diffuse from a longer distance than albumin. This is most clearly evidenced with the 40 μm microspheres and higher molecular weight PLGA, where erosion is slower, allowing such diffusion characteristics to be observed; and at the lower molecular weight PLGA, where the trend becomes increasingly pronounced with increased microsphere diameter. However, both the 25 kDa and 48 kDa PLGA exhibit this trend to a lesser degree. Instead, the rate of albumin release decreases with microsphere diameter. This is a direct result of erosion rate and diffusion characteristics, as well. The higher molecular weight PLGA erodes more slowly than the 11 kDa PLGA. In addition, the albumin must diffuse longer distances through the larger diameter microspheres. The larger diffusion distance, coupled with slower degradation and erosion cause the albumin to remain trapped inside the microsphere.

Table 3.6 Lysozyme vs. Albumin Percent Increase in Release from Burst

Lysozyme Microspheres	% Burst	Albumin Microspheres	% Burst
44 µm, 11 kDa	17.2	45 µm, 11 kDa	8.3
58 µm, 11 kDa	25.0	65 µm, 11 kDa	9..3
82 µm, 11 kDa	34.9	83 µm, 11 kDa	13.4
43 µm, 25 kDa	16.9	39 µm, 25 kDa	20.0
62 µm, 25 kDa	18.9	63 µm, 25 kDa	15.9
80 µm, 25 kDa	33.2	80 µm, 25 kDa	7.1
40 µm, 48 kDa	18.9	38 µm, 48 kDa	31.9
60 µm, 48 kDa	31.6	57 µm, 48 kDa	17.7
80 µm, 48 kDa	43.8	79 µm, 48 kDa	49.1

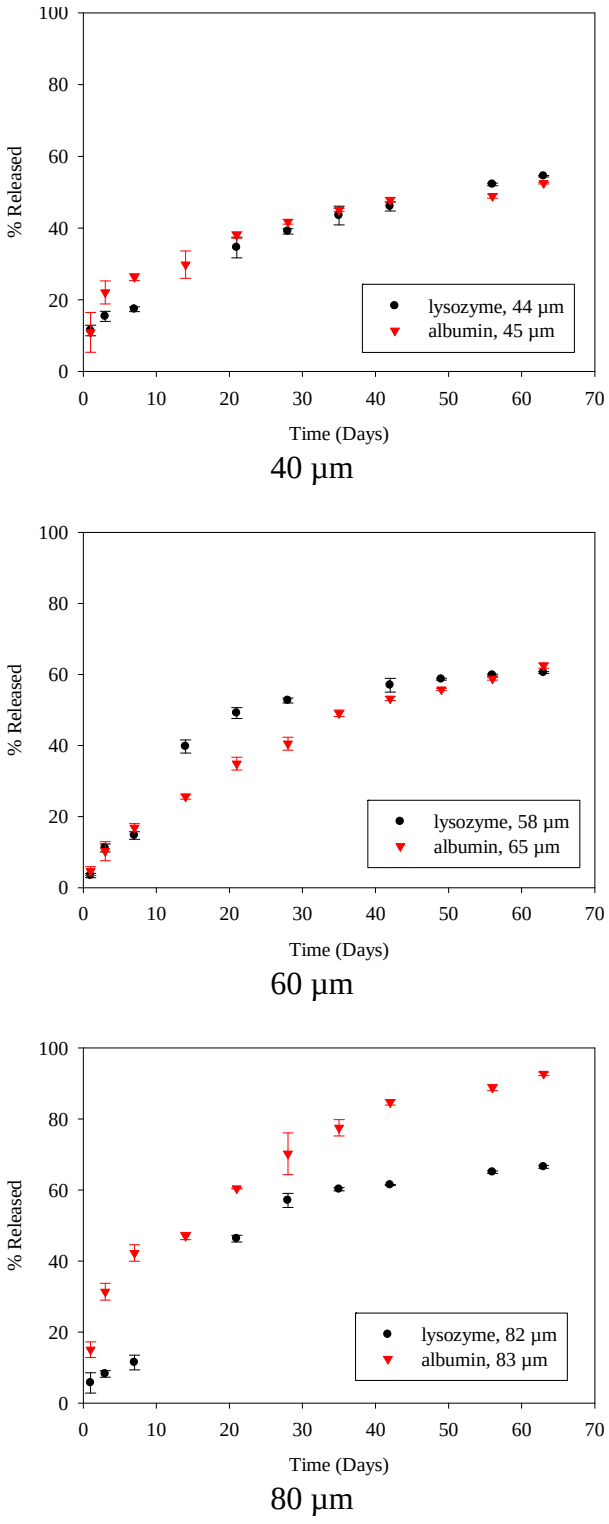

Figure 3.17. Lysozyme vs. albumin release from 11 kDa PLGA microspheres showing fastest release from 80 µm albumin-loaded microspheres.

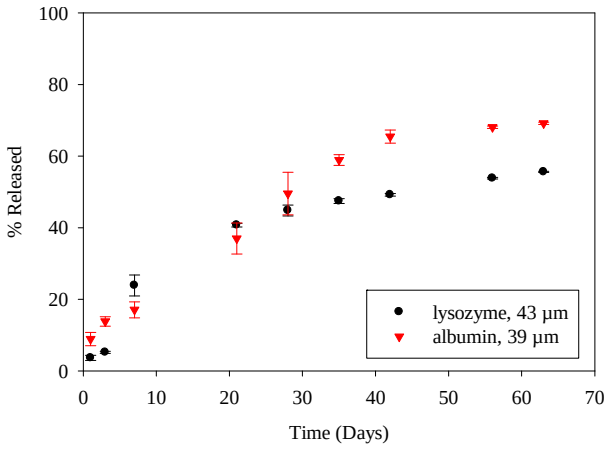

40 µm

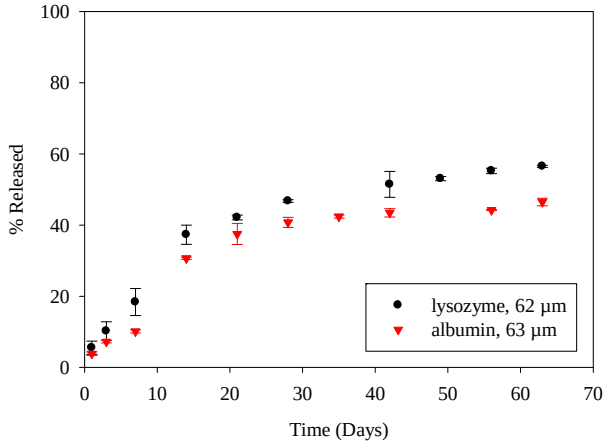

60 µm

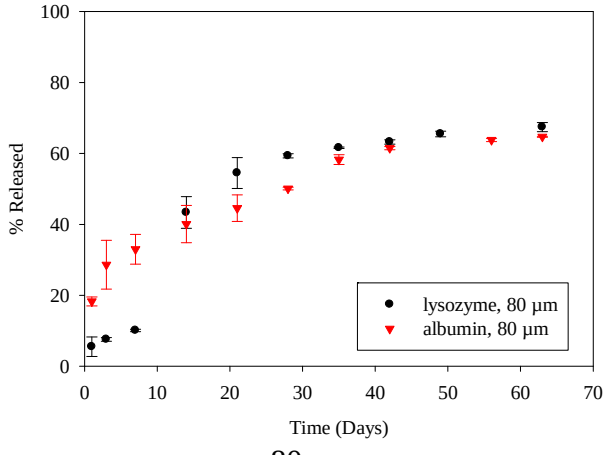

80 µm

Figure 3.18. Lysozyme vs. Albumin Release from 25 kDa PLGA microspheres showing fastest release from albumin-loaded microspheres, becoming incrementally less distinctive in 60 µm and 80 µm microspheres.

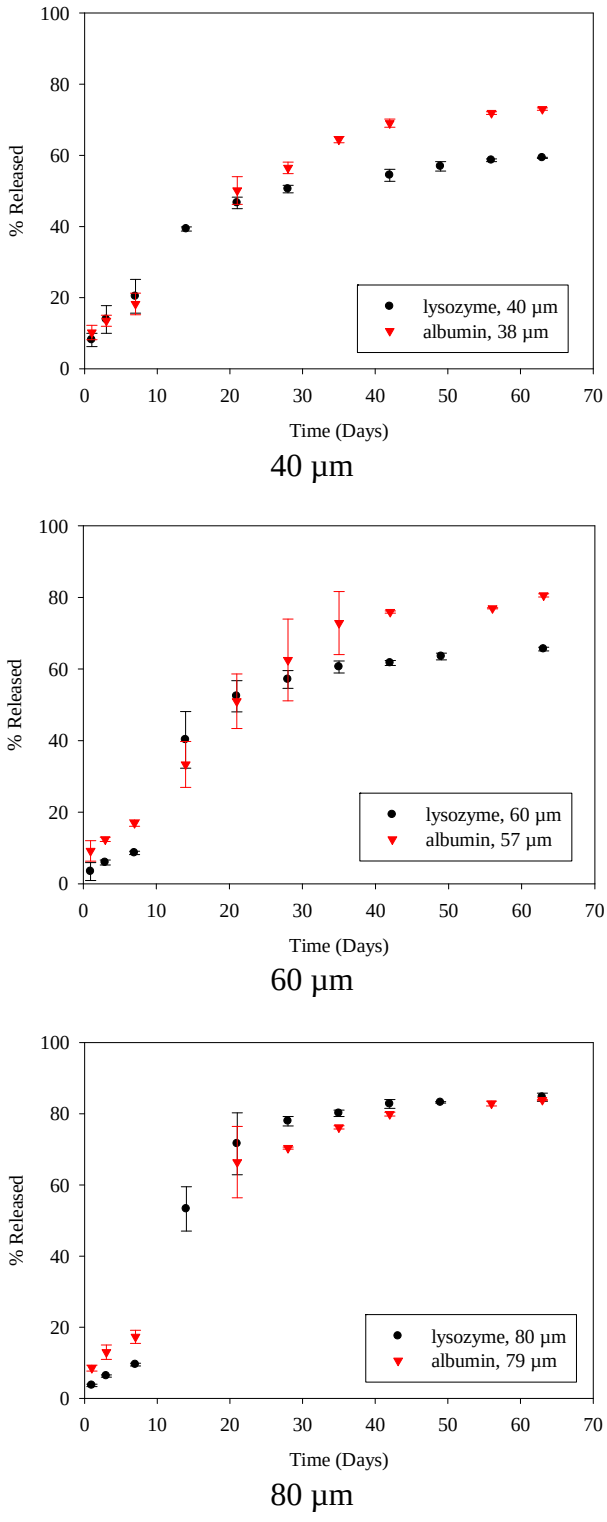

Figure 3.19. Lysozyme vs. albumin release from 48 kDa PLGA microspheres showing fastest release from albumin-loaded microsphere, with less distinctive release profiles in 80 µm microspheres.

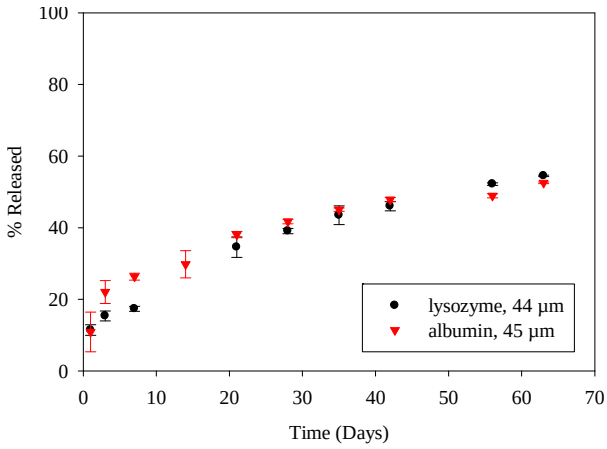

11 kDa

/

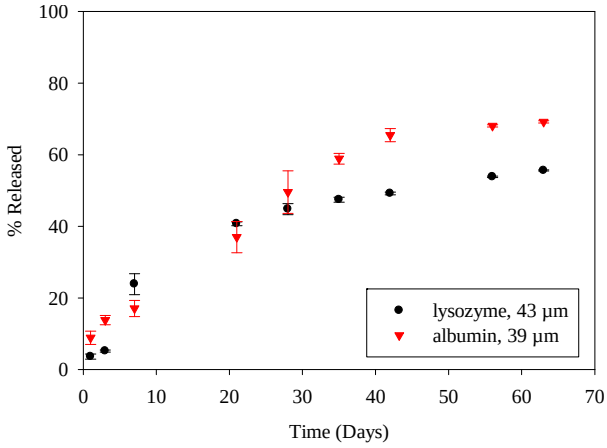

25 kDa

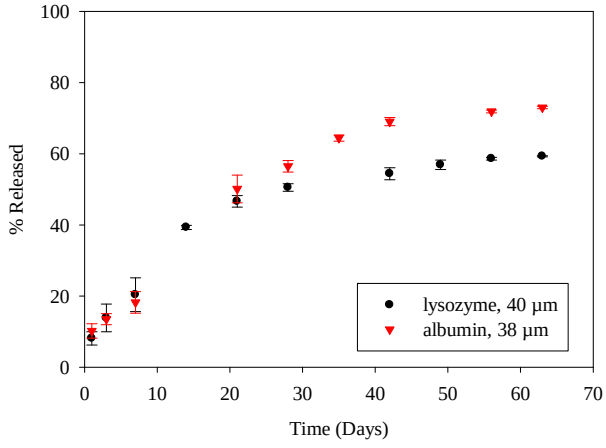

48 kDa

Figure 3.20. Lysozyme vs. albumin Release from 40 µm PLGA microspheres showing more distinctive increase in albumin release at larger PLGA molecular weight.

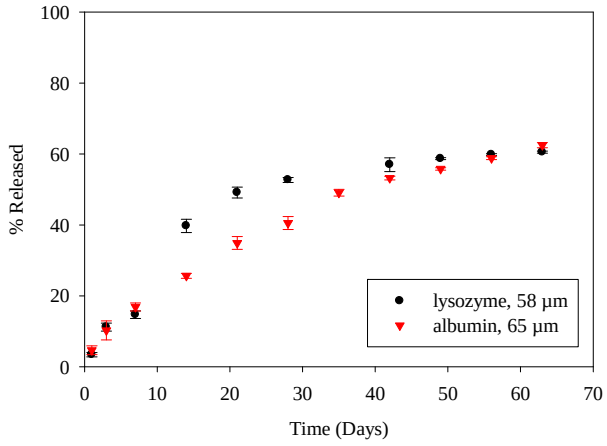

11 kDa

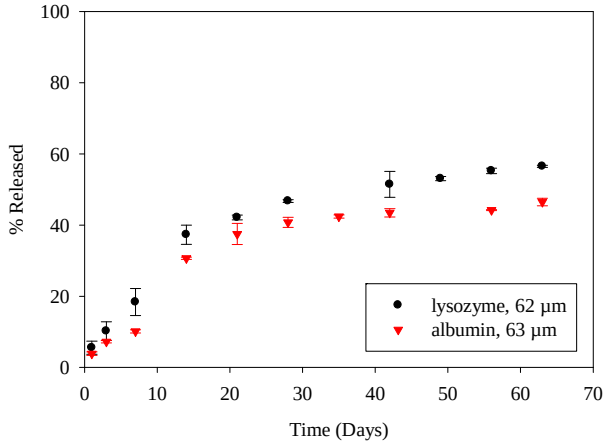

25 kDa

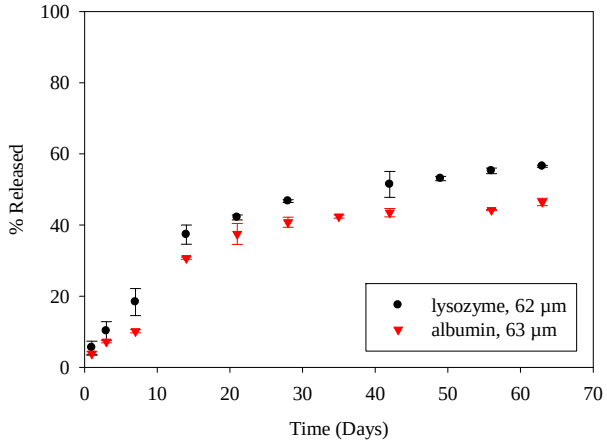

48 kDa

Figure 3.21. Lysozyme vs. albumin release from 60 µm PLGA microspheres showing more similar release profiles with increasing PLGA molecular weight.

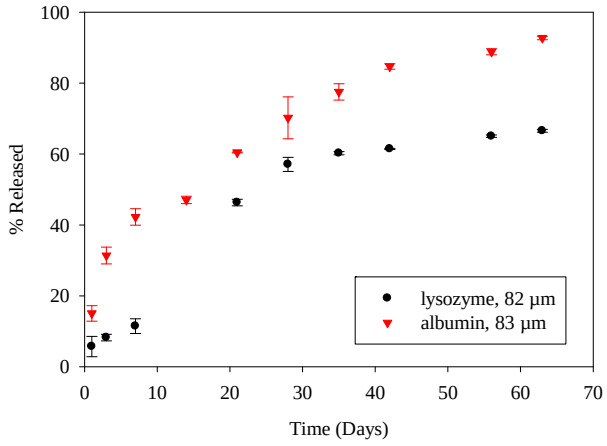

11 kDa

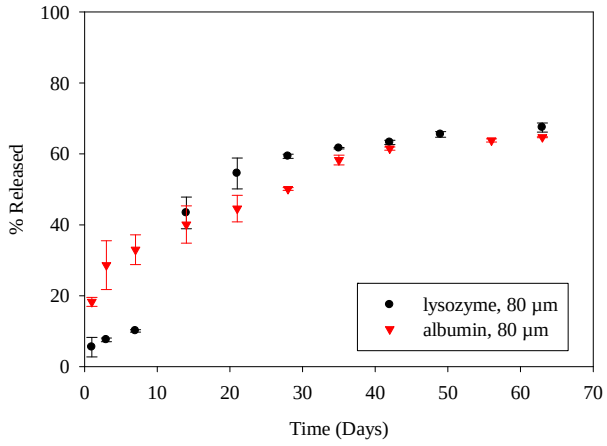

25 kDa

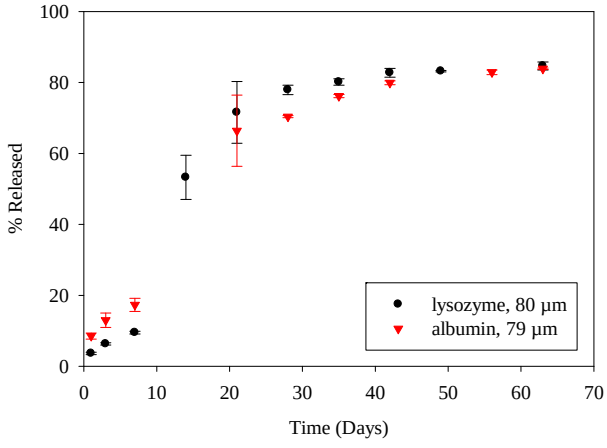

48 kDa

Figure 3.22. Lysozyme vs. albumin release from 80 µm PLGA microspheres showing more similar release profiles with increasing PLGA molecular weight.

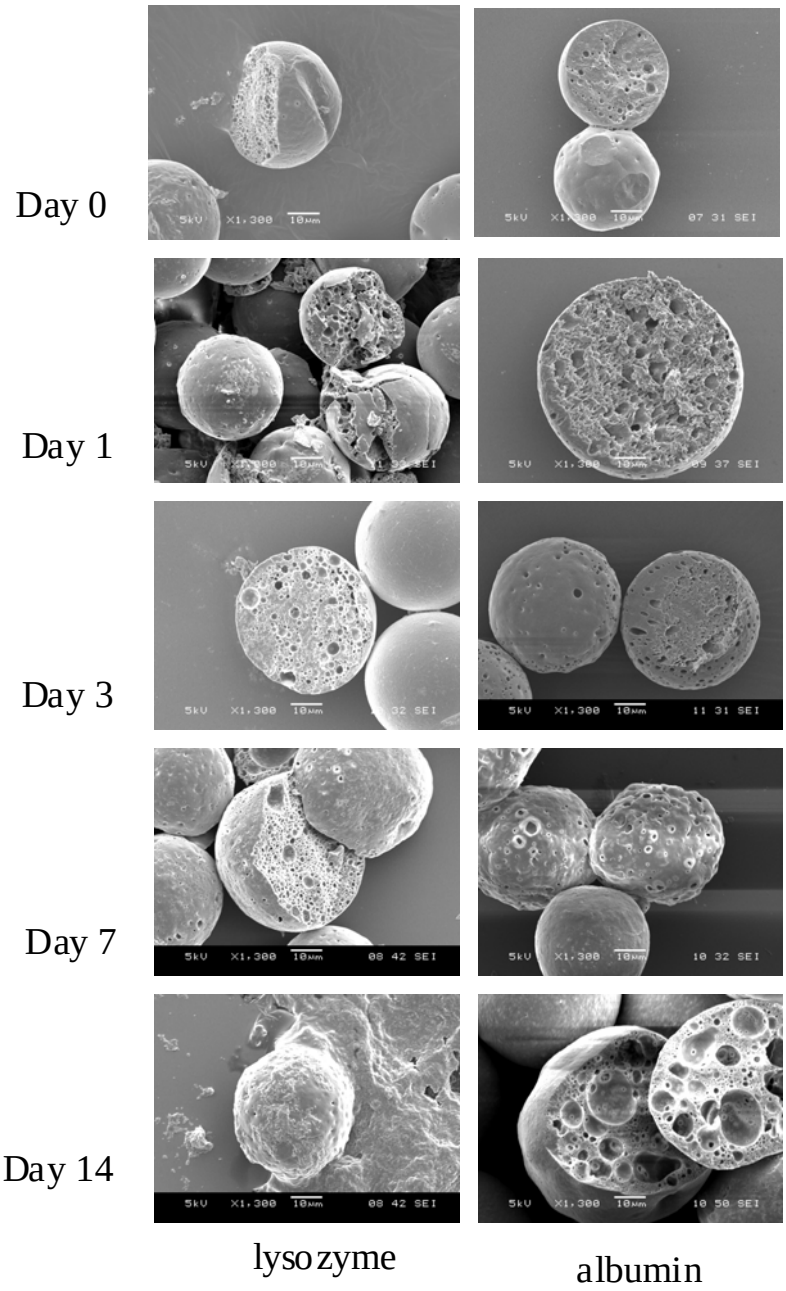

Figure 3.23. Representative scanning electron micrographs of cross-sectioned microspheres through day 14, showing similar internal porosity and spherical structure over time between lysozyme and albumin loaded microspheres.

3.4 Conclusions and Future Work

This study has explored the effect of microsphere size and PLGA molecular weight on the release properties of two macromolecules of different size, conformation, and PLGA affinity. The results of this study suggest that there may be a slight potential for characteristics of a macromolecule to influence the encapsulation and release observed from PLGA microspheres of various sizes and PLGA molecular weight. However, this study has shown that the microsphere size and PLGA molecular weight play more significant roles in determining the release rate of the macromolecule. Albumin, a larger more globular protein, exhibited higher encapsulation and faster release than lysozyme, a smaller more elongated enzyme. Albumin's propensity for both greater encapsulation and faster release are a result of its better dispersion throughout the microsphere and its ionic interaction with PLGA. The propensity of lysozyme to aggregate toward the surface of the microsphere during fabrication and its ionic attraction to PLGA leads to a larger burst release at the threshold of pore network formation. More notably, larger diameter microspheres made using higher molecular weight PLGA can reduce the extent to which the larger macromolecule release exceeds that of smaller macromolecule. It would be of great interest to know the extent to which each macromolecule aggregates during the release process, and whether the degree and time frame of acidity inside the microspheres affect the formation of aggregates with respect to the size and conformation of these molecules. Such information would provide greater insight into the behavior and stability of macromolecules inside PLGA microspheres.

3.5 References

[1] Najib, N., M. Suleiman, and A. Malakh. Characteristics of the In-Vitro Release of Ibuprofen from Polyvinylpyrrolidone Solid Dispersions. International Journal of Pharmaceutics, 32(2-3):229–236, 1986.

[2] Shukla, A., and J. Price. Effect of Drug Loading and Molecular Weight of Cellulose Acetate Propionate on the Release Characteristics of Theophylline Microspheres. Pharmaceutical Research, 8(11):1396–1400, 1991.

[3] Bezemer, J., R. Radersma, D. Grijpma, P. Dijkstra, C. van Blitterswijk, and F. Feijen. Microspheres for Protein Delivery Preprared from Amphiphilic Multiblock Copolymers 2. Journal of Controlled Release, 67(2-3):249–260, 2000.

[4] Ouellette, A., and N. Peppas. Controlled Release of Triamterene from Poly(dl-lactide-co-glycolide) Microspheres. Materials Research Society Symposium Proceedings, 331 (Biomaterials for drug and cell delivery), 91–96, 1994.

[5] Berkland, C., K. Kim, and D. Pack. Fabrication of PLGA Microspheres with Precisely Controlled and Monodisperse Size Distributions. Journal of Controlled Release, 73:59–74, 2001.
[6] Berkland, C., K. Kim, and D. Pack. PLGA Microsphere Size Controls Drug Release Rate Through Several Competing Factors. Pharmaceutical Research, 20(7):1055–1062, 2003.
[7] Blanco, D., and M. Alonso. Protein Encapsulation and Release from Poly(lactide-co-glycolide) Microspheres: Effect of the Protein and Polymer Properties and of the co-Encapsulation of Surfactants. European Journal of Pharmaceutics and Biopharmaceutics, 45:285–294, 1998.
[8] Calis, S., S. Bozdag, H. Kas, M. Tuncay, and A. Hincal. Influence of Irradiation Sterilization on poly(lactide-co-glycolide) Microspheres Containing Anti-Inflammatory drugs. Farmaco, 57(1):55–62, 2002.
[9] Sandor, M., D. Enscore, P. Weston, and E. Mathiowitz, Effect of Protein Molecular Weight on Release from Micron Sized PLGA Microspheres. Journal of Controlled Release, 76:297–311, 2001.
[10] Schugens, Ch., N. Laurelle, N. Nihant, Ch. Grandfils, R. Je´rome, Ph. Teyssie´, Effect of the Emulsion Stability on the Morphology and Porosity of Semicrystalline Poly l-lactide Microparticles Prepared by w/o/w Double Emulsion-Evaporation. Journal of Controlled Release, 32:161–176, 1994.
[11] Blanco, D., M. Alonso. Protein Encapsulation and Release from Poly(Lactide-co-glycolide) Microspheres: Effect of the Protein and Polymer Properties and of the Co-Encapsulation of Surfactants. European Journal of Pharmaceutics and Biopharmaceutics, 45:285-294, 1998.
[12] Raman, C. Computational and Experimental Studies of Controlled Release Drug Delivery: Effect of Microsphere Diameter and Drug Size on In-Vitro Release Kinetics. Dissertation University of Illinois at Urbana-Champaign, 2005.
[13] Van de Weert, M., W. Hennink, W. Jiskoot. Protein Instability in Poly(Lactic-co-Glycolic Acid) Microparticles. Pharmaceutical Research, 17(10):1159- 1167, 2000.
[14] Sah, H. Protein Instability Toward Organic Solvent/Water Emulsification: Implications for Protein Microencapsulation into Microspheres. Journal of Pharmaceutical Science and Technology, 1999.
[15] Li, W., K. Anderson, R. Mehta, P. DeLuca. Prediction of Solvent Removal Profile and Effect on Properties for Peptide-Loaded PLGA Microspheres Prepared by Solvent Extraction / Evaporation Method. Journal of Controlled Release, 37:199–214, 1995.

Chapter 4. Effect of Fabrication Technique on Microsphere Surface Morphology and Protein Release

4.1 Motivation

A range of techniques employing various fundamental principles are used to fabricate polymeric microparticles for use in drug delivery applications. Spray drying is a common technique used in industry [1-2], along with fluid-aided solvent extraction such as with homogenization. However, each technique has proven to have advantages and disadvantages. Spray drying offers rapid gas-aided solvent extraction, but typically has low particle yield. Higher particle yield is accomplished through the use of solution-aided solvent extraction. However, studies have shown that the encapsulation efficiency of water soluble compounds is typically lower with fluid-aided solvent extraction than with gas-aided solvent extraction [1, 3-5]. Equally, studies have shown the ability to control the porosity of particles in both solution and gas-aided drying [5,8]. However, the capacity of the process to produce narrow size distributions of particles with high encapsulation efficiency and high yield varies between techniques. It has been shown that the solvent extraction rate plays a significant role in the encapsulation behavior and particle formation behavior [6], and that the encapsulated compound of interest may also affect particle formation and encapsulation efficiency [6-7]. However, studies have provided little insight into the direct effect of the the mechanism of droplet disruption on particle formation and encapsulant loading. Herein, two very similar techniques that use solution-aided drying are compared to more closely examine the significance of shear-induced droplet disruption on protein encapsulation and release rates.

Though the use of spray drying would be a useful step, this study focuses on two fabrication techniques of great similarity – one being precision fabrication, the other homogenization. These techniques are separated by the direct treatment of the polymer-drug emulsion during particle formation, which will allow determination of the effect of shearing on the initial surface morphology and protein loading, and subsequent protein release and polymer erosion behavior. Future studies involving spray drying and electrospraying will incorporate the added effect of the drying process on microsphere formation.

In precision fabrication, a laminar polymer-solvent jet is disrupted by periodic acoustic waves to form droplets. Thereafter, the droplets are subjected to no further physical breakage, given that the proper stir rate during the hardening phase is used to prevent shearing. Additionally, solvent extraction at the surface of the particle is aided by the presence of the carrier phase, which provides shearing to the polymer-drug stream prior to breaking. With homogenization, however, the polymer phase is initially formed as a relatively large droplet when it is introduced to the non-solvent bath. Particles are then subjected to additional physical break up by the homogenizer. In this case, particles can be broken multiple times.

This study aims to directly observe the effect of each of these techniques on the initial surface morphology, including surface smoothness and surface and internal porosity on PLGA microspheres, as well as protein encapsulation efficiency. Subsequently, protein release and microsphere morphology changes during the degradation process are compared between the techniques.

4.2 Methods

4.2.1 Materials

Poly(D,L-lactide-*co*-glycolide) (PLGA) polymers of 50:50 lactide:glycolide ratio and inherent viscosities (i.v.) of 0.20, 0.41, and 0.61 dL/g, were obtained from Durect Corporation. These PLGA polymers are hereafter referred to by their relative molecular weights of 11 kDa, 25 kDa, and 48 kDa, respectively. Lyophilized bovine serum albumin was obtained from Sigma-Aldrich. Tween 80 was obtained from Fisher Scientific, and used as a surfactant during release studies. Phosphate buffered saline tablets were obtained from MP Biomedicals, and dissolved in milli-Q water. Poly(vinyl alcohol) (PVA), 88% hydrolyzed, was obtained from Polysciences, dissolved in Milli-Q water, and diluted to the specified concentrations. Reagent grade dichloromethane (DCM) and HPLC grade chloroform were obtained from Fisher Scientific.

4.2.2 Microsphere Fabrication

Both broadly and narrowly size-distributed microspheres were fabricated for this study using two techniques that vary dominantly in the amount of shearing that occurs at the PLGA particle surface during fabrication. PPF microspheres of roughly 40 µm diameter were fabricated using the precision fabrication technique described in chapter 1. In short, PLGA was dissolved in DCM at 10 % (w/v). Lysozyme or albumin was dissolved in milli-Q water. The amount of water used was maintained at a 1:10 (H_2O : DCM) ratio. Lysozyme and albumin concentrations were selected to provide 10 % (w/w) loading of the PLGA. The PLGA and macromolecule solutions were emulsified by sonication on ice at 60% amplitude for 1 minute, and fed into the precision fabricator. Carrier phase and emulsion phase flow rates, and frequency and amplitude of vibration were selected to produce the desired microsphere size. Microspheres were collected in 1% PVA solution, and allowed to harden under stirring for three hours. Microspheres were subsequently washed with three aliquots of milli-Q water, then frozen and lyophilized for 48 hours prior to use.

Broader distribution microspheres were prepared by homogenization. As with precision fabrication, microspheres were prepared by encapsulating bovine serum albumin at 10% loading inside PLGA microspheres, using 11 kDa, 25 kDa, and 48 kDa 50:50 PLGA. Dissolved PLGA and albumin were emulsified as previously described. The emulsion was then fed into 1% PVA using a syringe, while the bath was homogenized at a speed conducive to the production of dominantly 40 µm or 20 µm particles, depending on the batch. Microspheres were then hardened under stirring for 3 hours prior to sieving. Microspheres were sieved using Endecotts Ltd. 63 µm, 40 µm, and 20 µm Laboratory Test Seives.

Lyophilized microspheres were stored at -20ºC under desiccant. Microspheres were sized using a Beckman-Coulter Multi-Sizer III, with a minimum count of 10,000 microspheres. Microsphere diameters are reported as the mean diameter, and include the standard deviation and R_{90}, which is the ratio of the largest to smallest microsphere within the 10% outer limits of measurement.

4.2.3 Albumin Loading

For each set of microspheres, approximately 5 mg of microspheres were dissolved in 100 µL of DMSO. Twenty microliters of the dissolved PLGA and macromolecule solution were pipetted into 1 mL of PBS while vortexing. Samples were then incubated at 37ºC for 1 hour with agitation, then centrifuged at 10000 rpm for 10 minutes to pellet the polymer. The supernatant was removed and replaced with 1 mL of fresh PBS while vortexing. The samples were then incubated for an additional 30 minutes at 37ºC. The concentration of protein in the supernatant was determined for both supernatants using BCA assay, then summed per set of microspheres. The encapsulation efficiency or loading is reported as the measured concentration of macromolecule as a percent of theoretical loading during encapsulation.

4.2.4 In-Vitro Albumin Release and PLGA Degradation Studies

Microspheres were subjected to protein release and PLGA degradation using the protocol given in chapter 2. Briefly, 10 mg of microspheres were suspended in 1.25 mL of PBS with 0.05% Tween 80 (pH 7.2 ± 0.05), and incubated at 37ºC with agitation. One mL of supernatant was extracted at various time points, and replaced with fresh buffer. Protein concentration in supernatants was determined using BCA assay.

Microsphere surface morphology and porosity changes were observed by scanning electron microscopy. Microspheres were washed with milli-Q water three times, then freeze-fractured and mounted on carbon tape, and allowed to dry. Prepped samples were sputter coated for 30 seconds at 20 mA with gold-palladium using a Emitech K-575 Sputter Coater. Scanning electron micrographs were then acquired using a JEOL 6060 LV scanning electron microscope at 5 kV accelerating voltage.

PLGA molecular weight changes were monitored using gel permeation chromatography. Briefly, samples were washed with milli-Q water three times to remove PBS salt residue, then frozen and lyophilized. Lyophilized samples were dissolved in HPLC grade chloroform at 0.1 g/mL, and then filtered using a 0.45 µm filter. Samples were then analyzed using a Waters 1515 Isocratic HPLC Pump in conjunction with a Waters 717Plus Autosampler and Waters 2414 Refractive Index Detector. Three Waters Styragel columns HR 3, HR 4, and HR 4E were used to separate

the molecular weights. The relative molecular weights were determined against polystyrene standards at 0.1g/mL ranging from 580 Da to 299,400 Da. Samples were injected at 40ºC with a flow of 1.0 mL/min and HPLC grade chloroform as the mobile phase. Two injections were made per sample.

4.3 Results and Discussion

4.3.1 Microsphere Fabrication

Albumin-encapsulating PLGA microspheres were produced using both precision particle fabrication and conventional homogenization/solvent extraction as described above. Microspheres fabricated using 11 kDa, 25 kDa, and 48 kDa PLGA and of a wide size-distribution, were then sieved to 20 µm or 40 µm mean size. Precision fabricated microspheres were fabricated in the 40 µm range to compare with homogenizer microspheres. The average diameter with standard deviation and albumin loading of both the PPF and homogenizer microspheres are shown in Table 4.1. The size distributions of homogenizer microspheres are shown in Figure 4.1. The homogenizer distribution is overlaid with the distribution of PPF microspheres of comparable size and same PLGA molecular weight in Figure 4.2. As expected, the R_{90} value for the homogenizer microspheres is 2.0 and above, alluding to the broader size distribution. The precision fabricated microspheres are more uniform, with an R_{90} of 1.1 for each. The breadth of the size distributions from each technique are shown in Figure 4.3. Albumin loading is between 10% and 38% higher in microspheres of comparable size produced using precision fabrication at the highest and lowest PLGA molecular weights, but is 4% lower in microspheres using 25 kDa PLGA. The large difference in loading can be attributed to the greater instance of breakage each droplet experiences. During homogenization initially large droplets are broken into smaller particles, affording previously entrapped protein the opportunity to escape.

Table 4.1 Average Diameter of Microspheres

	Homogenizer Microspheres		PPF Microspheres	
PLGA Molecular Weight	**Diameter (μm) ± St. Dev. / R_{90}**	**Albumin Loading (%)**	**Diameter (μm) ± St. Dev. / R_{90}**	**Albumin Loading (%)**
11 kDa	43 ± 14 / 2.1	61.2	45 ± 3 / 1.1	99.4
	21 ± 7 / 2.5	81.2	---	---
25 kDa	41 ± 11 / 2.0	76.6	39 ± 6 / 1.1	72.3
	29 ± 10 / 2.5	74.3	---	---
48 kDa	45 ± 13 / 2.2	65.2	38 ± 5 / 1.1	76.7
	24 ± 7 / 2.0	65.5	---	---

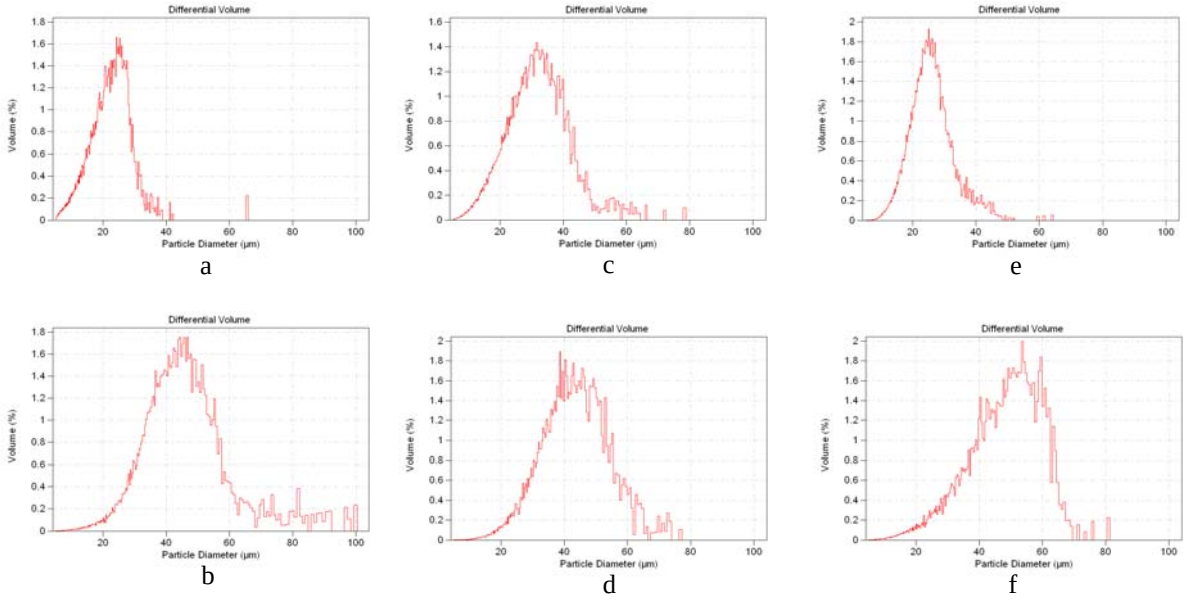

Figure 4.1. Size distribution of homogenizer microspheres. a) 21 µm, 11 kDa PLGA; b) 43 µm, 11 kDa PLGA; c) 29 µm, 25 kDa PLGA; d) 41 µm, 25 kDa PLGA; e) 24 µm, 48 kDa PLGA; f) 45 µm, 48 kDa PLGA.

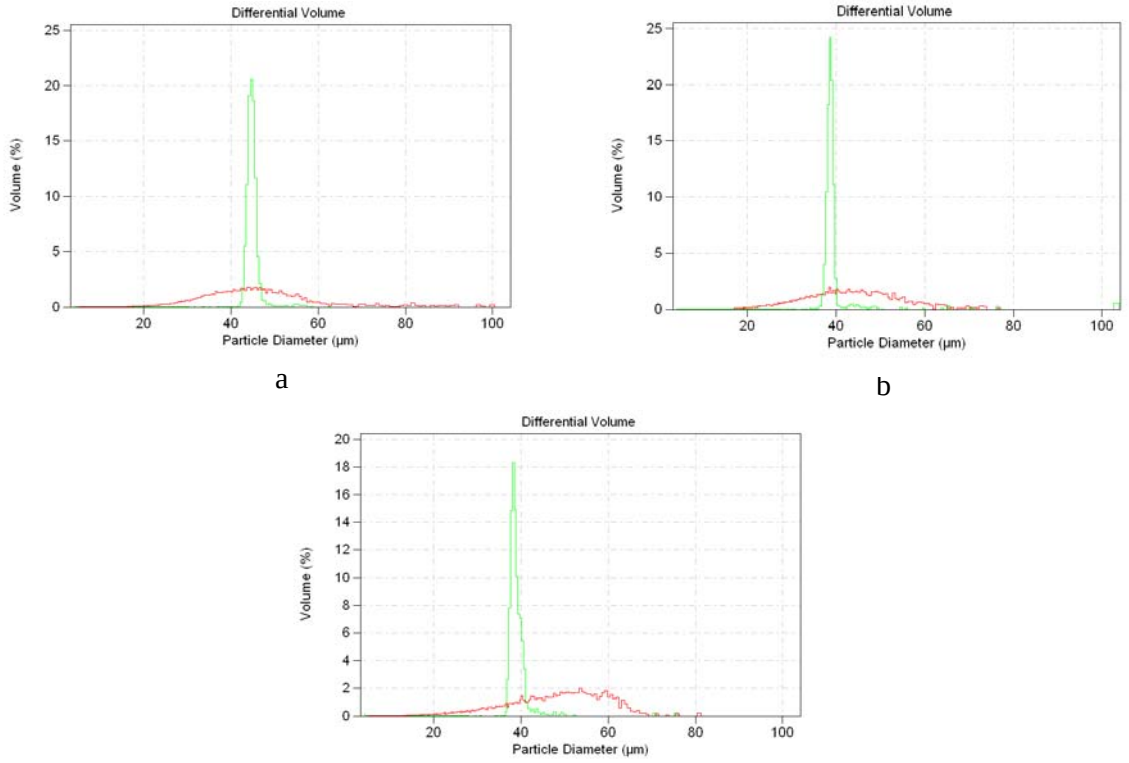

Figure 4.2. Overlay of PPF and homogenizer microspheres of ~40 µm mean diameter and a) 11 kDa, b) 25 kDa, and c) 48 kDa PLGA showing breadth of distribution per technique and the volume % at the peak size per batch.

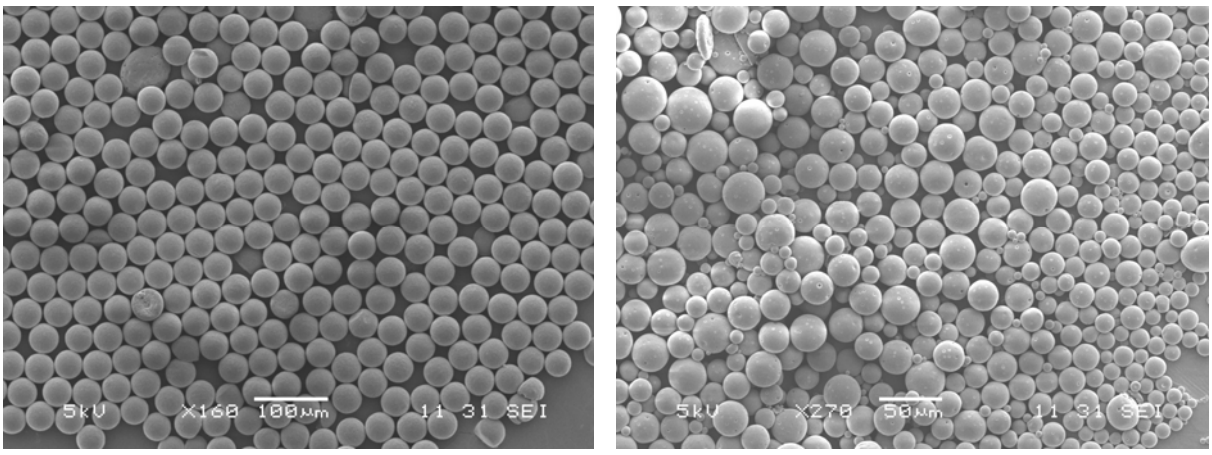

Figure 4.3 Scanning electron micrographs of PPF (left) and homogenizer (right) microspheres showing the breadth of the size distributions from each technique.

4.3.2. Microsphere Morphology, PLGA degradation, and In-Vitro Protein Release

Scanning electron micrographs of homogenizer 20 µm and 40 µm microspheres at various times during degradation are shown in Figure 4.4. The initial porosity throughout the microsphere is similar between different size batches of microspheres produced by homogenization. However, large pores inside some of the microspheres are present in each batch, as shown in Figure 4.5. Large pores at the center are visible in some microspheres of 40 µm and larger. This high porosity can be attributed first to the solvent evaporation rate, which at 10% PLGA concentration in 1% PVA is relatively fast compared with lower PLGA concentrations [10], causing the larger pores observed throughout. The hollow centers could in part be a result of droplets being broken multiple times and coalescing. Interestingly, the degree of shearing between batches fabricated by homogenization shows little effect on the degree of porosity or initial center pore formation. It should be noted that the smaller batch sizes were produced at 2500 rpms greater than the rpms for the larger batch sizes.

Figure 4.6 contains micrographs of both PPF and homogenizer microspheres in the 40 µm range at various times during degradation. After fabrication, both types of microspheres exhibit similar initial internal porosity when comparing only those homogenizer microspheres without large center pores. However, no microspheres with large center pores are noticeable in the PPF batches. Microspheres produced by both techniques appear to have smooth surfaces with submicron pores and some larger pores up to 3 µm. The similarities between the surface of the microspheres from both techniques allude to the likelihood that solvent evaporation rate during the hardening phase plays a greater role than initial shearing during fabrication in the formation of a smooth surface. However, the increased shearing that the homogenizer microspheres are subjected to greatly influences not only the batch size distribution, but the internal uniformity and loading efficiency of microspheres produced under such conditions.

Despite the large pores at the center, homogenizer and PPF microspheres exhibit similar erosion characteristics in surface and internal morphology over time, as evidenced in Figure 4.6. This is expected given the similarity between the surface and internal porosity of the microspheres. As shown in Figure 4.7 large center pores in homogenizer microspheres is still visible at day 21, but is not necessarily greater in size. Equally, microspheres with large center pores maintain their

shape and integrity just as well as more homogeneous microspheres. This is not surprising since the wall-thickness of these microspheres with large center pores is at least 45% of the total sphere diameter.

Albumin release from homogenizer microspheres of different size but same PLGA molecular weight are shown in Figures 4.8 – 4.10. Little burst release is observed; between 3% and 7% albumin is released in the first three days. A total of 16% to 17% of the albumin is released in the first 28 days from 48 kDa PLGA microspheres, and between 16% and 25% of the albumin is released in the first 28 days from 25 kDa PLGA.

A distinctively faster release rate is observed in the 40 µm microspheres than in the 20 µm microspheres from 11 kDa PLGA. This particular trend is not necessarily expected at this microsphere size range. Rather, it would be expected that due to diffusion time, the 40 µm microspheres would release slower than the 20 µm microspheres. However, the observed behavior is likely a result of fast PLGA degradation and easier diffusion of larger quantities of albumin out of the 40 µm microspheres due to the hollowing effect. This large porosity clearly exists even to the surface of some microspheres, and would allow shorter diffusion distances for the albumin over a larger surface area. Equally, more of these larger microspheres with large center pores are likely present in the 40 µm batches than the 20 µm batches, particularly with the lowest molecular weight PLGA, which would allow solvent diffusion to occur faster than the higher molecular weight PLGA. However, the percentage of hollowed microspheres per batch could not be determined; thus this is purely speculative.

With the 20 µm microspheres albumin release decreases with increasing PLGA molecular weight as shown in Figure 4.11. This is expected since higher molecular weight polymer degrades and erodes more slowly at smaller microsphere size. At 40 µm, shown in Figure 4.12, the lowest molecular weight PLGA is the fastest releasing, but the 25 kDa and 48 kDa PLGA have similar rates of albumin release.

Albumin release from PPF and homogenizer microspheres, shown in Figures 4.13 – 4.15, reveals a faster release of albumin from homogenizer microspheres made with 11 kDa PLGA, but that

albumin releases more slowly from homogenizer microspheres than PPF microspheres when 25 kDa and 48 kDa PLGA is used. The variability in the release observed can be attributed to several factors, dominantly, the breadth of the size distribution of homogenizer microspheres and an unknown percentage of those microspheres with large center pores. The data are easily skewed by either of these factors, and cannot be conclusively analyzed. However, the data may support the theory that a slower evaporation rate comes into play at higher molecular weight PLGA. Thus a higher percentage of microspheres with large center pores may actually be present in the 11 kDa PLGA microspheres, leading to faster release. But a smaller percentage of microspheres with large center pores may be present in the higher molecular weight PLGA microspheres, in part supporting slower release rates. This coupled with a much higher percentage of same size microspheres in the PPF batches may help explain the release observed.

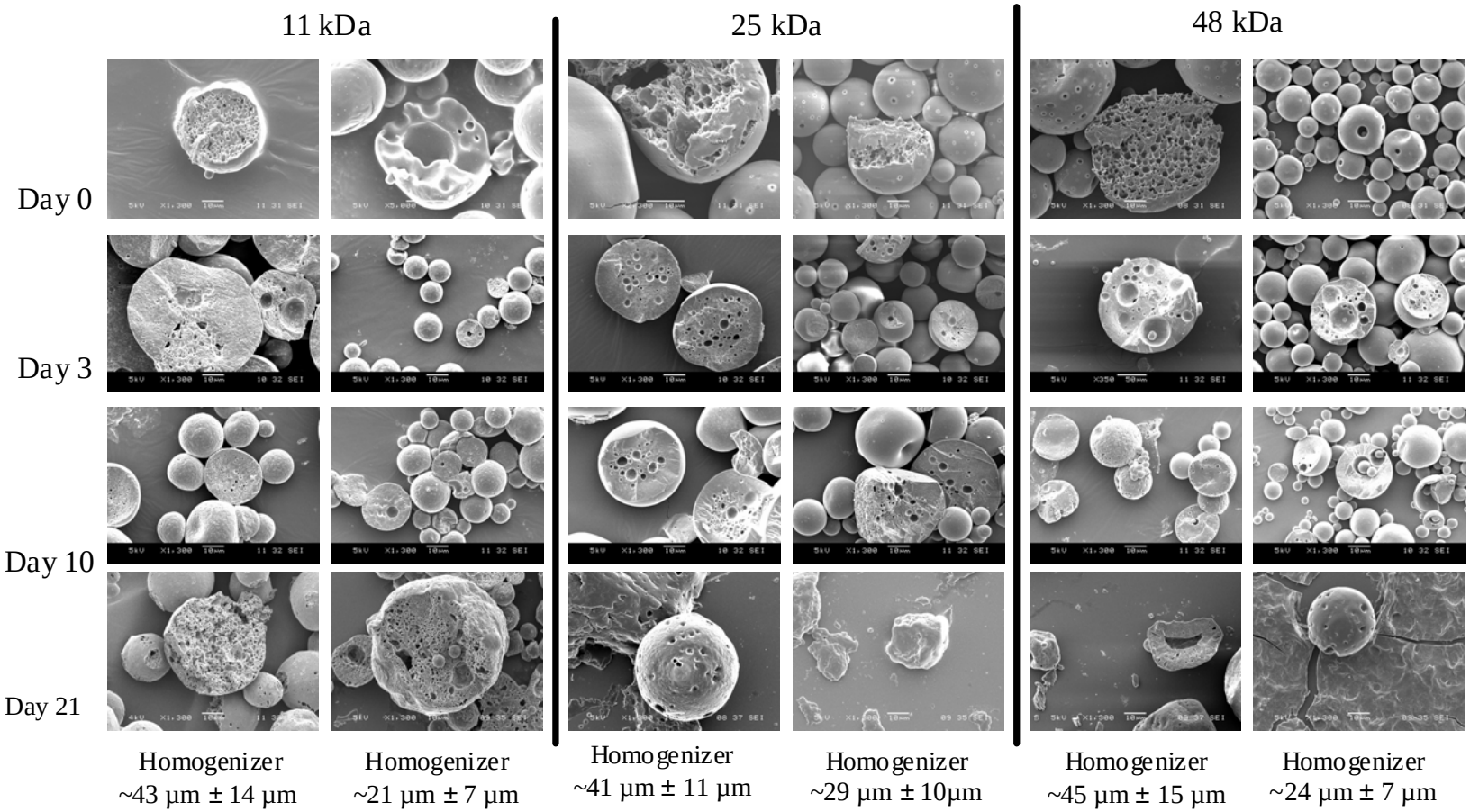

Figure 4.4. Scanning electron micrographs of homogenizer microsphere cross-sections during degradation, showing internal porosity.

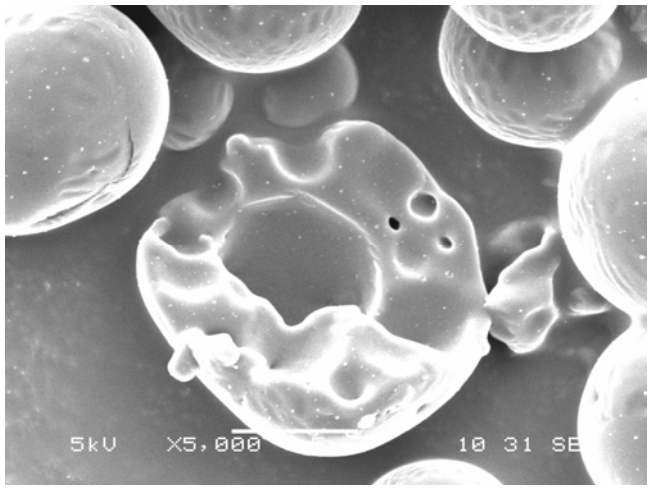

Figure 4.5. Scanning electron micrograph of homogenizer microspheres showing large pore at center, day 0.

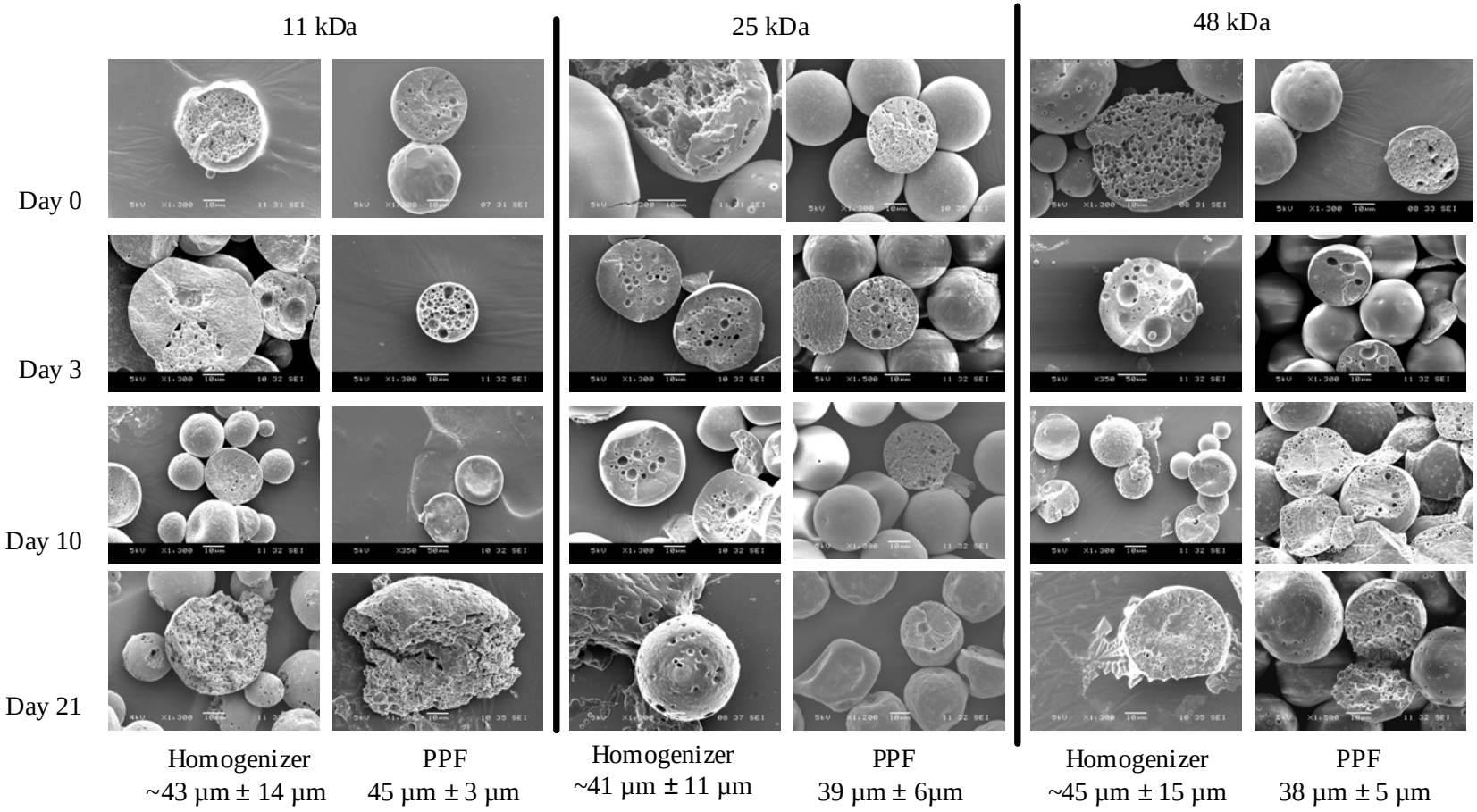

Figure 4.6. Scanning electron micrographs of homogenizer and PPF ~40 µm microsphere cross-sections, showing similarities in internal porosity during degradation.

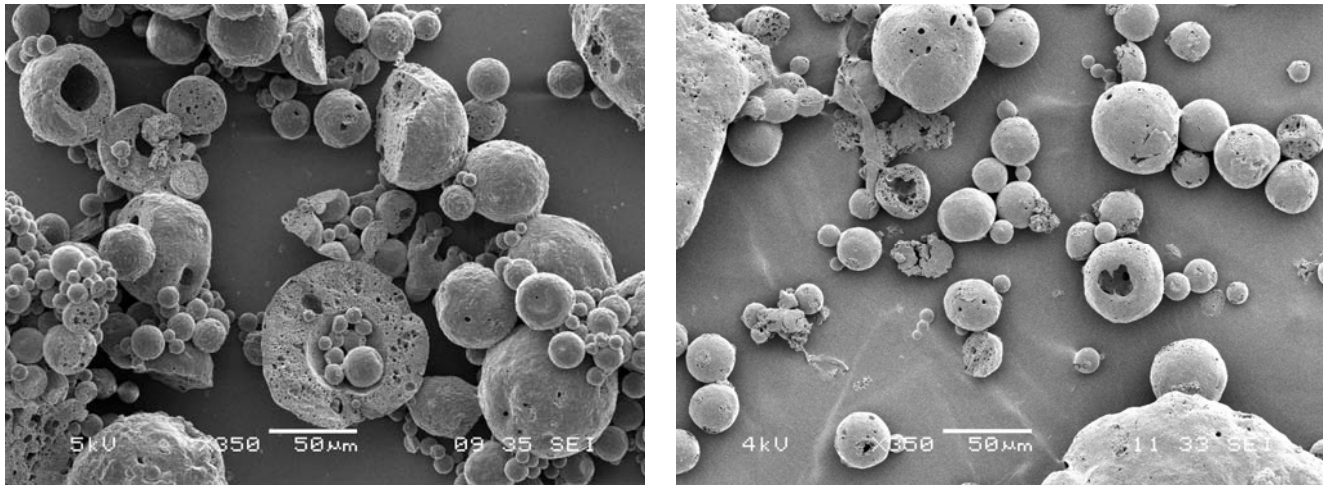

Figure 4.7. Scanning electron micrographs of homogenizer microspheres showing large pores at center and surface, day 21.

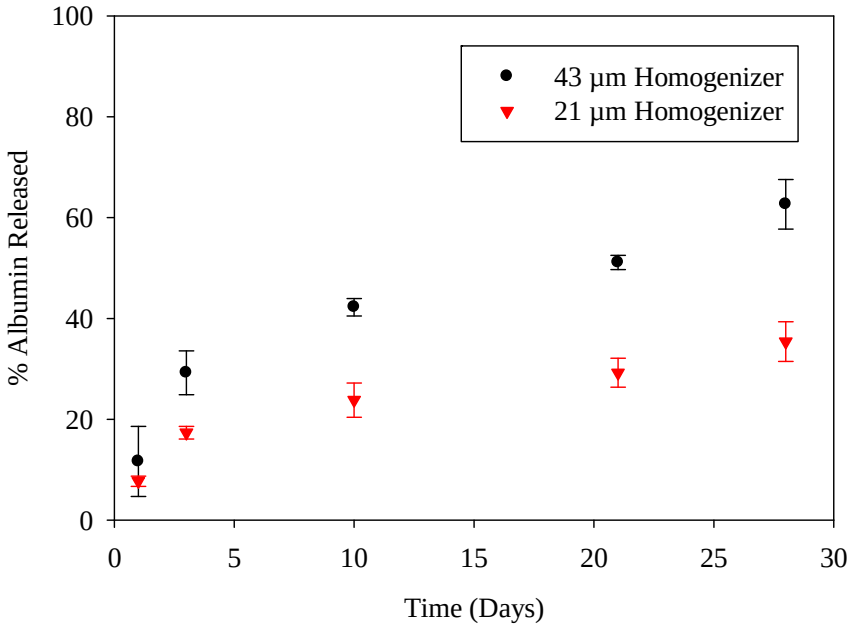

Figure 4.8 Albumin release from 20 µm and 40 µm 11 kDa PLGA microspheres showing faster release from the 40 µm microspheres.

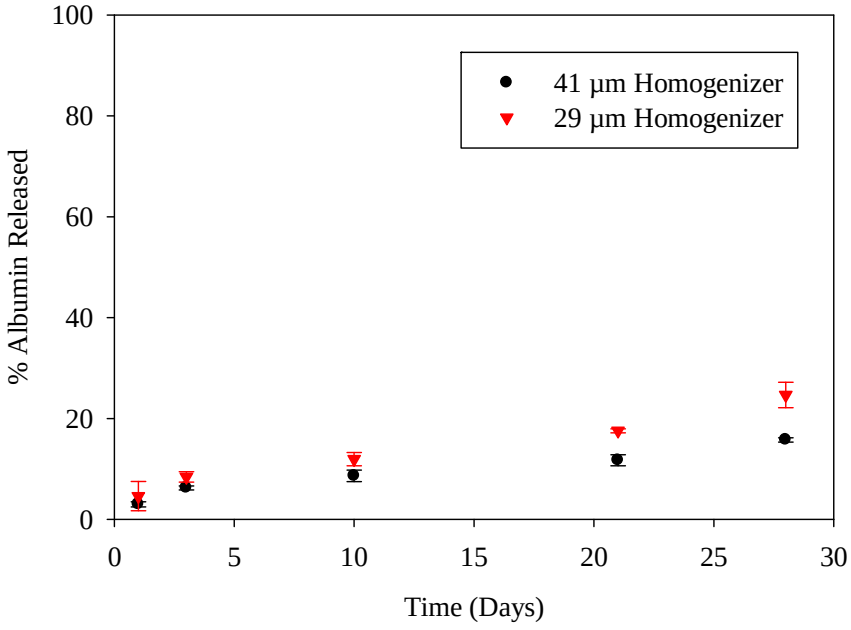

Figure 4.9 Albumin release from 20 µm and 40 µm 25 kDa PLGA microspheres showing slightly faster release from 20 µm microspheres.

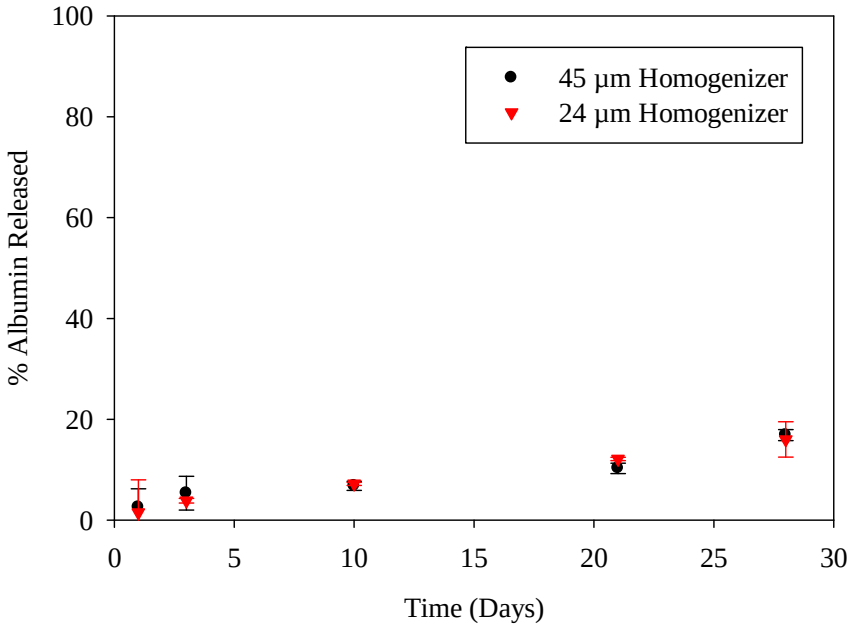

Figure 4.10 Albumin release from 20 µm and 40 µm 48 kDa PLGA microspheres showing similar release rates from the two.

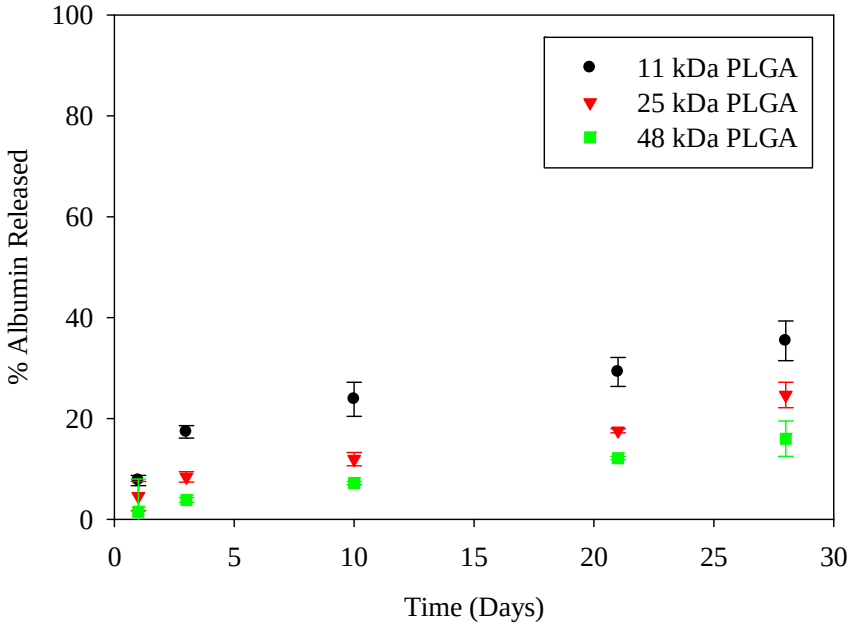

Figure 4.11 Albumin release from 20 µm PLGA microspheres showing incrementally slower release with increasing PLGA molecular weight.

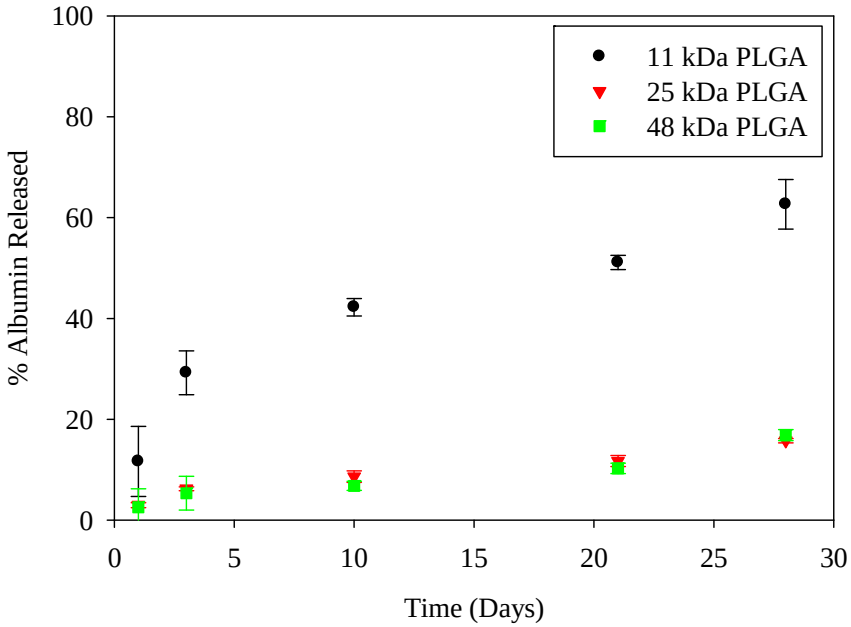

Figure 4.12 Albumin release from 40 µm PLGA microspheres showing fastest release from 40 µm microspheres.

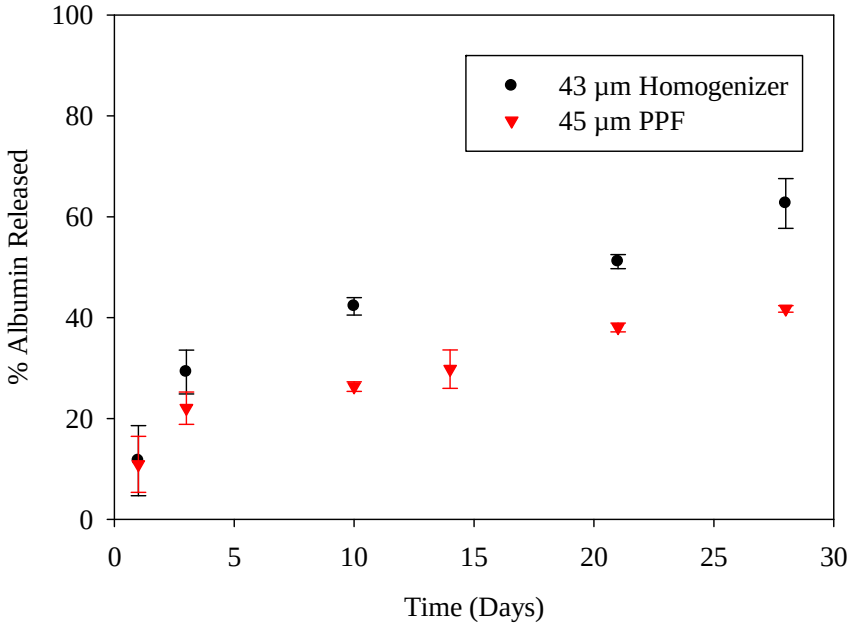

Figure 4.13 Albumin release from 40 µm 11 kDa PLGA homogenizer and PPF microspheres, showing faster release from homogenizer microspheres.

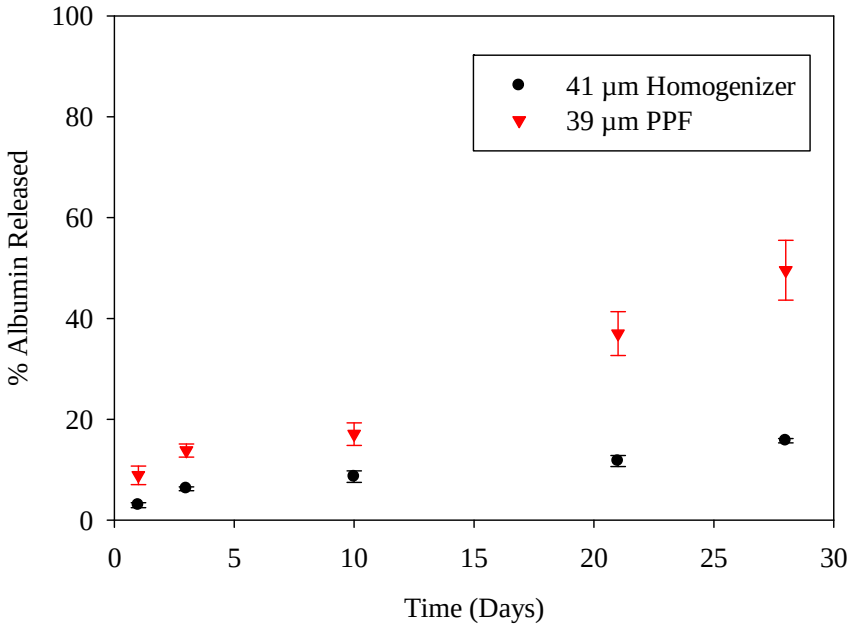

Figure 4.14 Albumin release from 40 µm 25 kDa PLGA homogenizer and PPF microspheres showing faster release from PPF microspheres, and distinctive burst release from PPF microspheres.

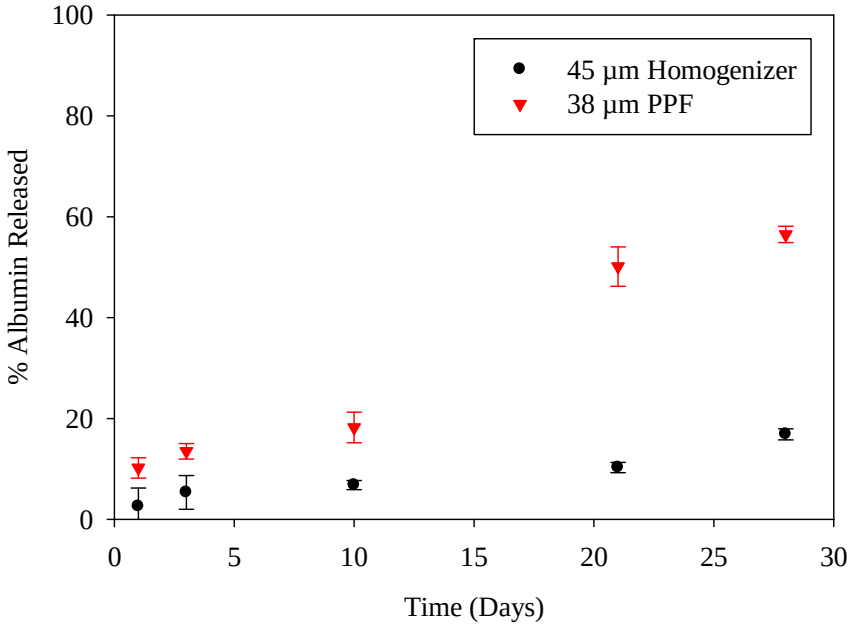

Figure 4.15 Albumin release from 40 µm 48 kDa PLGA homogenizer and PPF microspheres showing faster release from PPF microspheres, and distinctive burst release from PPF microspheres.

4.4 Conclusions and Future Work

Shear forces can be damaging to the formation of PLGA microspheres, as demonstrated herein. In particular, greater shearing during the fabrication process can lead to the development of less homogeneous microparticles with lower protein encapsulation efficiencies and faster release rates than desired due to a higher available surface area and shorter diffusion distances. The application of greatly reduced shear forces allows fundamental diffusion principles to more exclusively govern the homogeneity of microspheres and therapeutic encapsulation and retention.

To more definitively characterize the effect of shearing on PLGA microspheres, it would be of great benefit to expand this study to include multiple concentrations of PLGA, as well as single solution (as opposed to double emulsion) protein encapsulation. The initial emulsion or solution factors into the degree of porosity in newly formed PLGA microspheres, as well. Quantifying the results of an expanded study in a model that relates shear to porosity would also be worthwhile. Furthermore, measuring the porosity of the microspheres directly could give greater insight into the percentage of microspheres that hollow during formation.

4.5 References

[1] Johnson, K. Preparation of Peptide and Protein Powders for Inhalation. Advanced Drug Delivery Reviews 26:3–15, 1997.

[2] Bodmeier, R., and H. Chen. Preparation of Biodegradable Poly(+/-)lactide Microparticles Using a Spray-Drying Technique. Journal of Pharmacy and Pharmacology, 40(11):754–757, 1988.

[3] Chan, H., A. Clark, I. Gonda, M. Mumenthaler and C. Hsu, Spray dried powders and powder blends of recombinant human deoxyribonuclease (rhDNase) for aerosol delivery. Pharmaceutical Research 14 (1997), pp. 431–437.

[4] Maa, Y., P. Nguyen, T. Sweeney, S. Shire, and C. Hsu. Protein Inhalation Powders: Spray Drying vs. Spray Freeze Drying. Pharmaceutical Research, 16:249–254, 1999.

[5] Li, W., K. Anderson, R. Mehta, P. DeLuca. Prediction of Solvent Removal Profile and Effect on Properties for Peptide-Loaded PLGA Microspheres Prepared by Solvent Extraction / Evaporation Method. Journal of Controlled Release, 37:199–214, 1995.

[6] Pavanetto, F., B. Conti, I. Genta, P. Giunchedi. Solvent Evaporation, Solvent Extraction and Spray Drying for Polylactide Microsphere Preparation. International Journal of Pharmaceutic, 84(2):151-159, 1992.

[7] Sandor, M., D. Enscore, P. Weston, and E. Mathiowitz, Effect of Protein Molecular Weight on Release from Micron Sized PLGA Microspheres. Journal of Controlled Release, 76:291–311, 2001.

[8] Blanco, D., M. Alonso. Protein Encapsulation and Release from Poly(Lactide-co-glycolide) Microspheres: Effect of the Protein and Polymer Properties and of the Co-Encapsulation of Surfactants. European Journal of Pharmaceutics and Biopharmaceutics, 45:285-294, 1998.

[9] O'Donnell, P., J. McGinity. Preparation of Microspheres by the Solvent Evaporation Technique Advanced Drug Delivery Reviews, 28:25–42, 1997.

[10] Li, W., K. Anderson, R. Mehta, P. DeLuca. Prediction of Solvent Removal Profile and Effect on Properties for Peptide-Loaded PLGA Microspheres Prepared by Solvent Extraction / Evaporation Method. Journal of Controlled Release, 37:199–214, 1995.